AUG 1976

1 /13/78

FEB 14 1980

AN INVESTIGATION OF SEPARATED FLOW ABOUT A HEMISPHERE-CYLINDER AT 0- TO 19-DEG INCIDENCE IN THE MACH NUMBER RANGE FROM 0.6 TO 1.5

PROPULSION WIND TUNNEL FACILITY
ARNOLD ENGINEERING DEVELOPMENT CENTER
AIR FORCE SYSTEMS COMMAND
ARNOLD AIR FORCE STATION, TENNESSEE 37389

November 1976

Final Report for Period October 1974 — June 1976

Prepared for

AIR FORCE FLIGHT DYNAMICS LABORATORY (FGC)
WRIGHT-PATTERSON AFB, OHIO 45433

This report has been reviewed by the Information Office (OI) and is releasable to the National Technical Information Service (NTIS). At NTIS, it will be available to the general public, including foreign nations.

APPROVAL STATEMENT

This technical report has been reviewed and is approved for publication.

FOR THE COMMANDER

JOHN M. RAMPY
Analysis and Evaluation Division
Directorate of Test

ALAN L. DEVEREAUX
Colonel, USAF
Director of Test

REPORT DOCUMENTATION PAGE		READ INSTRUCTIONS BEFORE COMPLETING FORM
1 REPORT NUMBER AEDC-TR-76-112	2 GOVT ACCESSION NO	3 RECIPIENT'S CATALOG NUMBER
4 TITLE (and Subtitle) AN INVESTIGATION OF SEPARATED FLOW ABOUT A HEMISPHERE-CYLINDER AT 0- TO 19-DEG INCIDENCE IN THE MACH NUMBER RANGE FROM 0.6 TO 1.5		5 TYPE OF REPORT & PERIOD COVERED Final Report - October 1974 - June 1976
		6 PERFORMING ORG REPORT NUMBER
7 AUTHOR(s) T. Hsieh, ARO, Inc.		8 CONTRACT OR GRANT NUMBER(s)
9 PERFORMING ORGANIZATION NAME AND ADDRESS Arnold Engineering Development Center (XO) Air Force Systems Command Arnold Air Force Station, Tennessee 37389		10 PROGRAM ELEMENT PROJECT, TASK AREA & WORK UNIT NUMBERS Program Element 62201F Project 8219
11 CONTROLLING OFFICE NAME AND ADDRESS Arnold Engineering Development Center (DYFS) Arnold Air Force Station, Tennessee 37389		12 REPORT DATE November 1976
		13 NUMBER OF PAGES 118
14 MONITORING AGENCY NAME & ADDRESS(if different from Controlling Office)		15 SECURITY CLASS (of this report) UNCLASSIFIED
		15a DECLASSIFICATION/DOWNGRADING SCHEDULE N/A

16 DISTRIBUTION STATEMENT (of this Report)

Approved for public release; distribution unlimited.

17 DISTRIBUTION STATEMENT (of the abstract entered in Block 20, if different from Report)

18 SUPPLEMENTARY NOTES

Available in DDC

19 KEY WORDS (Continue on reverse side if necessary and identify by block number)

wind tunnel	Mach numbers
test methods	transonic flow
flow (separated)	laser velocimeters
cylindrical bodies	

20 ABSTRACT (Continue on reverse side if necessary and identify by block number)

A wind tunnel investigation was conducted of the separated flow about a hemisphere-cylinder at incidence from 0 to 19 deg in the Mach number range from 0.6 to 1.5. At zero incidence, a nose separation bubble is revealed from analysis of shadowgraphs and surface pressure distributions between Mach numbers 0.7 and 0.9. The basic differences between the present nose separation bubble

DD FORM 1473 1 JAN 73 EDITION OF 1 NOV 65 IS OBSOLETE

20.   ABSTRACT (Continued)

and the leading-edge separation bubble of airfoils are discussed.
A multiple shock system, consisting of a lambda shape shock and
two normal shocks, prevails in the flow field as a result of the
viscous/inviscid interaction which is strongest at $M_\infty = 0.85$.
Velocity field measurements utilizing a laser velocimeter were
obtained for $M_\infty = 0.85$.   The concept of an effective body and the
particle dynamics are used to analyze the velocity.   For incidences
from 5 to 19 deg, shadowgraphs, surface pressures, and oil flow
pictures showing the separation patterns and limiting streamlines
were obtained through the Mach number range.   Two separation
regions, the nose separation bubble and the crossflow separation
zone, were found to exist simultaneously.   Concentrated vortices
standing at the leeside forebody were found, and the mechanism
and condition for their appearance are discussed.   The distribution
of normal-force, total normal-force and axial-force coefficients,
and center of pressure are presented and compared with available
data and a simple theoretical prediction.

AFSC
Arnold AFS Tenn

PREFACE

The work presented herein was conducted by the Arnold Engineering
Development Center (AEDC), Air Force System Command (AFSC), at the
request of the Air Force Flight Dynamics Laboratory (AFFDL/FGC) under
Program Element 62201F, Project 8219. The AFFDL project monitor was
Eugene Fleeman. The results of the research were obtained by ARO, Inc.
(a subsidiary of Sverdrup & Parcel and Associates, Inc.), contract
operator of AEDC, AFSC, Arnold Air Force Station, Tennessee, under ARO
Project Numbers P34A-C-7A and P43C-C4A. The author of this report was
T. Hsieh, ARO, Inc. The manuscript (ARO Control No. ARO-PWT-TR-76-49)
was submitted for publication on May 11, 1976.

CONTENTS

ILLUSTRATIONS

APPENDIXES

1.0 INTRODUCTION

The maneuverability requirements of modern missiles have stimulated the renewed interest in basic aerodynamics of bodies of revolution at large incidence, particularly for those vehicles which perform slewing maneuvers. The maximum incidence for such missiles can reach 180 deg (Refs. 1 and 2). As the incidence increases beyond 20 deg, side force and yawing moment begin to develop because of the occurrence of asymmetrical vortex pattern in the leeside flow field of the missile. In the high subsonic, transonic, and low supersonic flow regime, the magnitude of the side force can sometimes reach as large as 60 percent of the normal force at an incidence between 30 to 50 deg (Refs. 3 and 4). It has been reported in Refs. 3 and 4 that one way of reducing the side force and yawing moment is by increasing the bluntness of the nose. The bluntness of the nose also has the effect to delay the onset of asymmetrical vortex shedding (Ref. 4). Therefore, for missiles designed for large incidence, a blunt nose may be considered as a shape for the purpose of increasing lateral stability.

Unlike the sharp nose bodies of revolution, the flow field about a blunt nose body of revolution in the transonic and low supersonic Mach number range has not drawn much attention. With the advantage of increasing lateral stability at large incidence, there is a need to study the flow field of a blunt nose body of revolution in detail. A hemisphere-cylinder was selected as a model of blunt nose body of revolution for the experimental investigation in this report. The flow field about a hemisphere-cylinder at incidences up to 19 deg is reported. In this range of incidence, significant side force and yawing moment are not expected; therefore, a symmetrical flow field is assumed.

In Ref. 5, a theoretical and experimental study of the flow field about a hemisphere-cylinder at zero incidence in the transonic and low supersonic Mach number range is presented. It was found that at zero incidence the flow field can be satisfactorily predicted by inviscid

theory for $M_\infty > 1.05$ while for $0.7 < M_\infty < 0.95$ the inviscid calculation is not satisfactory because of viscous/inviscid interaction with boundary-layer separation. In this report, a detailed investigation of the viscous/inviscid interaction phenomena is presented for Mach numbers from 0.6 to 0.9. Results of laser velocimeter (LV) measurements of the velocity field for $M_\infty = 0.85$, which has the strongest viscous/inviscid interaction, are also presented and analyzed by using the concept of effective body.

As a first step to understand the separated flow field, experimental results including shadowgraphs, oil flow pictures showing the separation patterns and limiting streamlines, and surface pressure are presented and interpreted. Of great interest is the formation of concentrated vortices standing in the leeside forebody and the mechanism and condition for their appearance are discussed. Also two separation regions, the nose separation bubble and the crossflow separation zone, are found to exist simultaneously. By integrating the surface pressure, distribution of local normal-force coefficient, the total normal- and axial-force coefficients, and the center of pressure were determined and are presented for comparison with available data of other investigators and a simple theoretical prediction.

2.0 TEST APPARATUS, EXPERIMENTAL TECHNIQUE, AND TEST CONDITIONS

2.1 WIND TUNNEL FACILITY

The experiments described herein were performed in the AEDC Aero-dynamic Wind Tunnel (1T). This facility is a continuous flow, nonreturn wind tunnel capable of being operated at Mach numbers from 0.2 to 1.5 utilizing variable nozzle contours above $M_\infty = 1.1$. The test section is 1 ft square and 37.5 in. long with six-percent porous walls in the top and bottom and two plexiglass side walls for flow visualization. The accuracy of Mach number in the test section is ±0.003. Details of the test facility can be found in Ref. 6.

2.2 MODEL, SUPPORT SYSTEM, AND PRESSURE MEASUREMENTS

The model used in the test is a hemisphere-cylinder 1 in. in diameter and 10 in. long and is made of stainless steel. Eighteen pressure orifices are located along a single plane as shown in Fig. 1. The model is sting mounted with a sting diameter of 0.75 in. An adapter is used in order to cover the incidence range up to 19 deg and consists of a vertical support strut and a sting support yoke. The sting support yoke is attached on the vertical support to a sliding strut and a lead screw to provide pitch capability. The accuracy of model incidence is estimated to be ±0.15 deg. The model can be rolled manually every 15 deg by lining up pinholes in the sting and the adapter. A system of Scanivalves® was used for pressure measurements with accuracy of $\Delta C_p = \pm 0.01$.

2.3 LASER VELOCIMETER SYSTEM

The LV used for the present experiment is a two-component, dual-scatter, Bragg-cell-type system operating in the on-axis, back-scatter collection mode with a 1.5-watt argon ion laser. The system includes an opaque tube and confocal lens which allow low noise, on-axis collection by isolating stray light from the transmitter section. The system is capable of measuring velocity in the range from -500 to 1,600 ft/sec for the horizontal component and ±400 ft/sec for the vertical. The probe volume can be approximated by a 0.3-mm-diam cylinder, 5 mm long, depending on the size of pinhole used. The entire optical system is mounted on a three axis transverse mechanism with an accuracy of ±0.001 in. in all three directions.

The scattering sources (or tracer particles) are the natural aerosol particles entrained in the flow medium. In order to obtain a sound statistical sample, about 1,000 samples were taken in each measurement. A data reduction computer program has been designed to obtain both mean and mode (peak) values of the sample distribution or histogram. Details of the LV system and the data reduction scheme can be found in Ref. 7.

2.4 FLOW VISUALIZATION

Two visualization methods were used in this experiment: shadow-
graphs and oil flow pictures. The shadowgraph system is an off-axis,
collimated beam, direct shadowgraph type. An air gap spark is the point
light source (effective diameter = 0.04 in.) and it provides exposure of
approximately one micro-second duration. The source is positioned at
the focus of a 16-in.-diam f/8 parabolic mirror. This mirror reflects
light from the source in a collimated beam through the wind tunnel test
section, perpendicular to the flow, and directly on to film (11 x 14 in.
to cover the field of interest).

The surface flow pattern is revealed by the technique of injecting
oil. The pressure tubes from the model were connected into an oil tank,
which was pressurized and set outside of the wind tunnel as shown in
Fig. 2. Pressure ports No. 1, 3, 5, 8, 10, and 14 (Fig. 1) were used
for oil injection. Black dye was added to the oil and the model was
sprayed with a light coat of white paint to increase the contrast.
Grids at intervals of 30 deg in the circumferential direction and every
1 in. in the longitudinal direction are marked on the model surface to
provide readings of separation lines. Circumferential angles of ϕ = 165,
120, 75, and 30 deg were chosen for oil injection in order to provide a
comparison of surface flow pattern and separation lines.

2.5 TEST CONDITIONS

The outline of the experiments is presented on the following page.

EXPERIMENTAL PLAN

M_∞	0.6	0.7	0.8	0.9	1.0	1.1	1.2	1.3	1.4	1.5
Re x 10^{-6}/ft	4.2	4.5	4.8	5.1	5.2	5.4	5.4	5.3	5.3	5.0
α	A[1]	A	A	A	A	A	A	A	A	A
Pressure	B[2]	C[3]	B	C	B	C	B	C	B	C
Shadowgraph	Yes	Yes	Yes	Yes	Yes	Yes	Yes	Yes	Yes	Yes
Oil Flow	Yes	No	Yes	No	Yes	No	Yes	No	Yes	No

Notes: 1. Plan A = 5, 10, 15, and 19 deg;

2. Plan B: ϕ = 0, 30, 60, 75, 90, 105, 135, and 180 deg;

3. Plan C: ϕ = 0, 90, and 180 deg; and

ϕ = 0 is the leeside plane of symmetry.

3.0 HEMISPHERE-CYLINDER AT ZERO INCIDENCE

3.1 EFFECT OF COMPRESSIBILITY ON FLOW SEPARATION AND SHOCK SYSTEM

In Ref. 5, flow separation about a hemisphere-cylinder at zero incidence was observed at M_∞ = 0.8. The effect of compressibility on flow separation is presented in this section for M_∞ = 0.6 to 0.9 within a Reynolds number range from 4.2 to 5.1 x 10^6 per foot. The variation of Reynolds number is negligible in the present experiment. Figure 3 shows the shadowgraph of flow past the hemisphere-cylinder for M_∞ = 0.6 to 0.9. At M_∞ = 0.6, the flow is well attached and no shock appears. Between M_∞ = 0.7 and 0.85, there is flow separation at the nose, a shock system, and reattachement. The most pronounced separation region occurs at M_∞ = 0.85. At M_∞ = 0.9 and above (Ref. 5) flow separation is not observed, and a well-defined normal shock appears. Therefore, the nose separation bubble occurs for the hemisphere-cylinder at Mach numbers between 0.7 and 0.9.

A comparison of the measured surface pressure with the inviscid theory (Refs. 5 and 8) for M_∞ = 0.6 to 1.0 is shown in Fig. 4. The

point of separation, reattachment, and the shock location (only the
major normal shock location is shown for multiple shock cases) as esti-
mated from an enlarged version of the shadowgraph of Fig. 3 are also
indicated in Fig. 4. The minimum pressure $C_{p_{min}}$ and the critical pressure
C_p^* (supercritical flow prevails when $C_{p_{min}} < C_p^*$) are plotted as a
function of Mach number (Fig. 5). At $M_\infty = 0.6$, the comparison between
theory and experiment is satisfactory and the flow is subsonic every-
where ($C_{p_{min}} > C_p^*$) with $C_{p_{min}}$ occurring ahead of the junction of the
hemisphere and cylinder. For $M_\infty > 0.7$, supercritical flow prevails.
From $M_\infty = 0.7$ to 0.85, poor agreement between theory and experiment is
found in the separated region as expected, while in the region of attached
flow (downstream) the agreement is still good. For $M_\infty = 0.9$ and above,
some difference in surface pressure between theory and experiment also
occurs in the region where the deviation of shock location is found
(Fig. 4 or Ref. 5). The discrepancy in shock location may be caused by
the interaction between the boundary layer and the shock (without flow
separation) which is not treated in the theory. This statement is based
on the fact that excellent agreement is shown in the same figure for
$M_\infty = 1.0$ without the presence of the shock on the body.

The phenomena of the nose separation bubble and the shock system
can now be explained. The nose separation bubble, as shown in Fig. 3,
appears to be similar to the shock-induced leading-edge separation
bubble discussed in great detail for airfoils (Ref. 9). However, there
are two basic differences between these types of separation in that (1)
the nose separation bubble presently investigated starts at a point
where the pressure ahead of separation is continuously decreasing (Fig.
4) and thus cannot be caused by the boundary-layer separation attrib-
utable to reversed pressure gradient or normal shock as in the case of
leading-edge separation bubble of airfoils, and (2) the appearance and
disappearance of nose separation at $M_\infty = 0.7$ and 0.9, respectively, also
suggests a basic difference in the mechanism of separation. The mech-
anism which leads to the separation is argued to be caused by the

recompression shock following an overexpansion zone. As shown in Fig. 5, the theoretical $C_{p_{min}}$ value for inviscid flow decreases as Mach number increases from 0.6; $C_{p_{min}}$ is minimum at $M_{\infty} = 0.75$ and then increases as Mach number further increases. The $C_{p_{min}}$ for $M_{\infty} > 0.6$ occurs at $Z/R = 1$; therefore, the flow at $Z/R < 1$ is under rapid expansion and may be overexpanded, depending on the $C_{p_{min}}$ value, to cause recompression shock. Such a recompression shock is indicated in the shadowgraphs of Fig. 3 for $M_{\infty} = 0.9$ without flow separation. When the strength of the recompression shock, which is proportional to $C_{p_{min}}$, is sufficiently large the sudden increase in pressure may initiate a flow separation. Once the flow separates, the sudden increase in boundary-layer thickness results in a flow which is similar to supersonic flow over a compression corner, or the so-called viscous ramp, as discussed in Ref. 9 with the difference that downstream of the "corner" the surface is curved. Therefore, the interaction of separated flow over a compression corner can describe the flow. From the above argument, a relation can be reached between the flow separation and the $C_{p_{min}}$ calculated from inviscid theory. A critical $C_{p_{min}}$, or $C_{p_{min,c}}$ is defined such that when $C_{p_{min}} < C_{p_{min,c}}$ a nose separation bubble is to be expected. The value of $C_{p_{min,c}}$ for the hemisphere-cylinder is estimated to be approximately -1.20 as shown in Fig. 5. The $C_{p_{min,c}}$ value may be different for different nose configurations and must be determined empirically. Therefore, it may be interpreted that for $M_{\infty} \leq 0.6$ or $M_{\infty} \geq 0.9$, the $C_{p_{min}}$ value is not low enough to initiate a flow separation.

The shock system as observed in Fig. 3 can generally be described by a lambda shape shock located immediately at the starting point of nose separation bubble and two normal shocks (the major and the minor, see Fig. 3 for $M_{\infty} = 0.8$ and 0.85 for example). The appearance of the lambda shape shock with a forward limb and a very weak rear limb is a direct result of the nose separation bubble. Two interesting points can be made since the reattachment of the bubble occurs only after the appearance of the normal shocks. First, the flow in the downstream

vicinity of the lambda shape shock is supersonic; therefore, a rapid reattachment is not possible and the bubble height is increasing (see discussion of Ref. 9, pp. 1197-1199). Second, the argument of Ref. 9 that the reattachment of the bubble over a curved surface can only be reached in the region where subsonic flow is reestablished holds also in the present investigation. Further illustration of the above discussion may be found in the following section.

3.2 ANALYSIS OF VISCOUS/INVISCID INTERACTION AT $M_\infty = 0.85$

As shown in Fig. 3, a strong viscous/inviscid interaction is found for $M_\infty = 0.85$. The questions of interest are (1) what is the size of the nose separation bubble, (2) is the mutlitple normal shock in the shadowgraph real, and (3) how much is the external inviscid flow field influenced by the flow separation? To answer these questions, a velocity measurement using the LV and a theoretical analysis using the concept of effective body are presented in this section. The velocity measurement using the LV for this type of flow is unique because the flow field is very sensitive to disturbance of any material probe. However, the LV system measures the velocity of the tracer particles entrained in the flow medium rather than the gas velocity itself. In general, there is a difference between the particle velocity and the gas velocity, so-called "particle lag." The particle lag in the AEDC Aerodyanamic Wind Tunnel (1T) has been analyzed* and is applied herein to the theoretical flow field computed for the effective body in order to compare with the LV data.

3.2.1 The Velocity Distribution

The measured U and V components (mean value from LV samplings) for flow about the hemisphere-cylinder at $M_\infty = 0.85$ are shown in Fig. 6 along the stagnation streamline Y/R = 0 and along the radial direction at various stations Z/R from -1 to 6.0. Also shown in Fig. 6 in the solid line is the results of the inviscid theory for the hemisphere-cylinder. The agreement between theory and experiment is fairly good

---

* Unpublished data from work conducted by T. Hsieh, PWT, AEDC.

for the region $Z/R \leq 0.4$, where the flow field is considered to be free
from viscous effects. (Note: The agreement between theory and experi-
ment is excellent when the particle lag is taken into account as deter-
mined by Hsieh or by the dash-and-dot curve in Fig. 6 as will be
discussed later in Sect. 3.2.2). The interaction region with flow
separation previously observed in the shadowgraph extends from $Z/R = 0.7$
to 3.0 approximately. It can be seen that the velocity predicted by
inviscid theory differs significantly from the experiment in this region
also. For $Z/R \geq 3.0$, a thick boundary layer is indicated by experi-
mental results.

LV measurements inside the separation bubble were not satisfactory
because of the type of nose or leading-edge separation encountered. As
shown in Fig. 7, the majority of tracer particles in the separated
region do not follow the gas. Tracer particles with inertia may pene-
trate through the separated region. Only particles sufficiently small
in size would follow the streamlines and not enter the separated region
(a reduction of data rate in the separated region was distinctly indi-
cated). Some of the small particles may enter the separated region at
the reattachment location E, and these trapped particles can follow the
gas even in the separated region. The evidence is that in the LV samples
obtained in the separated region show simultaneous positive (about 600
ft/sec) and negative (as large as -350 ft/sec) velocities with about 15
percent or less in total samples for the latter. Such sampled results
confirm that the flow is indeed separated (otherwise no negative velocity
samples can possibly be detected), but the local velocity cannot be very
well represented because of the large number of particles penetrating
the bubble by inertia as shown in Fig. 7. Hence, no data in the sepa-
rated region are presented.

3.2.2 Effective Body

An exact analysis of the interaction region requires solution to
the viscous equations. However, a simple analysis for the external
inviscid flow only and the approximate size of the separated region may
be accomplished by using the concept of effective body.

15

An effective body is defined to be a body that will give the
measured surface pressure of the hemisphere-cylinder. To do this, the
computer program used in obtaining inviscid flow field for pressure
curves as shown in Fig. 4 was modified for the purpose of constructing
the effective body. The scheme used is one of trial and error. The
body shape was gradually adjusted to obtain the required surface pres-
sure distribution. In the course of the trial-and-error process, it was
found that specifying the body curvature and integrating for the body
shape would speed up the convergence of surface pressure. The resulting
effective body is shown in Fig. 8. A satisfactory comparison of the
computed surface pressure for the effective body with the experimental
data is shown in Fig. 9. A plot of curvature distribution for the
effective body is included in Fig. 9. Also shown in Figs. 8 and 9 are
the inviscid results for the hemisphere-cylinder (dash curve) for com-
parison. To determine the precise shape of separated region from the
shadowgraph is difficult, but an approximate estimation can be made as
shown in Fig. 8 and is seen to be comparable to the shape of computed
effective body in the fore portion.

It is interesting to point out that a decrease in the thickness of
the profile from distance $Z/R > 2.0$ for the effective body (Fig. 8) is
necessary in order to match the experimental pressure data at $Z/R = 2.0$
(Fig. 9). This also confirms the bubble type separation. The choice of
$Z/R = 2.7$ for the end of curved body (Fig. 8) was made to match the
experimental pressure data at $Z/R = 3.0$ (Fig. 9), which also agrees with
the pressure curve for the hemisphere-cylinder. Downstream of $Z/R = 2.7$,
the body is approximated by a cylinder 11 percent larger in radius to
simulate the thick boundary-layer development after flow reattachment.
This approximation is justified since the pressure for $Z/R \geq 2.7$ is very
near the free-stream pressure and is not important to the present study.
In Fig. 9, the appearance of an expansion followed by a compression
resulting in a hump in the surface pressure curve after the shock is
theoretically sound (Ref. 10).

A plot of the Mach number and pressure distribution in the external field for the effective body is shown in Fig. 10. The corresponding shock locations for the lambda shape shock and the major and minor normal shocks, as seen from the shadowgraph, are also plotted in Fig. 10. It is interesting to note that there are two supersonic pockets given by the effective body corresponding to the major and minor normal shocks, respectively, as observed. The exact location of the shocks are generally not given by the theory because of the lack of a shock-fitting scheme in the numerical computation. (In Ref. 5, however, the shock location is represented by the sonic location for the hemisphere-cylinder with a single normal shock, and the predicted shock location is found to be slightly ahead of the experimentally observed one.) The significance of the appearance of the second supersonic pocket is that the observed minor shock is physically possible. This is considered to be a fruitful result of using the effective body to analyze the flow field. The location for the lambda shape shock is inside the first supersonic pocket as is consistent with the nature of an oblique shock as discussed in Section 3.0. The plot of pressure distribution in Fig. 10 does not show any pressure discontinuity across any of the shocks (particularly the lambda shape shock and the minor shock). This is attributed to the lack of a shock fitting in the theory.

Now, a comparison can be made between the velocity field as predicted by the effective body and the experiments. The comparison is also shown in Fig. 6 by the dash curve. In the regions $Z/R \leq 0.4$ and $Z/R \geq 3.0$, no significant change is shown between the results for the effective body (dash curve) and that for the hemisphere-cylinder (solid curve); this indicates that the influence of flow separation has a negligible effect on the velocity distribution in these two regions. In the interaction region, $0.8 \leq Z/R \leq 2.0$, however, the dash curve at all stations shown does more correctly match the experimental data. In addition, in order to account for the particle lag, an effective particle with radius of 2 μm and density of 0.8 gr/cc was used to compute

17

for the particle velocity components U_p and V_p in the external flow field associated with the effective body and results are also plotted in Fig. 5 by the chain (dash and dot) curve. The surprisingly good agreement between the chain curve and the experimental data for stations at $Z/R \leq 0.8$ definitely indicates that the flow field is well represented by the effective body for $Z/R \leq 0.8$. For the station at $Z/R = 1.2$, it is interesting to notice that the U_p component does not agree satisfactorily with the data, but the comparison for the V_p component is surprisingly good. Such a result can be reasoned by the fact that the shock system in the flow field under investigation is not very well computed by the theory as discussed in the last paragraph and these shocks generally have negligible influence on the V component of the gas velocity. In the interaction zone ($1.2 \leq Z/R \leq 2.0$), the U component predicted by the theory is slightly large. The lambda shock starts at about $Z/R = 0.7$, hence for region $Z/R \leq 0.8$ the U_p, V_p are not yet affected by the shocks and good comparisons are expected.

4.0 HEMISPHERE-CYLINDER AT INCIDENCE FROM 5 TO 19 DEG

The results of experimental investigation of flow field about a hemisphere-cylinder at incidence from 5 to 19 deg in the Mach number range from 0.6 to 1.5 are described in this section.

4.1 FLOW VISUALIZATION BY SHADOWGRAPHS

Figure 11 shows the shadowgraphs of the hemisphere-cylinder at incidence for Mach numbers from 0.6 to 1.5. For $M_\infty \geq 1.1$, the shock standoff distance and shock shape in the plane of symmetry can be obtained from the shadowgraphs. A plot of the shock standoff distance at both the body axis and the wind axis is shown in Fig. 12. It is seen that for $M_\infty \geq 1.2$ the shock standoff distance in the wind axis is approximately constant for a given Mach number over the range of incidence under investigation. In addition, the shock shapes for $\alpha = 0$ to 19 deg at $M_\infty = 1.2$ and 1.5 are shown in Fig. 13 by the solid lines.

Also, in Fig. 13 the shock shapes for α > 0 given by rotating the shock shape obtained at α = 0 by angle of attack are shown by dash lines. It is seen that the solid line and dash line coincide very well for the case of M_∞ = 1.5 and only differ slightly for M_∞ = 1.2. Therefore, the flow field in the nose portion for α = 0 can be used to approximate the flow field in the nose portion for α > 0 by rotating the entire flow with angle of attack as successfully treated in Ref. 11. It should be pointed out that the flow in the nose region does not separate until 15 to 19 deg for 1.1 ≤ M_∞ ≤ 1.5 as shown by the shadowgraphs, hence the approximation by rotation is useful for inviscid computation as in Ref. 11.

For M_∞ ≤ 1.0, the following points of interest are noticed: (1) as incidence increases the normal shock as observed at zero incidence gradually diminishes on the windside for a given Mach number; in the leeside, the flow separates with a thick separation layer and the normal shock breaks up into multiple shocks or disappears; and (2) at M_∞ = 0.8, the separation is the most serious of the cases studied. Flow separation even shows in the windside and persists until α = 19 deg. Hence, at M_∞ = 0.8, a ring shape of separated flow prevails on the forebody for α ≤ 15 deg.

4.2 SEPARATION CHARACTERISTICS

Surface flow patterns of the hemisphere-cylinder at incidence are revealed by oil flow pictures as shown in Figs. 14a and b. Figure 14a shows the different features of separation and Fig. 14b shows various cases. Important characteristics about the separated flow can be observed from the pictures in conjunction with the shadowgraphs (Fig. 11) as described below.

4.2.1 Regions of Separation I and II

As sketched in Fig. 15, the region of separation I is identified as the crossflow separation zone caused by the crossflow pressure gradient, a direct consequence of incidence. As a result, a pair of leeside

vortex sheets appear which is well known. The region of separation II is identified as the leeside nose separation bubble caused by the meridional pressure gradient (similar nose separation also occurs at $\alpha = 0$), a consequence of both the bluntness of the nose and the incidence. In Ref. 12, the separation patterns of elongated body of revolution at incidence are discussed in great detail. A simultaneous appearance of both separation regions I and II as described herein was not mentioned in Ref. 12 and hence adds a new separation phenomenon for blunt nose body at incidence. A sketch of the limiting streamlines in the plane of symmetry for the nose separation bubble and in the crossflow plane for the crossflow separation zone is shown in Figs. 15b and c, respectively.

For the nose separation bubble, the bubble-type separation concept of Maskell (Ref. 13) describes the flow well. A figure of Maskell's bubble-type separation as described in Fig. 14a of Ref. 12 is reproduced as shown in Fig. 15d. It is noted that inside the bubble a circumferential velocity gradient can develop on the body surface near the separation line II and causes the limiting streamline to curve in a counterclockwise direction (note: discussion is made only for flow on the left side of the plane of symmetry facing upstream) toward the separation line. A reattachment of the nose separation bubble to the body has been shown for the zero incidence case (see Section 3.2). At low incidence, the bubble size is small and a closed bubble can also be formed with a reattachment zone. As the incidence increases, the bubble size grows by extending downstream. When the bubble size becomes sufficiently large, the flow may not reattach and the bubble becomes open as shown in Fig. 15a.

The open-type separation line as described in Ref. 12 with limiting streamlines penetrating from the windside into the leeside separation region I as sketched in Fig. 15e is clearly shown by the oil flow picture of Fig. 14a and also other cases in Fig. 14b for $M_\infty \geq 1.2$ at $\alpha = 19$ deg.

4.2.2 Appearance of a Concentrated Vortex

As shown in Fig. 14, a circulatory flow pattern appears on the cylinder surface near the nose for α = 15 deg, M_∞ = 1.0 and α = 19 deg, $M_\infty \geq 0.8$. This is identified as a standing concentrated vortex. Such a vortex on the leeside front surface has also been reported by Werle (Ref. 14). However, little understanding of such a vortex has been advanced since then and its real existence has even been questioned. With the pictures in Fig. 14, a reasonable explanation of the mechanism and condition for the formation of such a vortex can be made (Ref. 15).

For the hemisphere-cylinder at α = 0, a separation bubble may or may not appear, depending on the free-stream Mach number (see Section 3.0). When there is a separation bubble at α = 0 (M_∞ = 0.7 to 0.9), the limiting streamlines are shown in Fig. 16a. At low incidence, Fig. 16b, the region of separation I is formed far downstream while the region of separation II also starts to develop with the size of separation bubble depending on Mach number and angle of attack. For $M_\infty \leq 1$, the nose separation occurs at a lower incidence than for M_∞ > 1, where no nose separation occurs until $\alpha \geq 15$ deg. For Mach numbers from 0.7 to 0.9, the nose separation occurs at α = 0, then its shape changes as the incidence increases; that is, the bubble in the windside gradually disappears while that on the leeside grows. In this stage, regions of separation I and II are far apart and their interaction is negligible and the nose separation bubble is closed. At moderate incidence (for constant Mach number), the nose separation bubble grows and becomes open; meanwhile, the open-type separation line I moves forward. The situation is sketched in Fig. 16c. Since surface flow in the region of separation II near the plane of symmetry must flow upstream while that near the limiting streamlines AA (Fig. 16c) must flow downstream, a condition is provided for the reversal of surface flow in both meridional and circumferential components. Therefore, a concentrated vortex is formed as shown in Fig. 16c. The concentrated vortex can be identified in Fig. 14b for the cases of α = 15, M_∞ = 1.0 and α = 19, $M_\infty \geq 0.8$.

At high incidence, which is beyond the experimental range reported herein, it is believed that separation lines I and II will join together and separation regions I and II will merge to form a closed-type separation as sketched in Fig. 16d. Then, the concentrated vortex will disappear. A three-dimensional sketch of the flow field with the presence of the concentrated vortex tubes is given in Fig. 16e. It is seen that the axis of the concentrated vortex is first perpendicular to the body surface and is convected downstream above the body.

4.2.3 Secondary Separation

Also shown in the oil flow pictures of Fig. 14 is the existence of a secondary separation line III as sketched in Fig. 17a. The appearance of secondary separation has been reported, Ref. 16 for example. A sketch of the flow in the crossflow plane is shown in Fig. 17b, where S_1 and S_2 indicate the primary and secondary separation points, respectively, and V_1, V_2, and V_3 represent a possible appearance of vortices. It is noted that the region in between the primary and secondary separation lines seems to retain less oil than the other part of the surface. This may be interpreted to mean that the surface shear caused by the vortices is stronger in the region between separation lines I and III. The separation angles for the primary and secondary separation (read from the oil flow pictures) along the body axis are shown in Fig. 18. It is seen that the primary separation angle varies significantly as the Mach number increases at higher incidence, whereas the secondary separation angles are not very sensitive to the changes in Mach number and angle of attack.

4.3 DIFFICULTIES OF LASER VELOCIMETER MEASUREMENTS IN LEESIDE FLOW

An attempt was made to measure the leeside velocity field using the LV for $M_\infty = 0.6$ and 1.2 at station $X/R = 14$, where the leeside vortices in the crossflow plane should be well developed. However, the results were not satisfactory for the following reasons:

1. The probe volume of the LV system is too long relative to the size of vortex to be measured or relative to the model size used in the experiment. A sketch of the relative size of the model, the vortices, and the length of the LV probe volume is shown in Fig. 19a (note: the diameter of the probe volume is exaggerated in Fig. 17a). Therefore, with the large velocity gradient involved in the vortex region, the measured velocity is in error.

2. The tracer particles in the vortex region can hardly catch up with the real gas velocity because of the large velocity gradient involved.

3. At $M_\infty = 1.2$, as the laser beam passed through the vortex field, the beam was broken up, because of the lack of tracer particles in the regions where the vortex cores were located. A sketch of the situation is shown in Fig. 19b. It should be noted that the brightness of the beam is proportional to the number density of the tracer particle. The vortex rotating speed is so large that in the dark region all the tracer particles are thrown out by centrifugal force. This finding is consistent with the results of oil pictures which indicate that a strong vortex region exists between the separation lines I and III (Fig. 16).

4.4 SURFACE PRESSURE DISTRIBUTION

Surface pressure data are obtained for the cases shown in Section 2.5. The measured pressure distributions are given in Appendix A.

For $M_\infty \geq 1.2$ and $\alpha \leq 15$ deg, the flow in the fore portion of the hemisphere-cylinder is not separated and inviscid calculation has been performed for $M_\infty = 1.2$ and 1.5 as given in Ref. 11. An improvement of Ref. 11 (for $M_\infty = 1.2$ only) has been made after the publication of Ref. 11 and a new case of $M_\infty = 1.4$ has also been calculated. A modification of the three-dimensional method of characteristics computer

program was made in the surface pressure iteration subroutine, to obtain results further downstream on the body, to the locaton where crossflow separation is known to occur.

A comparison of the calculated and measured surface pressure is shown in Figs. 20 and 21 for M_∞ = 1.2 and 1.4, respectively. Two comments can be made as follows:

1. As shown in Figs. 20a and 21a and b, the surface pressure in the leeside (ϕ = 0) and the windside (ϕ = 180 deg) of the plane of symmetry as predicted by the inviscid theory differs from the general thinking that the two curves (solid and dash) should gradually approach each other toward the downstream end of the body. Instead, the two curves are observed to first cross over and then approach each other gradually. The cross-over character prevails for all cases computed. It is interesting to note that the cross-over character is also presented in the experimental data at M_∞ = 1.2 and 1.4 for α = 5 deg and for α = 10 deg to a less degree. Since for α = 5 deg crossflow separation occurs at far downstream end, the flow over the body fore portion is essentially inviscid. Therefore, the theoretically predicted cross-over character is indeed sound. As the incidence increases and the separation line I (Fig. 16) moves upstream, the cross-over character in the real flow is lost because of viscosity as shown by the experimental data.

2. In the low supersonic flow regime, the inviscid calculation for the hemisphere-cylinder is good for incidence up to 15 deg and from the nose down to the location where leeside crossflow separation occurs as shown in Figs. 20 and 21.

4.5 AERODYNAMIC COEFFICIENTS

The aerodynamic coefficients of the normal force, the pitching moment, and the center of pressure may be obtained by integrating the surface pressure. The method of integration is given in Appendix B. The normal-force distribution over the body length is shown in Fig. 22. A dip in the normal-force coefficient around $Z/R = 1$, the junction of the hemisphere and cylinder, is found at high incidence for all Mach numbers shown and is most pronounced at $M_\infty = 0.8$. The dip is caused by the separation of flow at the forebody (region of separation II, Fig. 15) and therefore significant lift is lost. Also shown in Fig. 22 is the normal force obtained by the method of crossflow drag coefficient of Ref. 1 which is briefly discussed in Appendix C along with other available methods. It is seen that the agreement between the experimental data and the prediction method of Ref. 1 is only approximately correct far downstream from the nose.

The integrated total normal-force coefficient, axial-force coefficients, and center of pressure from the present experiments are shown in Fig. 23. The data of Ref. 17 (fineness ratio 9) and Ref. 18 (fineness ratio 10), both using balances for force and moment measurements, are also presented in Fig. 23 for comparison. The comparison for C_N among the data is satisfactory. Data for $M_\infty = 0.6$ do not show significant difference from the incompressible case of Ref. 18. The crossflow model of Ref. 1 overpredicts C_N for $\alpha > 5$ deg and does not show Mach number effects as pronounced as the experimental data. The comparison of C_A shows some difference between the present data and the referenced experiments. This is expected because the present data do not include surface frictional drag. (Note: If a frictional resistance coefficient $C_f = 0.00025$ is assumed, the surface frictional drag in the present experiment is estimated to be about 0.1 which is about the magnitude of difference in C_A between the solid and open data in Fig. 23.) Theoretical values of C_A at $\alpha = 0$ are obtained from inviscid calculation (Ref. 5) and are seen to agree very well with the present experimental

data for $M_\infty \geq 1.2$. The cos α variation of axial force as given by the crossflow drag model (Ref. 1) is fairly good in the incidence range under investigation. The comparison of center of pressure $(Z/R)_{c.p.}$ from the nosetip in Fig. 23 shows that present data locate the center of pressure about 1 radius downstream compared to Ref. 17. This is because of difference in fineness ratio as expected. Present data for $(Z/R)_{c.p.}$ at $M_\infty = 0.6$ agree well with the incompressible data of Ref. 18 for α ≥ 10 deg. As α → 0, the crossflow model appears to give a wrong trend of the predicted center of pressure.

5.0 CONCLUSIONS

5.1 HEMISPHERE-CYLINDER AT ZERO INCIDENCE

1. A nose separation bubble is found to exist on the fore portion of the hemisphere-cylinder in the Mach number range from 0.7 to 0.9. The basic differences between the nose separation bubble and the leading-edge separation bubble of airfoils are discussed. The viscous/inviscid interaction is found to be most strong at $M_\infty = 0.85$.

2. A multiple shock system is observed as a result of flow separation. The shock system consists of a lambda shape shock and major and minor normal shocks.

3. At $M_\infty = 0.85$, an analysis using the concept of effective body can verify the flow field as observed from the shadowgraphs for the following interesting points: (a) the approximate size of the bubble, (b) two supersonic pockets corresponding to the major and minor normal shocks, and (c) the influence on the external velocity field as a result of the viscous/inviscid interaction.

For the engineering application of a hemisphere-cylinder as a probe or sensing device, the separation effects as described herein must be taken into consideration.

5.2 HEMISPHERE-CYLINDER AT INCIDENCE UP TO 19 DEG

1. For $M_\infty \geq 1.2$, it is shown that the flow field on the hemisphere portion of a hemisphere-cylinder at incidence may be approximated by rotating the zero incidence flow field by the amount of incidence.

2. For $M_\infty \geq 1.2$, inviscid computation for the surface pressure of a hemisphere-cylinder at incidence by the method of Ref. 11 is satisfactory for incidence up to 15 deg before the occurrence of nose separation and from the nose down to the location where the crossflow separation is known to occur.

3. Two separation regions, namely the nose separation bubble (region I) and the crossflow separation zone (enclosed by leeside separation sheets or region II), are shown to exist simultaneously.

4. By oil flow visualization, a pair of concentrated vortices are found for incidence of 15 deg or greater and Mach numbers between 0.8 and 1.4. Therefore, a circulatory surface flow pattern (in counterclockwise direction on the left side of the plane of symmetry when facing upstream) prevails on the leeside of the forebody near the nose.

5. The measured normal-force distribution at far downstream of the hemisphere-cylinder does not agree satisfactorily with the crossflow drag computation given by Ref. 1 for incidence greater than 10 deg. Because of the flow separation at the nose, a local drop of lift distribution at the junction of the

hemisphere and the cylinder is shown. The measured aero-
dynamic coefficients for the total normal force, axial force,
and center of pressure show a stronger influence of free-
stream Mach number than the predicted values using the cross-
flow drag model of Ref. 1.

The separated flow field as described herein for the hemisphere-
cylinder can also occur on bodies with blunt nose of different config-
urations at incidence.

REFERENCES

1. Jorgensen, L. H. "Prediction of Static Aerodynamic Characteristics
   for Space-Shuttle-Like and Other Bodies at Angles of Attack
   from 0° to 180°." NASA TN D-6996, January 1973.

2. Fleeman, E. L. and Nelson, R. C. "Aerodynamic Forces and Moments on
   a Slender Body with a Jet Plume for Angles of Attack Up to
   180 Degrees." AIAA Paper 74-110, 12th Aerospace Sciences
   Meeting, January 30 – February 1, 1974.

3. Pick, G. S. "Side Forces on Ogive-Cylinder Bodies at High Angles
   of Attack in Transonic Flow." AIAA Paper 71-570, 4th Fluid
   and Plasma Dynamic Conference, June 21 – 23, 1971 and Journal
   of Spacecraft and Rockets, Vol. 9, No. 6, June 1972, pp 389-
   390.

4. Keener, E. R. and Chapman, G. T. "Onset of Aerodynamic Side Forces
   at Zero Sideslip on Symmetric Forebodies at High Angles of
   Attack." AIAA Paper 74-770, Mechanics and Control of Flight
   Conference, August 5-9, 1974.

5. Hsieh, T. "Flow Field Study about a Hemispherical Cylinder in the Transonic and Low Supersonic Mach Number Range." AIAA Paper 75-83, 13th Aerospace Sciences Meeting, January 20-22, 1975; also AEDC-TR-76-114, AFATL-TR-75-132 (ADA018157), November 1975.

6. Jackson, F. M. and Sloan, E. H. "Calibration of the AEDC-PWT 1-ft Transonic Tunnel." AEDC-TR-68-4 (AD827912), February 1968.

7. Lo, C. F. "Transonic Flow Field Measurements Using a Laser Velocimeter." Symposium on Laser Anemometry, University of Minnesota, October 22-24, 1975.

8. South, J. C., and Jameson, A. "Relaxation Solutions for Inviscid Axisymmetric Transonic Flow over Blunt or Pointed Bodies." Proceedings of AIAA Computational Fluid Dynamics Conference, July 19-20, 1973.

9. Pearcey, H. H. "Shock Induced Separation and Its Prevention by Design and Boundary Layer Control." Boundary Layer and Flow Control, Pergamon Press, Vol. 2, 1961, pp 1177-1200.

10. Oswatitsch, K. and Zierep, J. "Das Problem des Senkrechten Stosses an Einer Gekrummten Wand." ZAMM, Vol. 40 Supplement, 1960, pp T143-T144.

11. Hsieh, T. "Low Supersonic, Three-Dimensional Flow About a Hemisphere-Cylinder." AIAA Paper 75-836, 8th Fluid and Plasma Dynamic Conference, June 16-18, 1975.

12. Wang, K. C. "Separation Patterns of Boundary Layer over an Inclined Body of Revolution." AIAA Journal, Vol. 10, No. 8, August 1972, pp 1044-1050.

13. Maskell, E. C. "Flow Separation in Three Dimensions." RAE Rept. Aero 2565, November 1955, Royal Aircraft Establishment, Bedford, England.

14. Werle, H. "Separation on Axisymmetrical Bodies at Low Speed." La Recherche Aeronautique, No. 90, September-October 1962.

15. Wang, K. C. and Hsieh, T. "Concentrated Vortex on the Front Nose of An Inclined Body." Paper Presented in 28th Division of Fluid Dynamic Meeting of American Physical Society, College Park, Maryland, November 24-26, 1975; also AIAA Journal, Vol. 14, No. 5, May 1976, pp. 698-700.

16. Rainbird, W. J., Crabbe, R. S., Peake, D. J., and Meyer, R. F. "Some Examples of Separation in Three-Dimensional Flows." Canadian Aeronautic and Space Journal, Vol. 12, No. 10, 1966, pp 409-423.

17. Anderson, C. F. and Henson, J. R. "Aerodynamic Characteristics of Several Bluff Bodies of Revolution at Mach Numbers from 0.6 to 1.5." AEDC-TR-71-130, AFATL-TR-71-82, (AD885911) July 1971.

18. Schindel, L. H. "Effects of Vortex Separation on the Lift Distribution on Bodies of Elliptic Cross Section." Journal of Aircraft, Vol. 6, No. 6, 1969, pp 537-542.
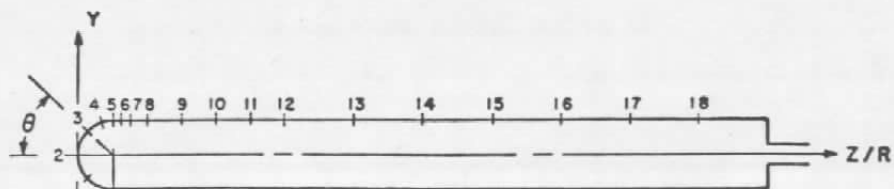
PRESSURE ORIFICE NO.	1	2	3	4	5	6	7	8	9	10	11	12	13	14	15	16	17	18
LOCATION, Z/R	.271	0	.271	.708	1.0	1.25	1.5	2.0	3.0	4.0	5.0	6.0	8.0	10.0	12.0	14.0	16.0	18.0
θ	-43°	0	43°	73°	90°													
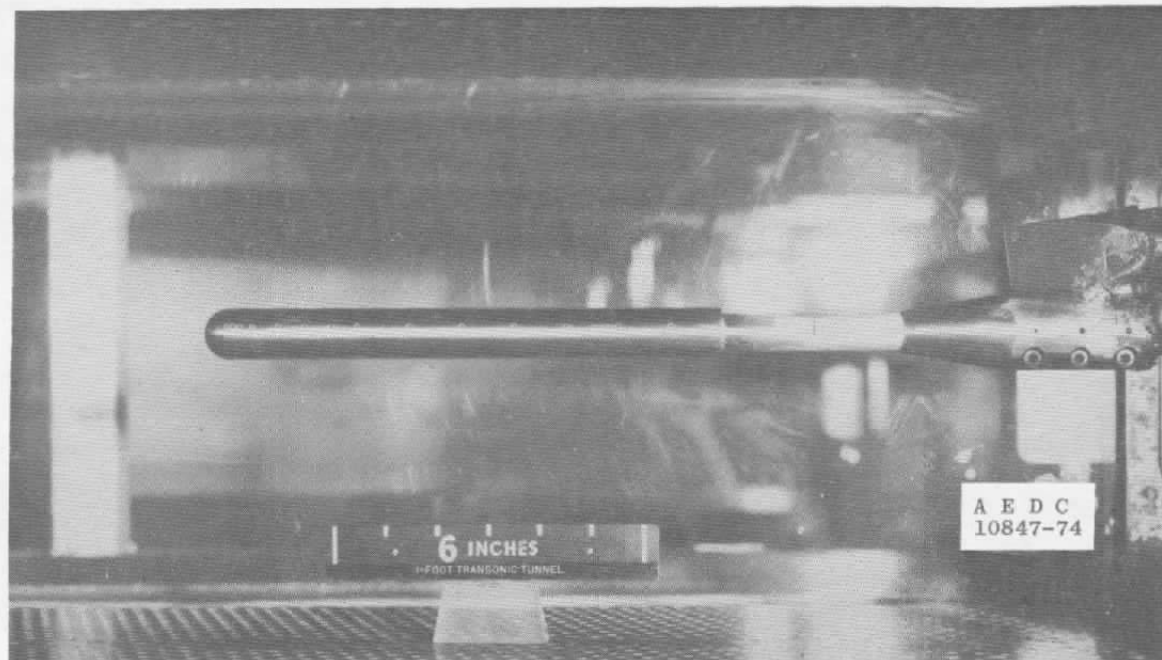
Figure 1. Model of hemisphere-cylinder.
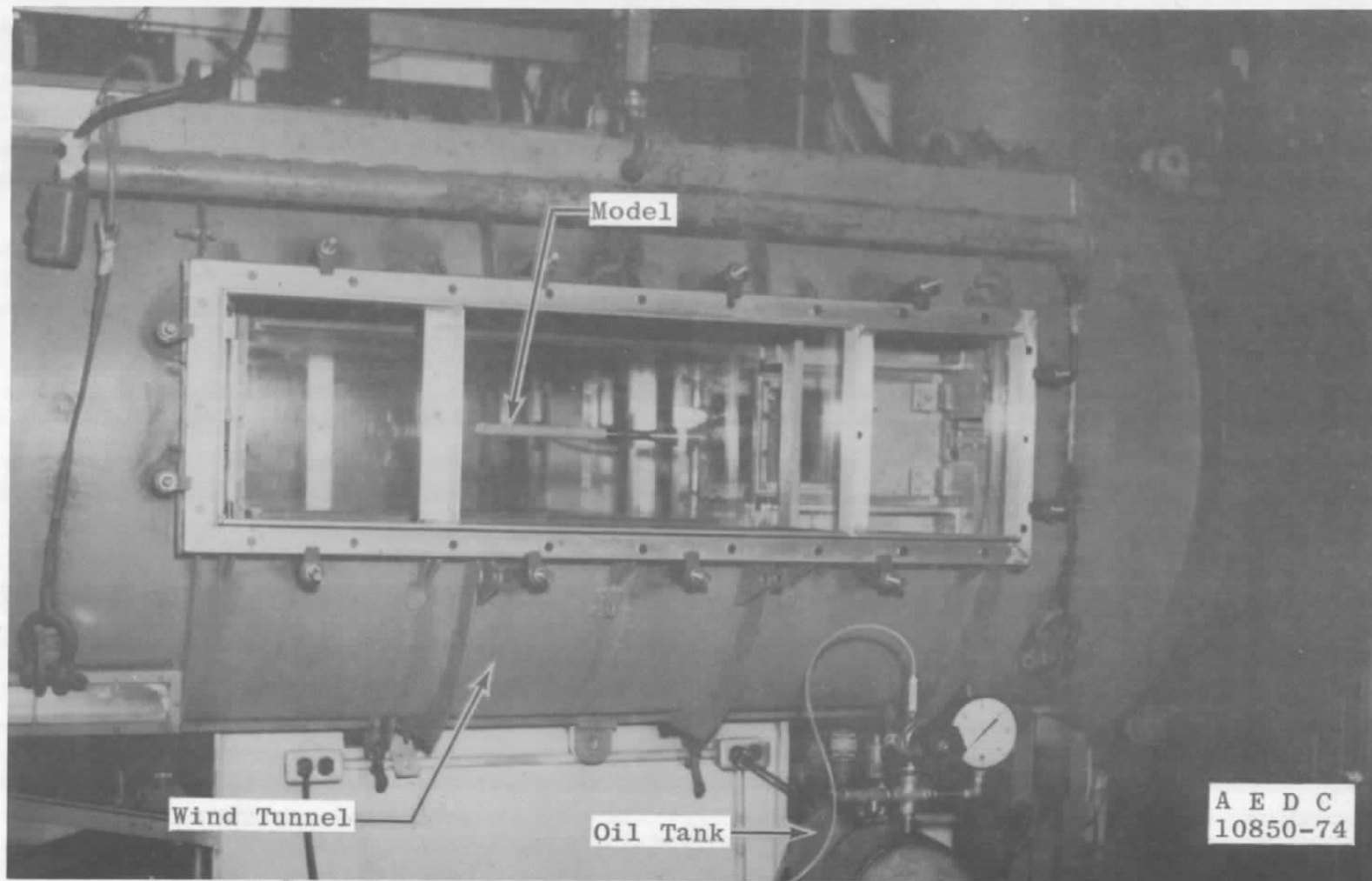
Figure 2. Wind tunnel, model, and oil tank.
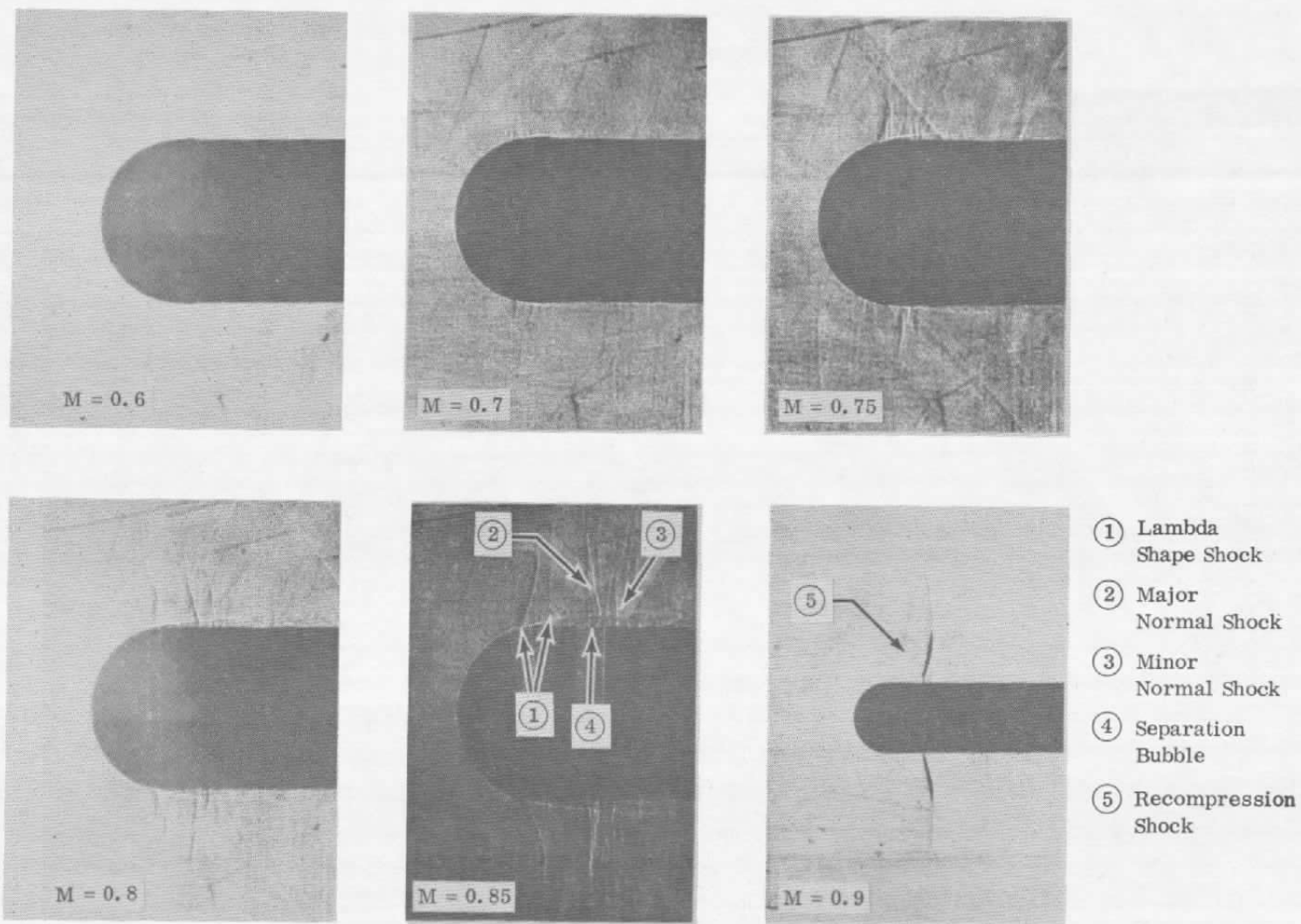
Figure 3. Shadowgraphs of flow past hemisphere-cylinder at $a = 0$.

M = 0.6

M = 0.7

M = 0.75

M = 0.8

M = 0.85

M = 0.9

① Lambda
Shape Shock

② Major
Normal Shock

③ Minor
Normal Shock

④ Separation
Bubble

⑤ Recompression
Shock
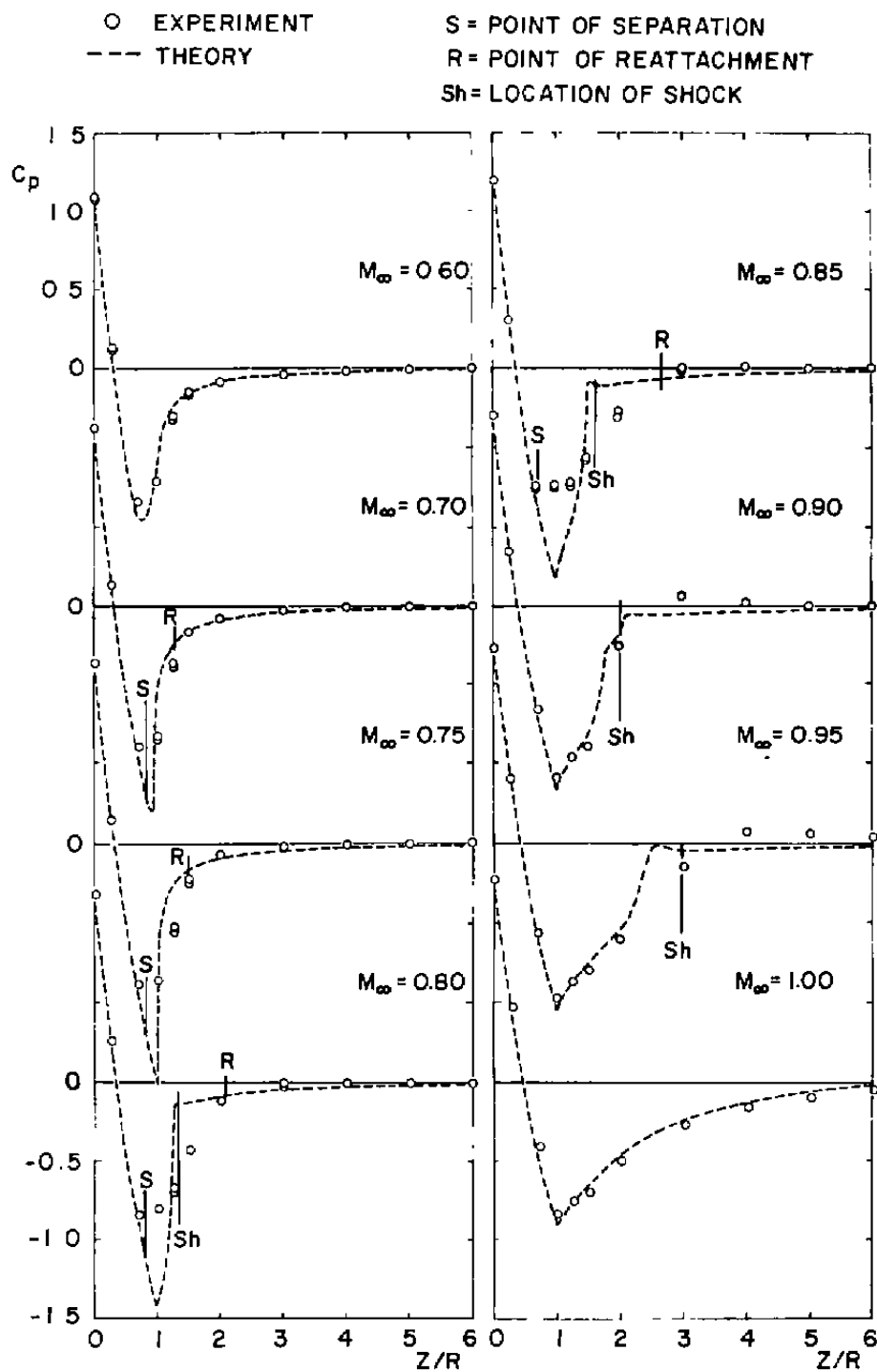
Figure 4. Comparison of surface pressure between
experiments and calculations.
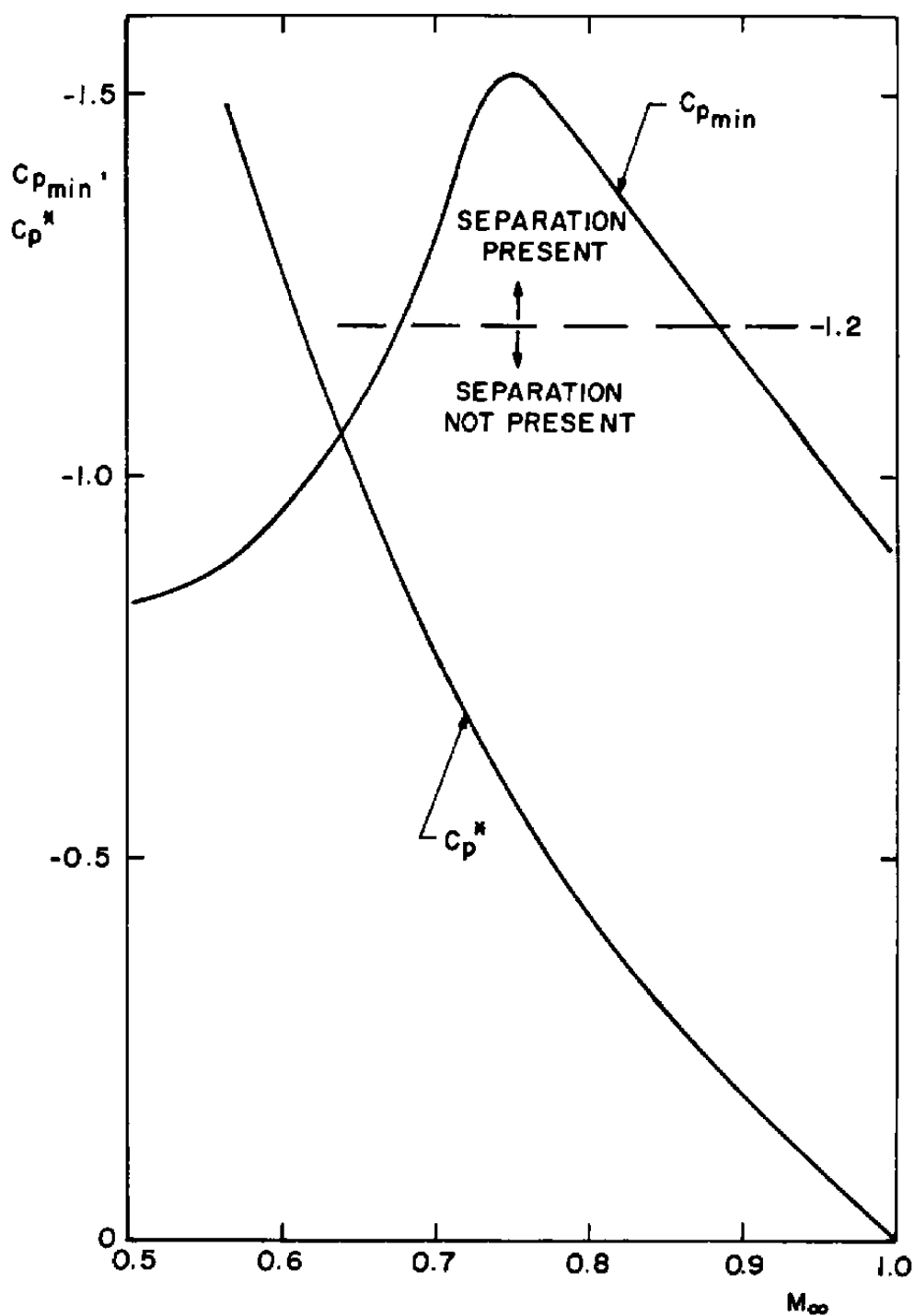
Figure 5. Minimum pressure and critical pressure as a function
of Mach number for hemisphere-cylinder.
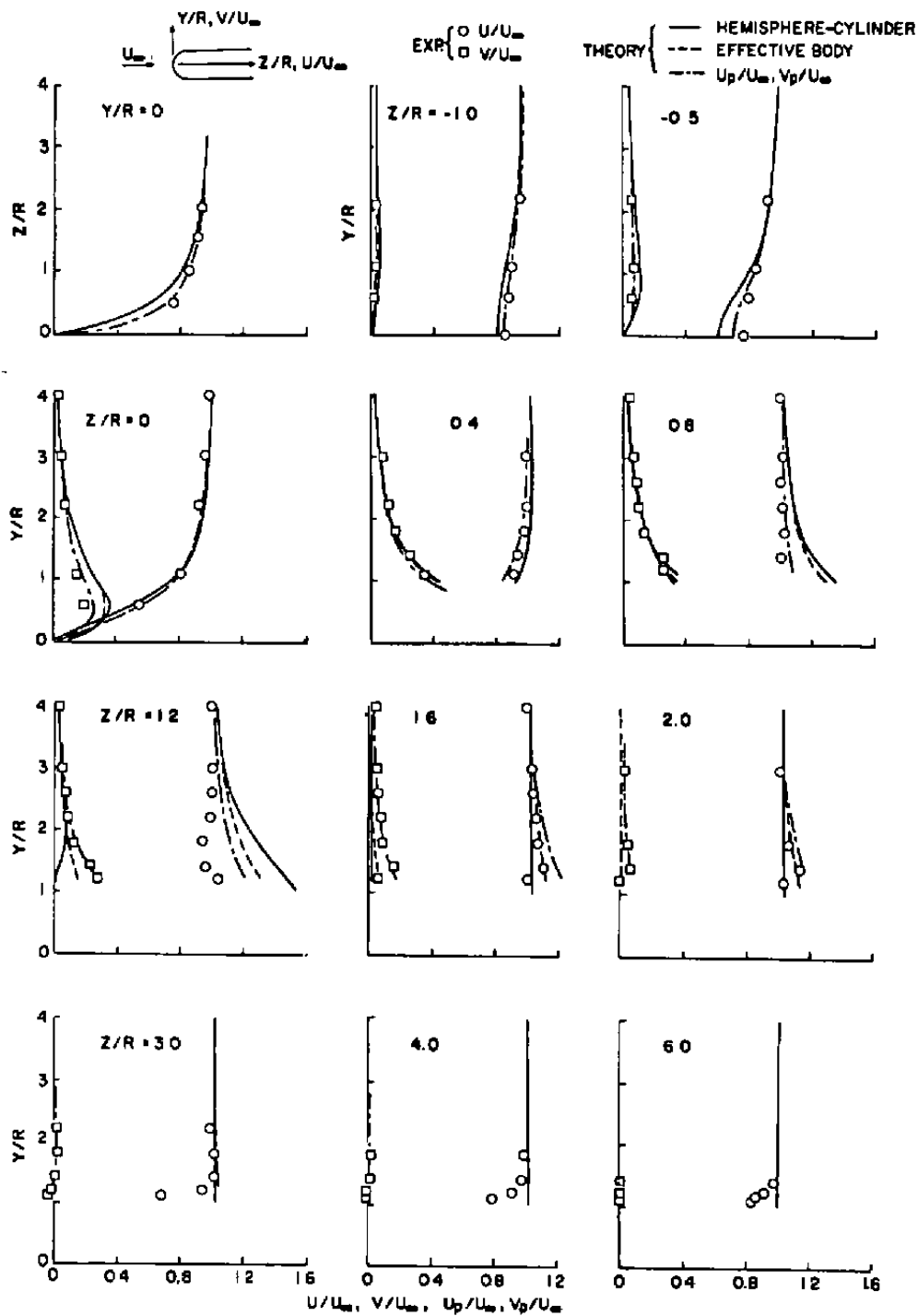
Figure 6. Velocity field about hemisphere-cylinder at zero
incidence and $M_\infty = 0.85$.

PARTICLE TRAJECTORIES
STREAMLINES

SEPARATED REGION
DIVIDING STREAMLINE

E
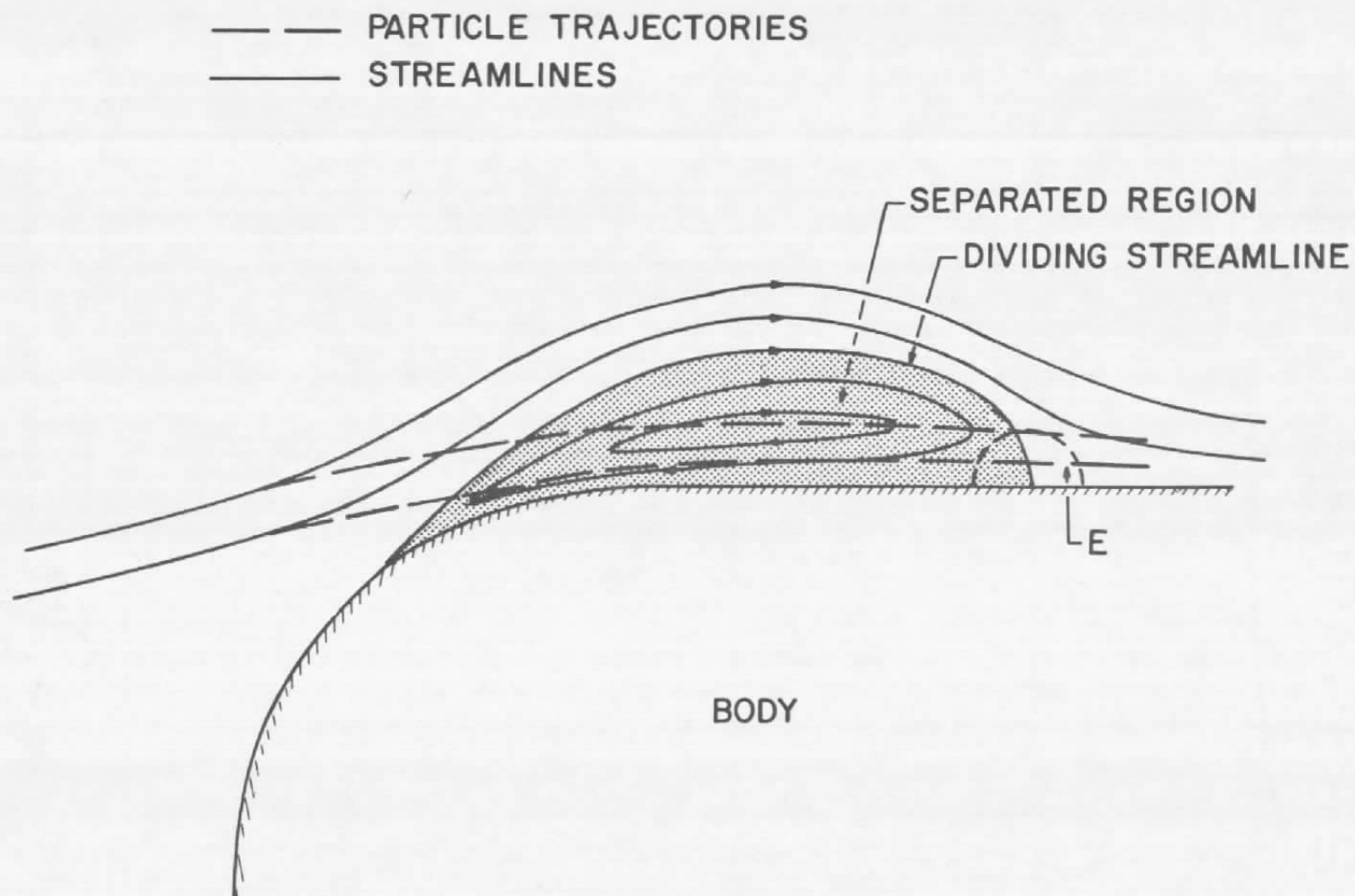
BODY

Figure 7. Possible particle trajectories over nose separation region.
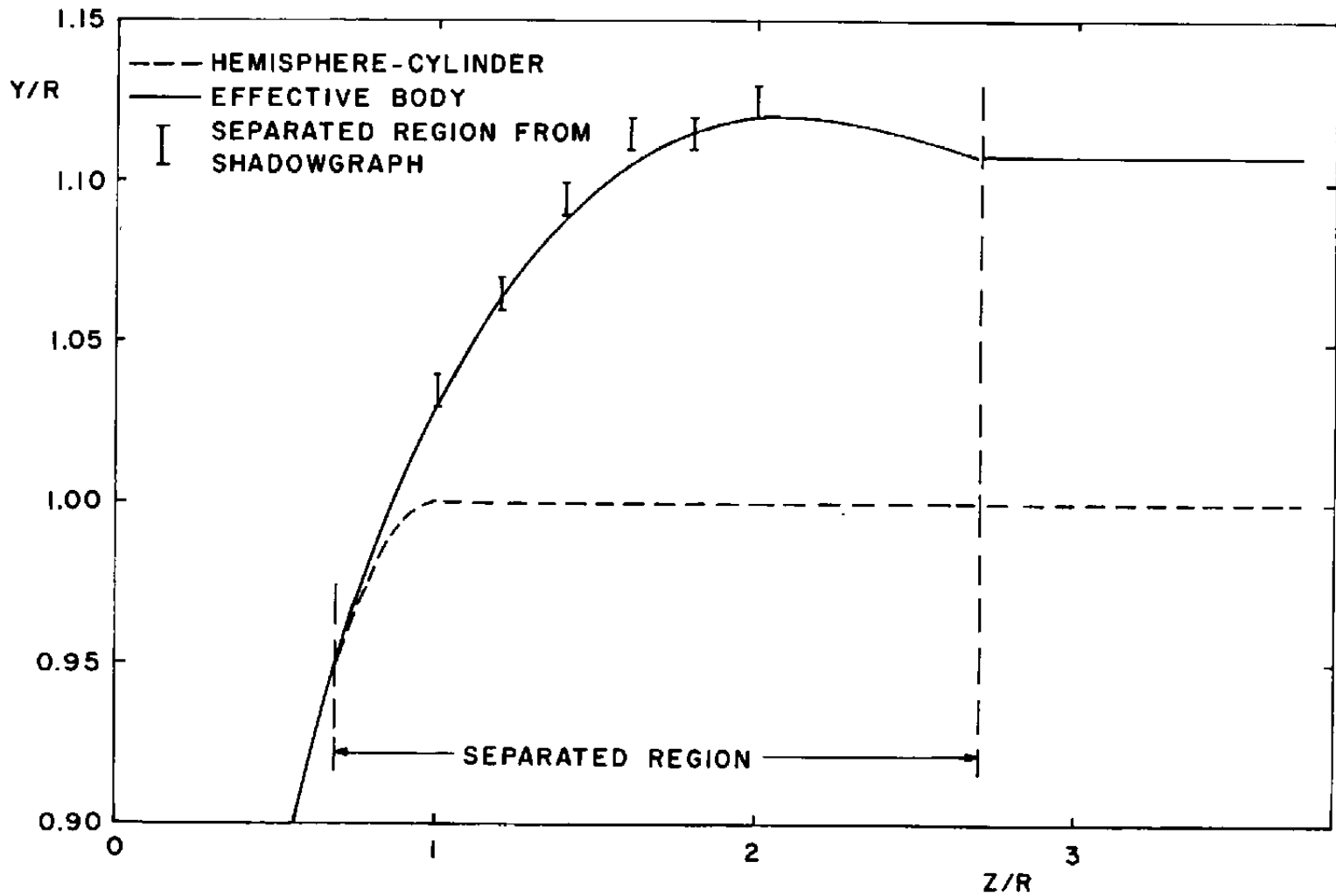
Figure 8. Comparison of the calculated effective body with shadowgraph at $M_\infty = 0.85$.
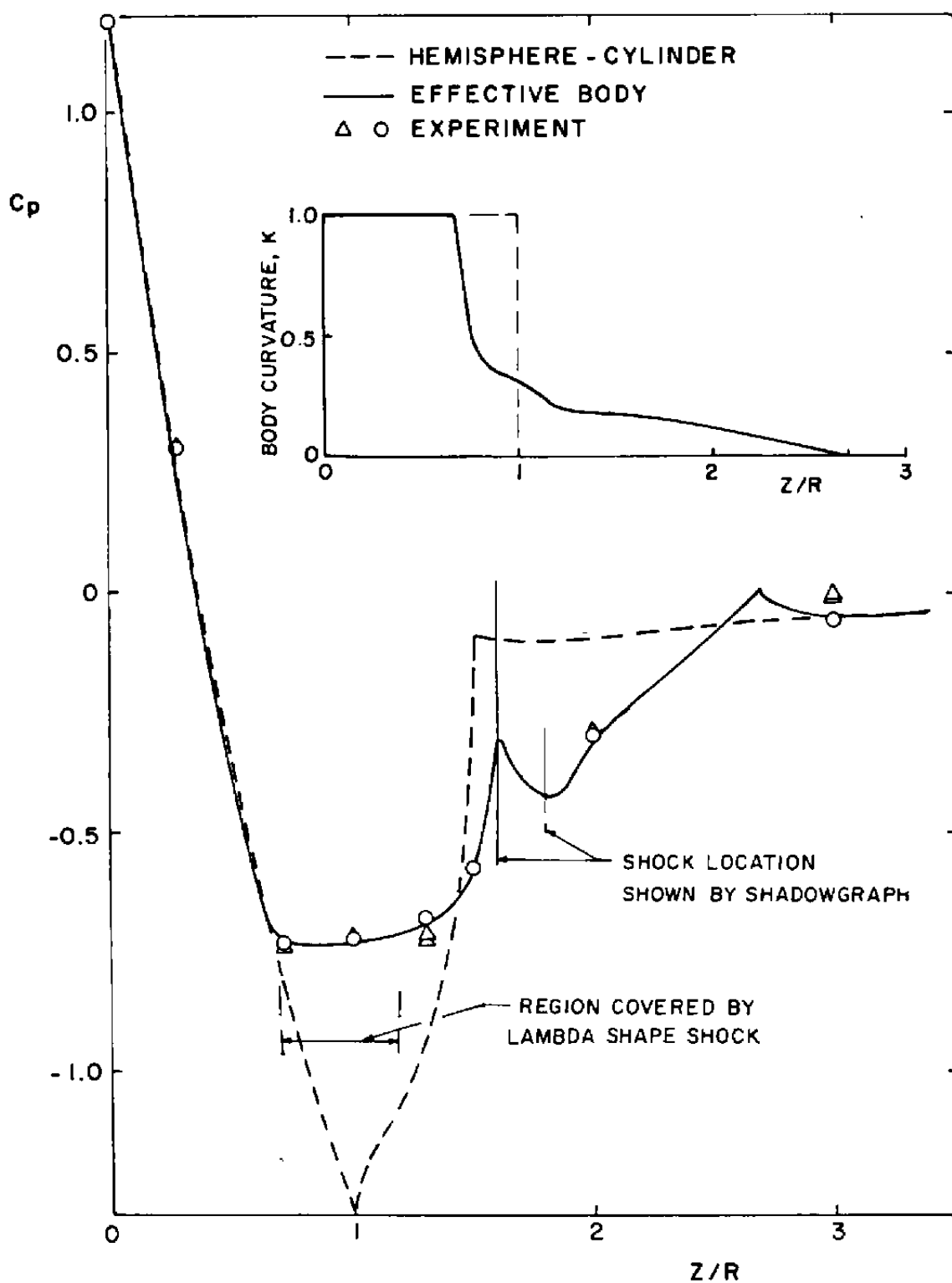
Figure 9. Surface pressure and curvature distribution over
effective body at M_∞ = 0.85.
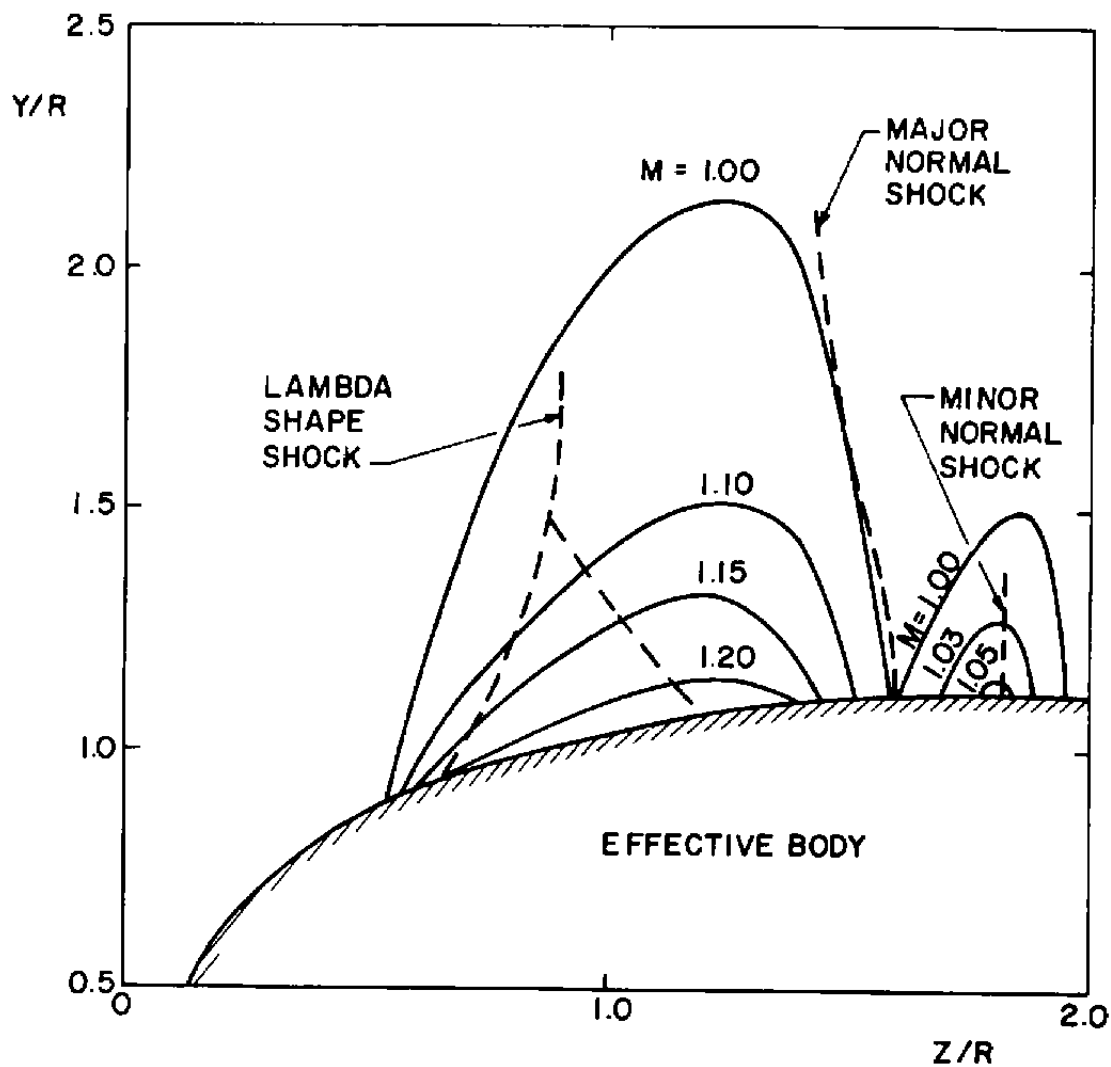
a. Mach number

Figure 10. Mach number and pressure distribution in the external
flow field of the effective body.
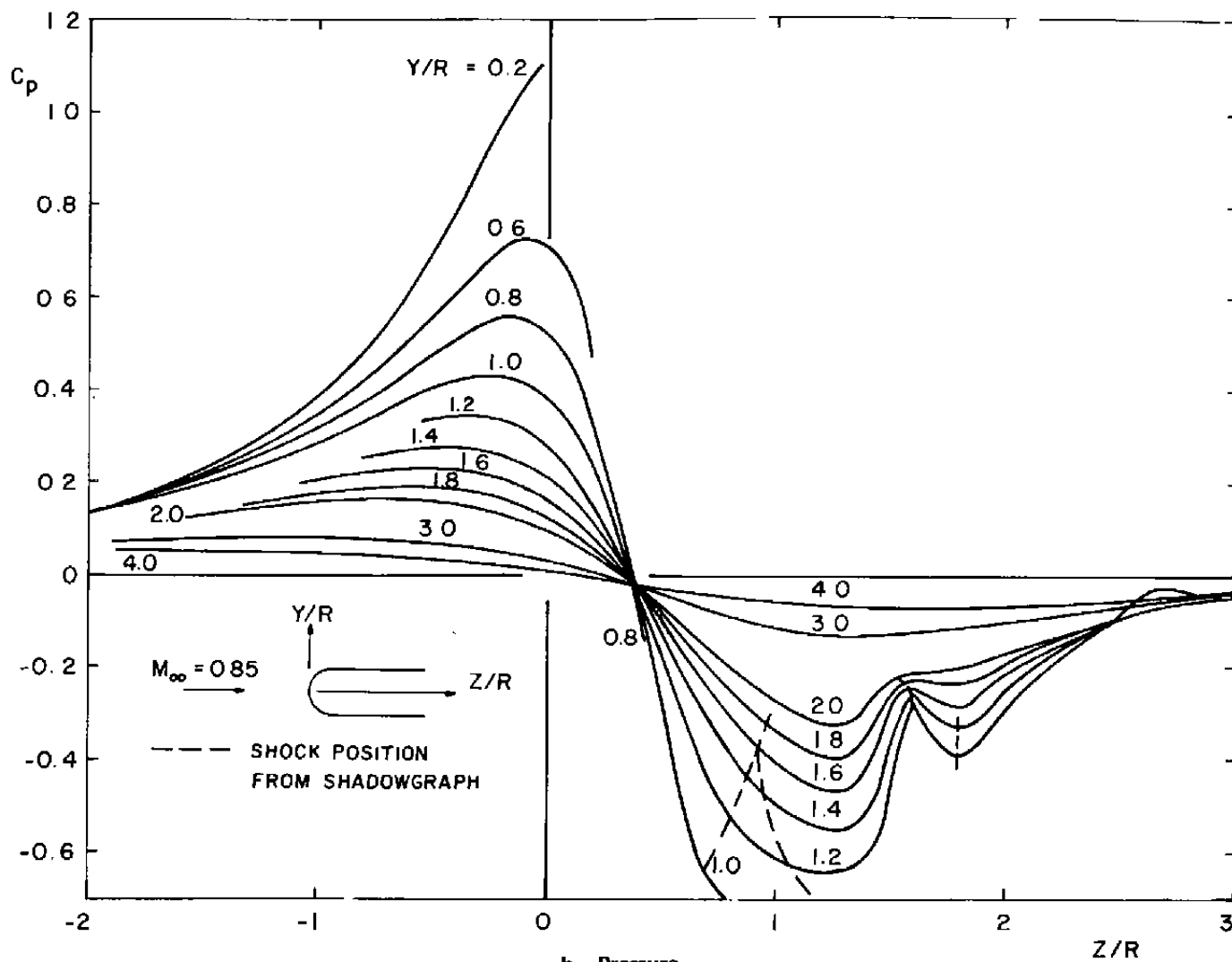
b. Pressure
Figure 10. Concluded.
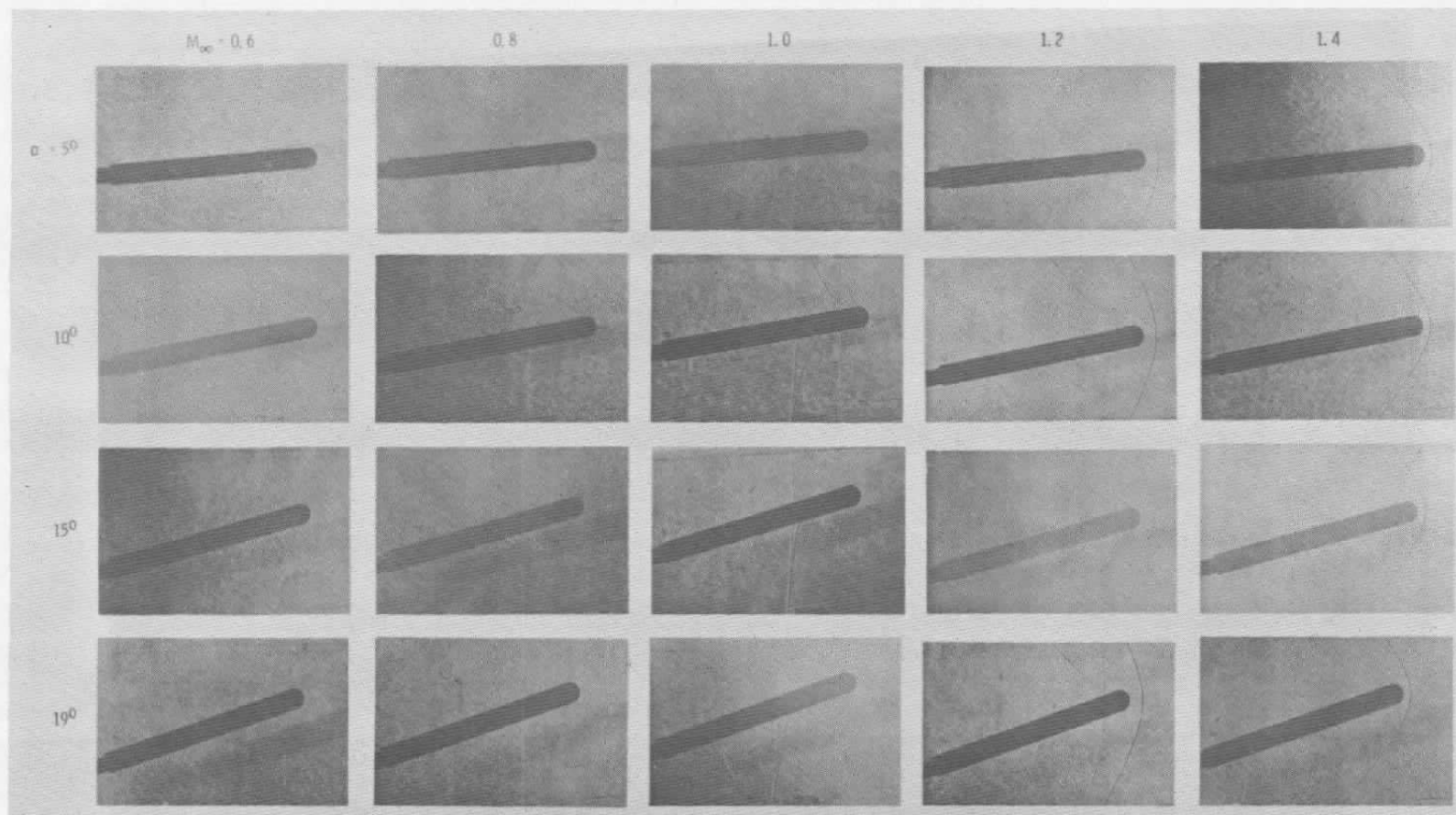
Figure 11. Shadowgraphs for flow past hemisphere-cylinder at incidence.
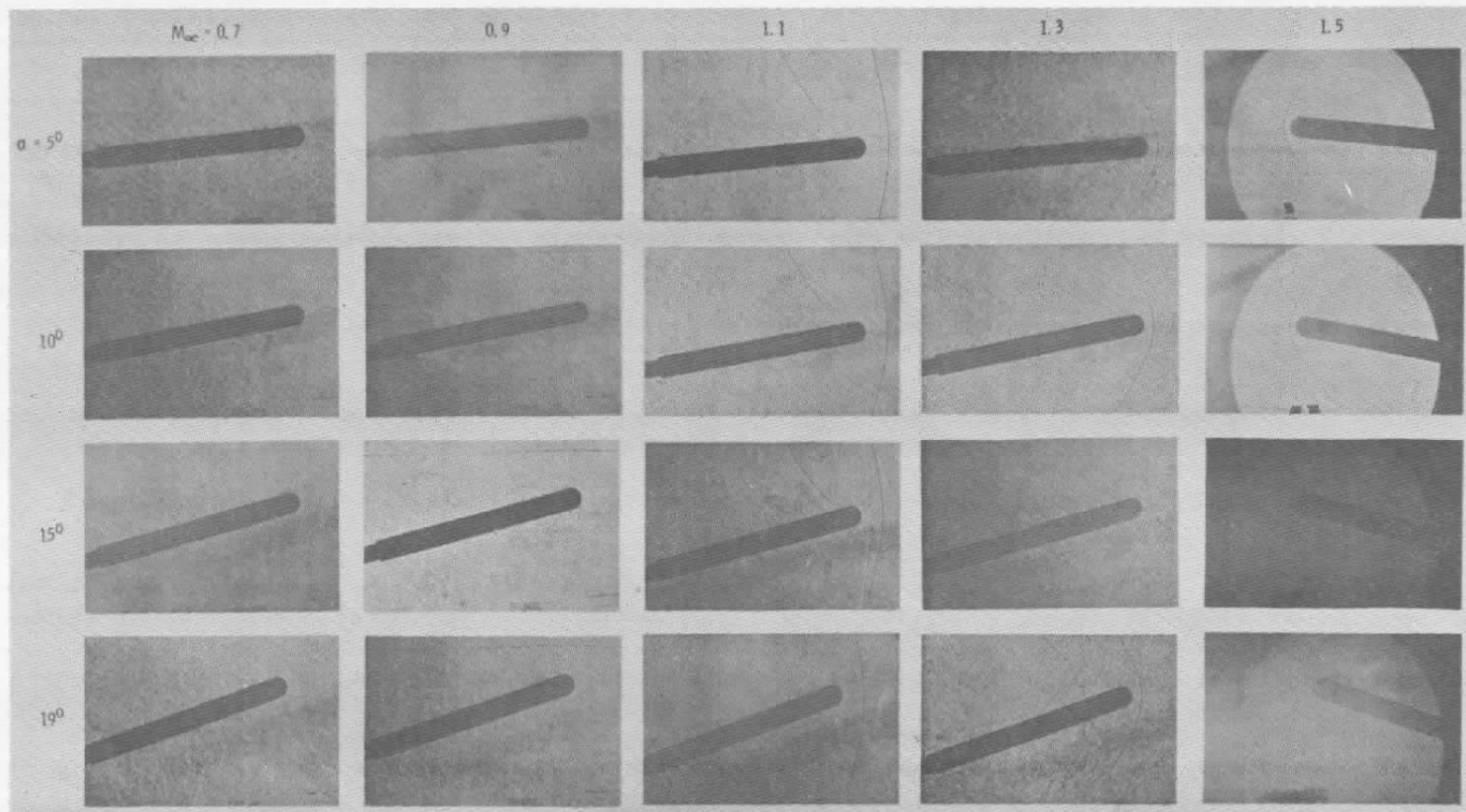
Figure 11. Concluded.
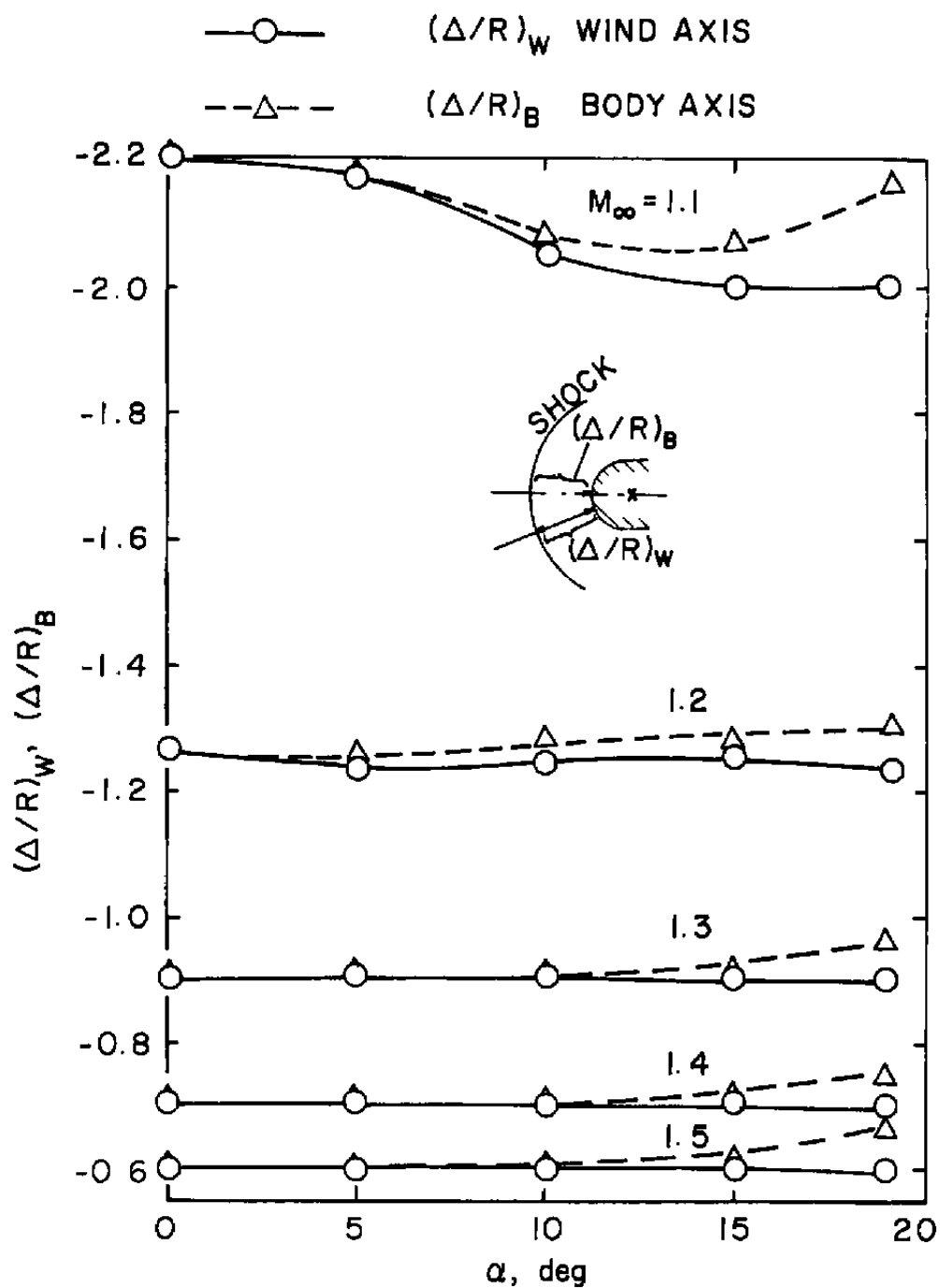
Figure 12. Shock standoff distance about hemisphere-cylinder at
incidence from shadowgraphs.
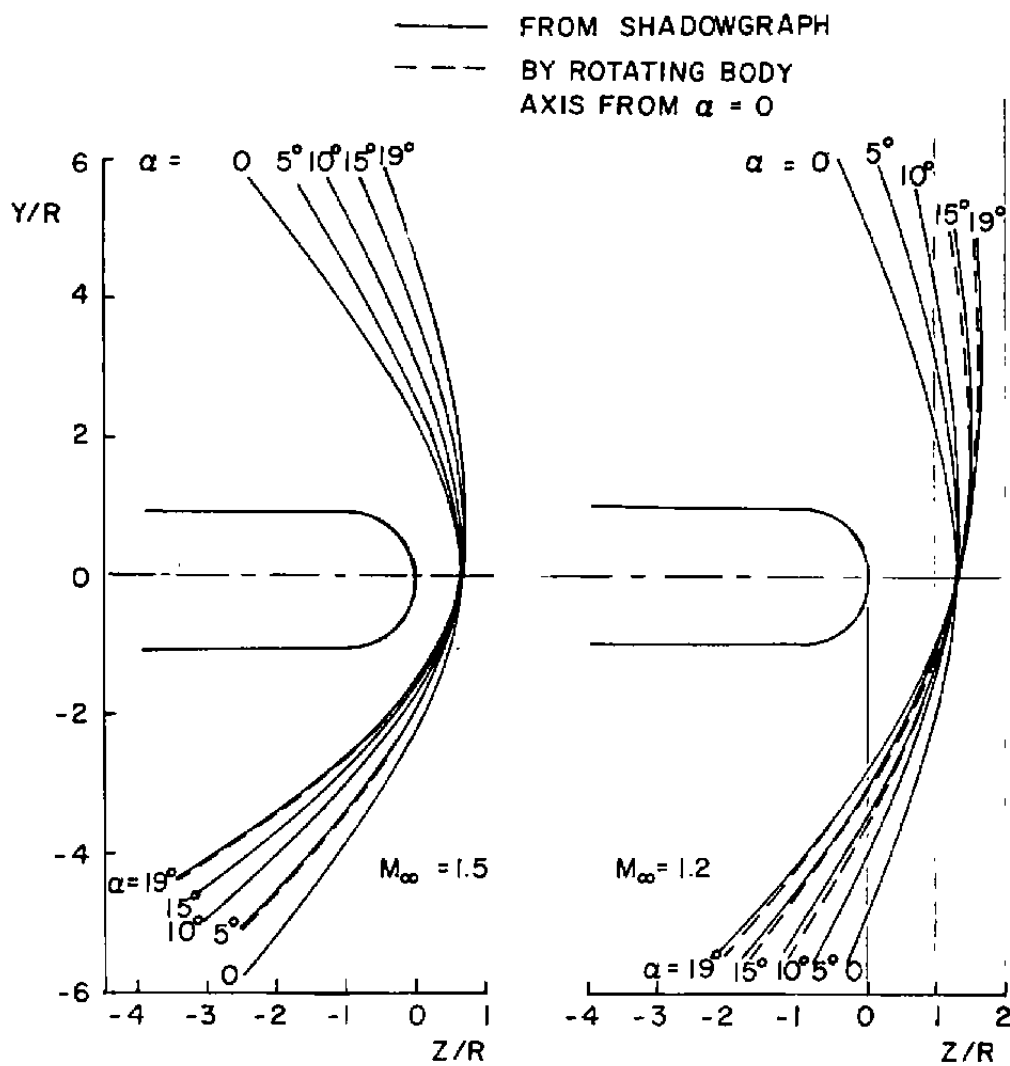
Figure 13. Shock positions for hemisphere-cylinder at various incidences.

(1) Nose
Separation
Line

(2) Concentrated
Vortex

(3) Secondary
Separation
Line
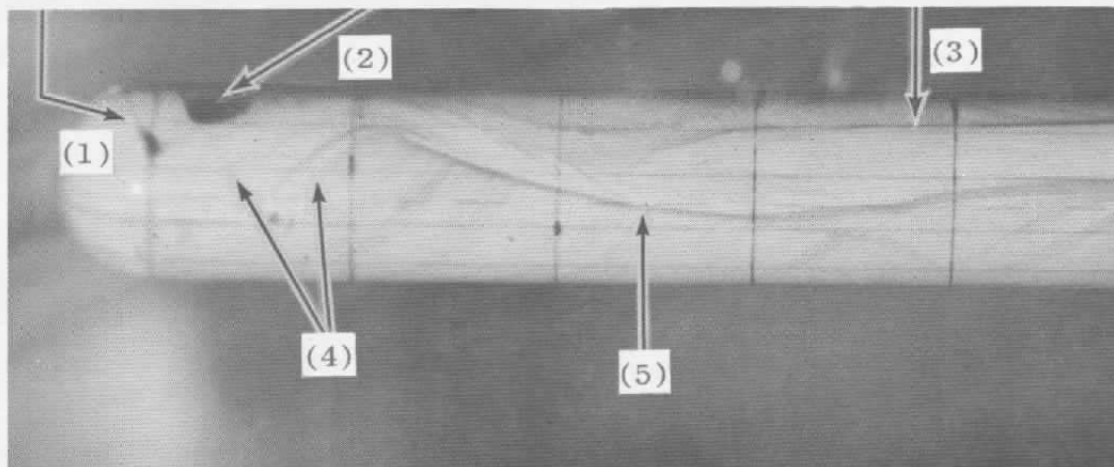
(4) Limiting Streamline of
Open-Type Separation

(5) Primary Separation Line

$$\alpha = 19$$
$$M_\infty = 1.2$$

a. Different features of separation
Figure 14. Oil flow pictures showing the surface flow pattern
about hemisphere-cylinder.
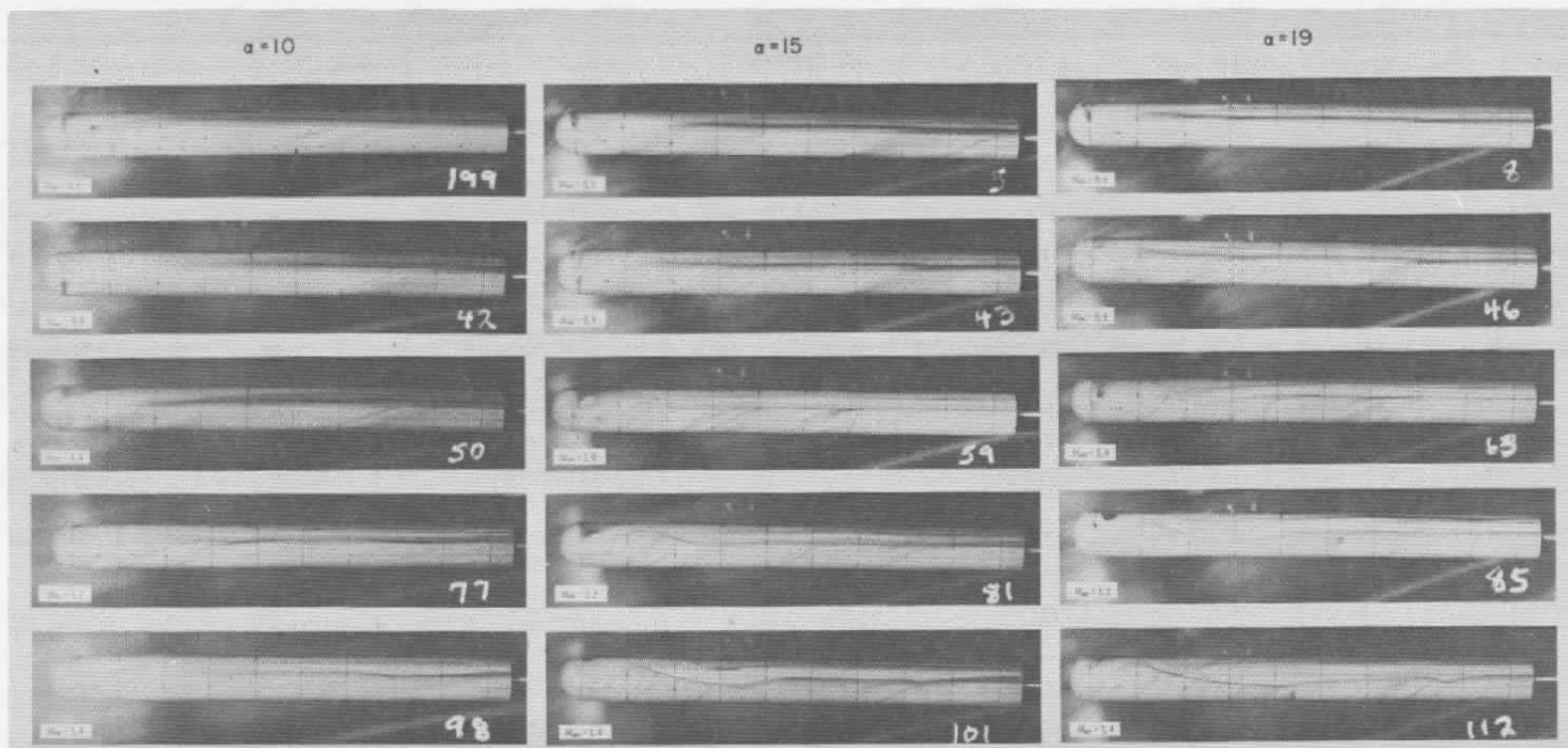
b. Various cases of separation
Figure 14. Concluded.

a. Region I and II

b. Separation II in plane of symmetry

c. Separation I in crossflow plane

d. Bubble flow pattern

e. Separation line I and II
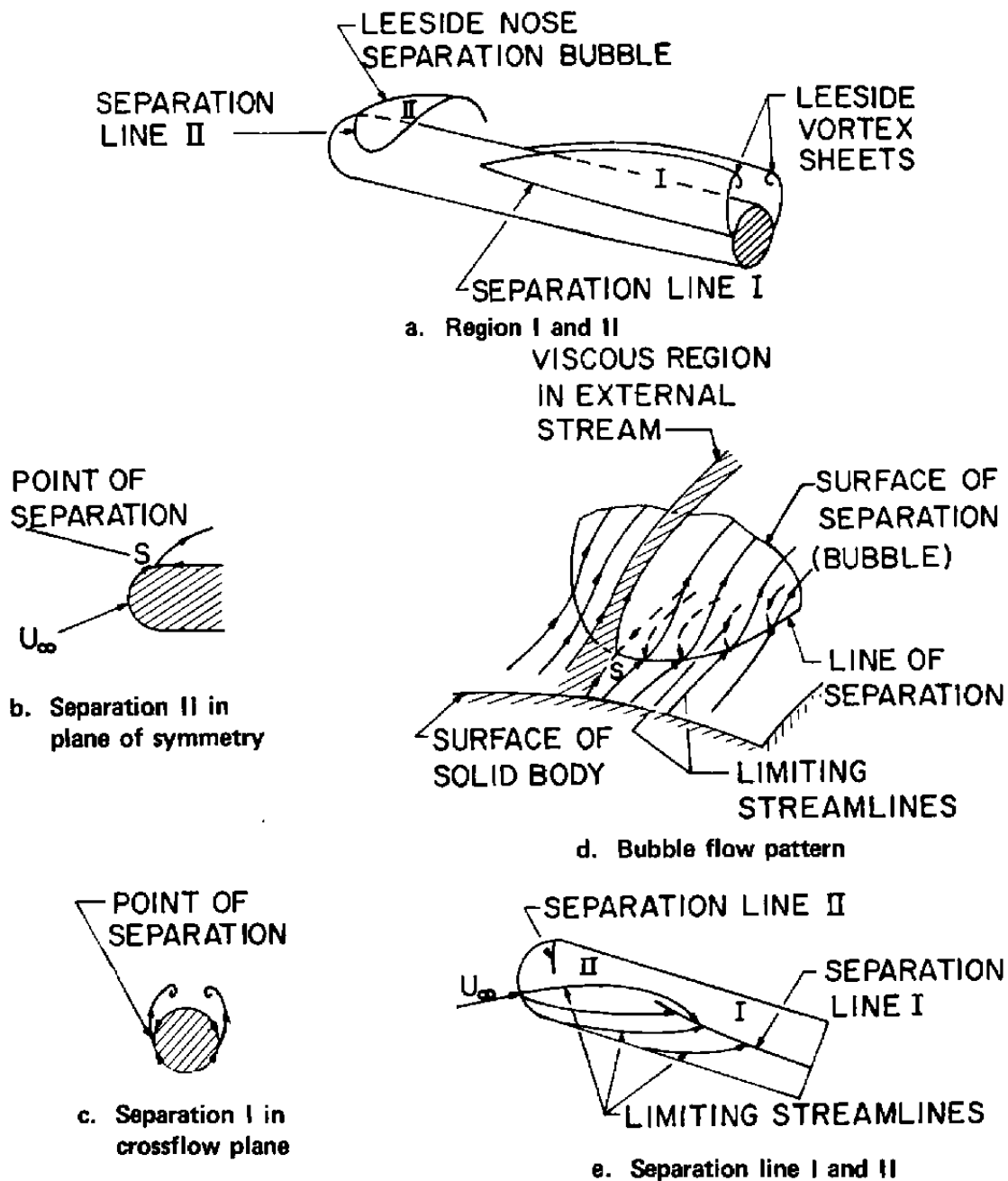
Figure 15. Description of separation regions I and II.

a. $\alpha = 0$

c. Intermediate incidence

b. Low incidence

d. High incidence

e. Leeside flow field with the presence of concentrated vortex tubes
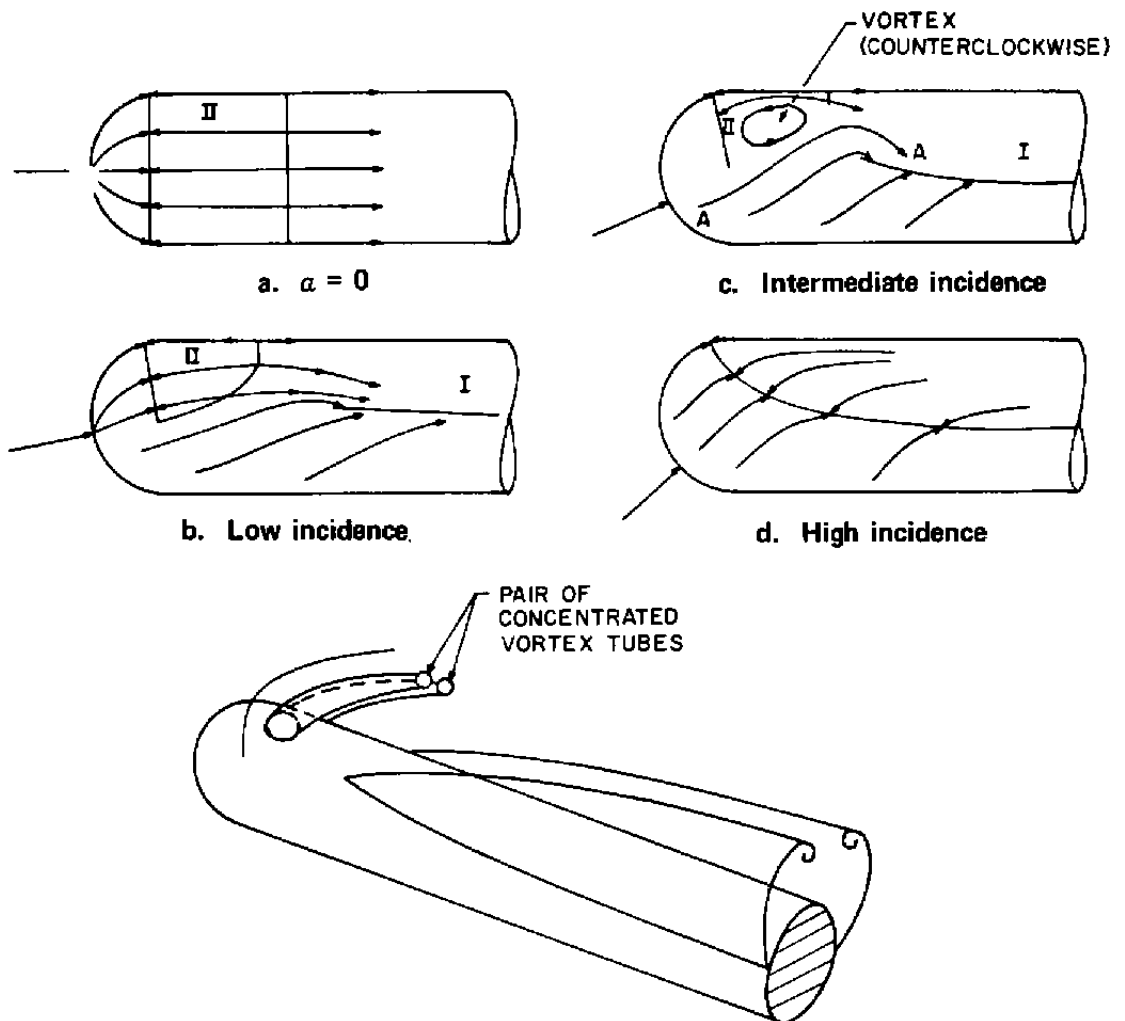
Figure 16. Mechanism and condition for the formation of the concentrated vortex.

SEPARATION LINE Ⅱ

SEPARATION
LINE Ⅲ

HIGH SURFACE SHEAR REGION

SEPARATION LINE Ⅰ

V_1

V_2

V_3

S_2

S_1
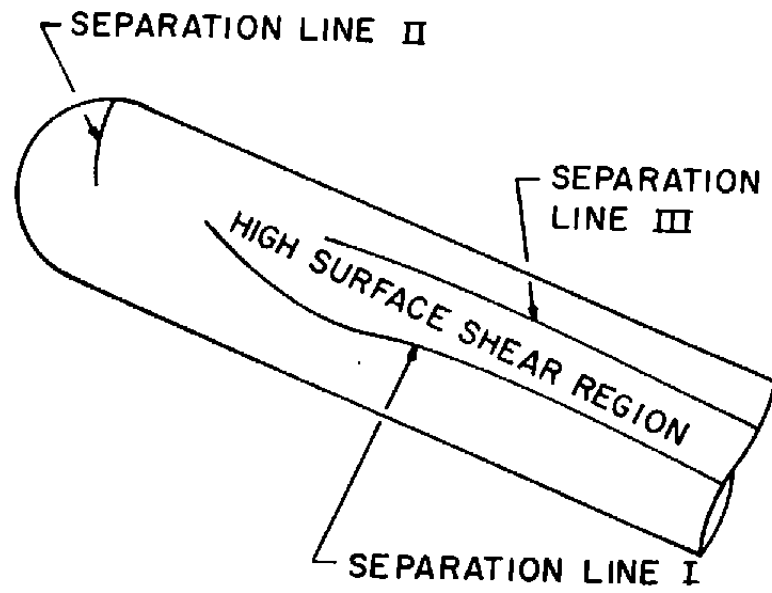
a. Separation lines
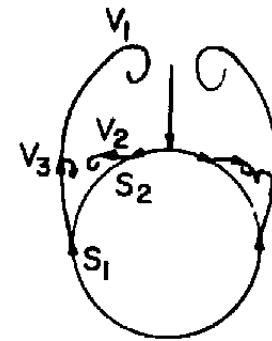
b. Cross-sectional view

Figure 17. Flow with secondary separation in the crossflow plane.
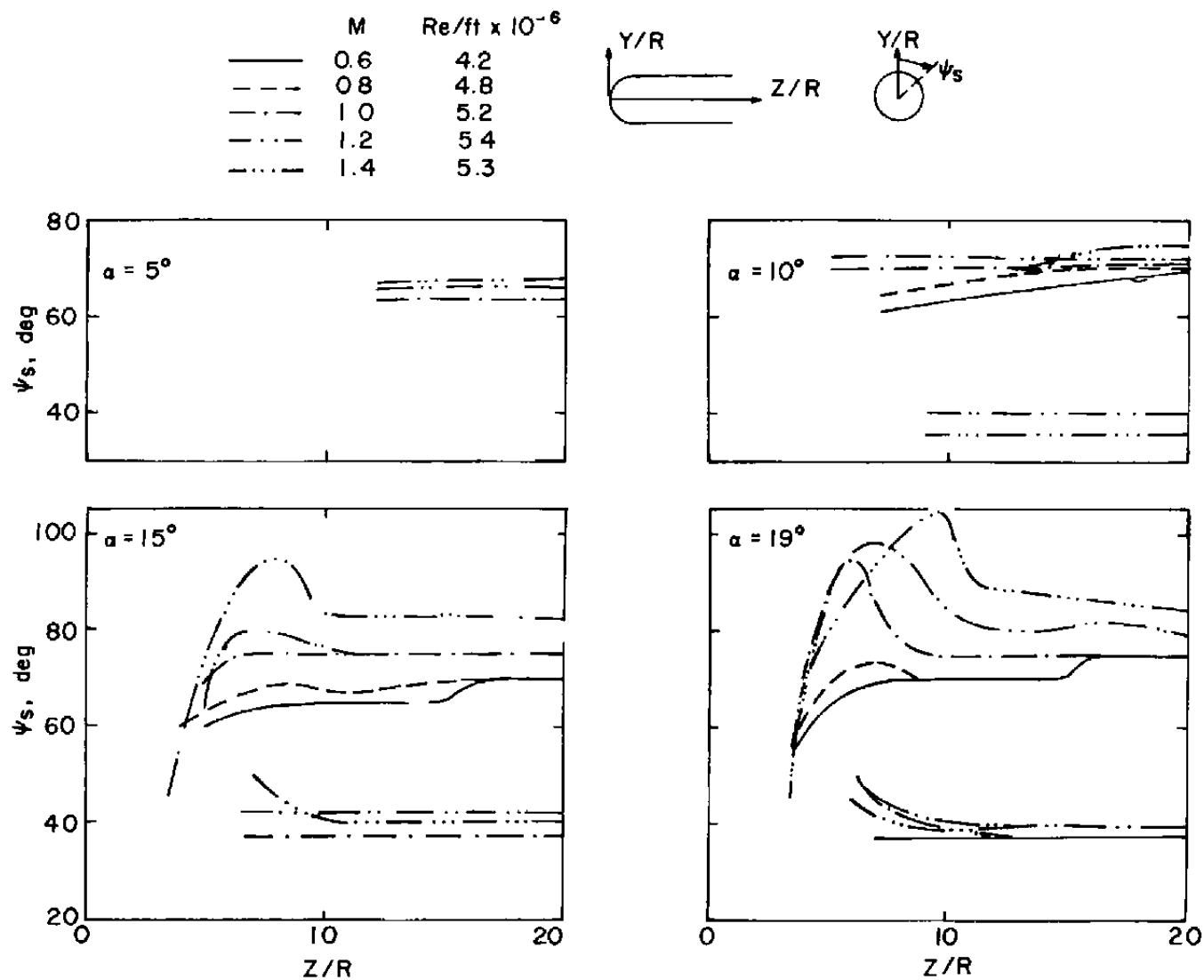
Figure 18. Separation angle as a function of Z/R, Mach number, and angle of attack for hemisphere-cylinder.

PROBE
VOLUME

BODY
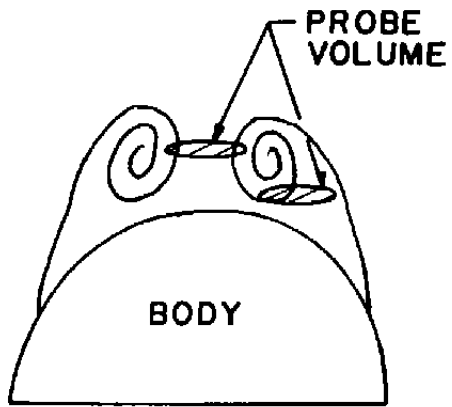
a. Probe volume and
   vortex size

1 BRIGHT
2 BRIGHTER
3 NOTHING
4 BRIGHTEST
5 NOT SO BRIGHT

1 2 3 4 5 4 3 2 1

LASER
BEAM

BODY
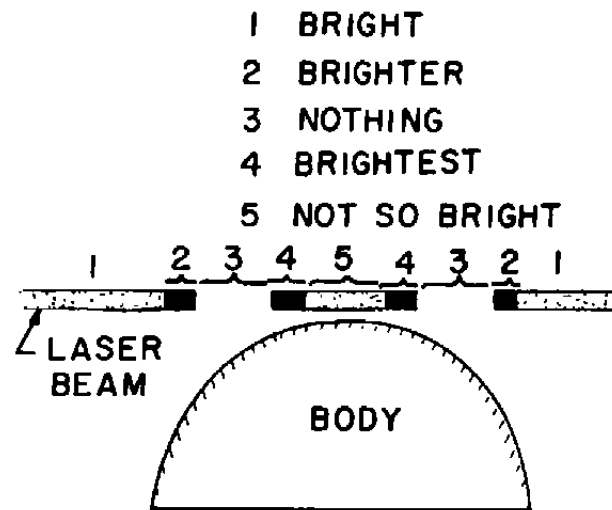
b. Laser beam over
   vortex wake

Figure 19. Relative length of probe volume to the vortex size
and laser beam over vortex wake.
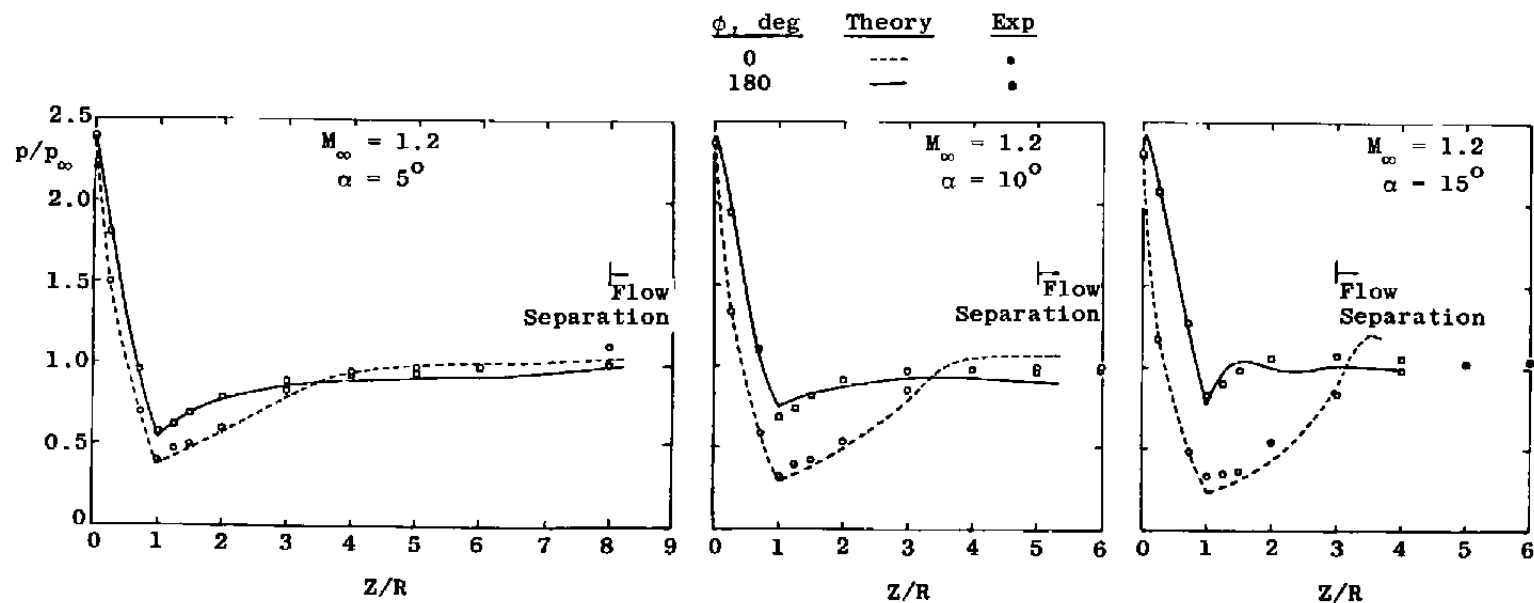
a. ϕ = 0 and 180 deg

Figure 20. Comparison of surface pressure between theory and
experiments at M_∞ = 1.2.
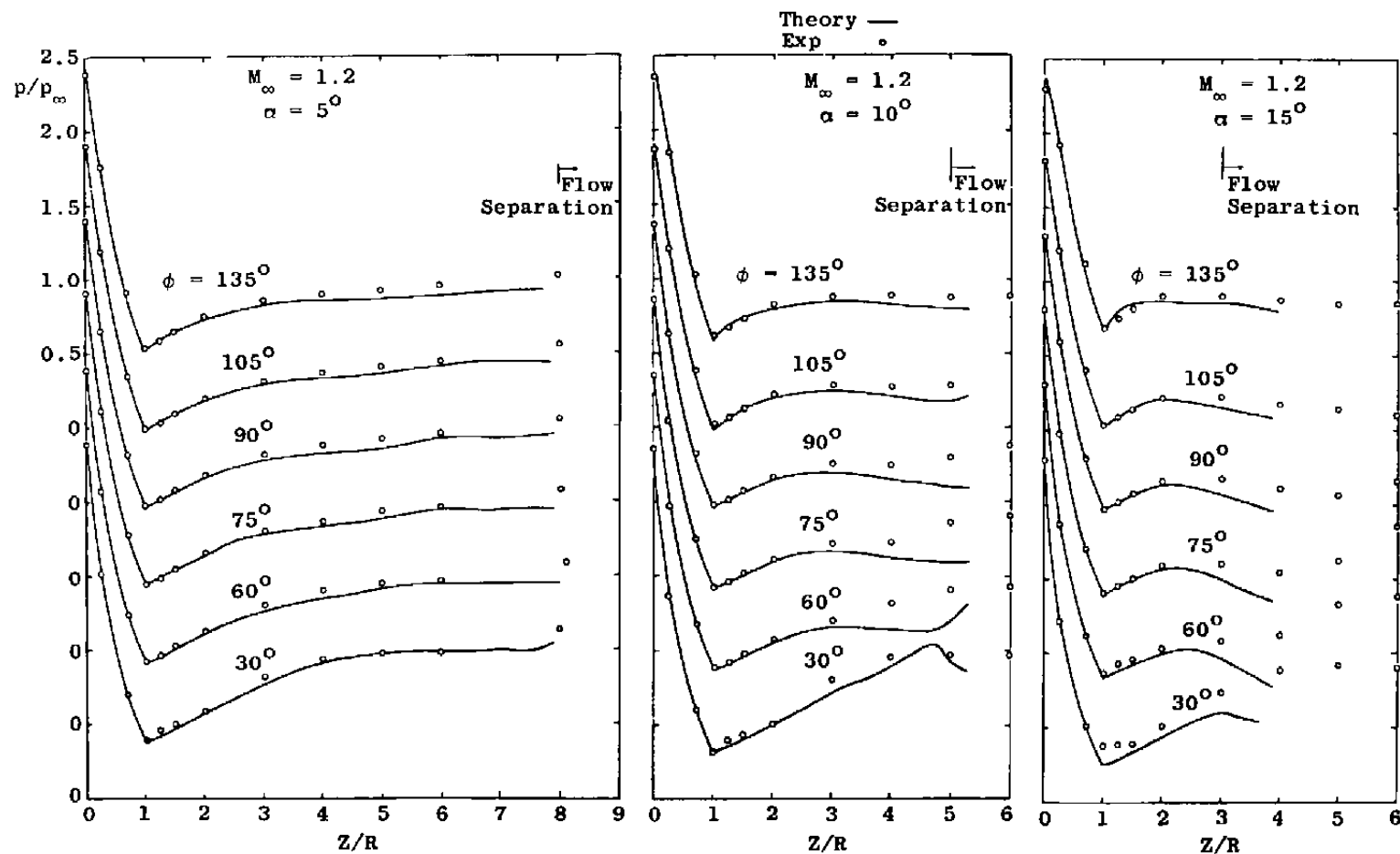
b. ϕ = 30 to 135 deg
Figure 20. Concluded.
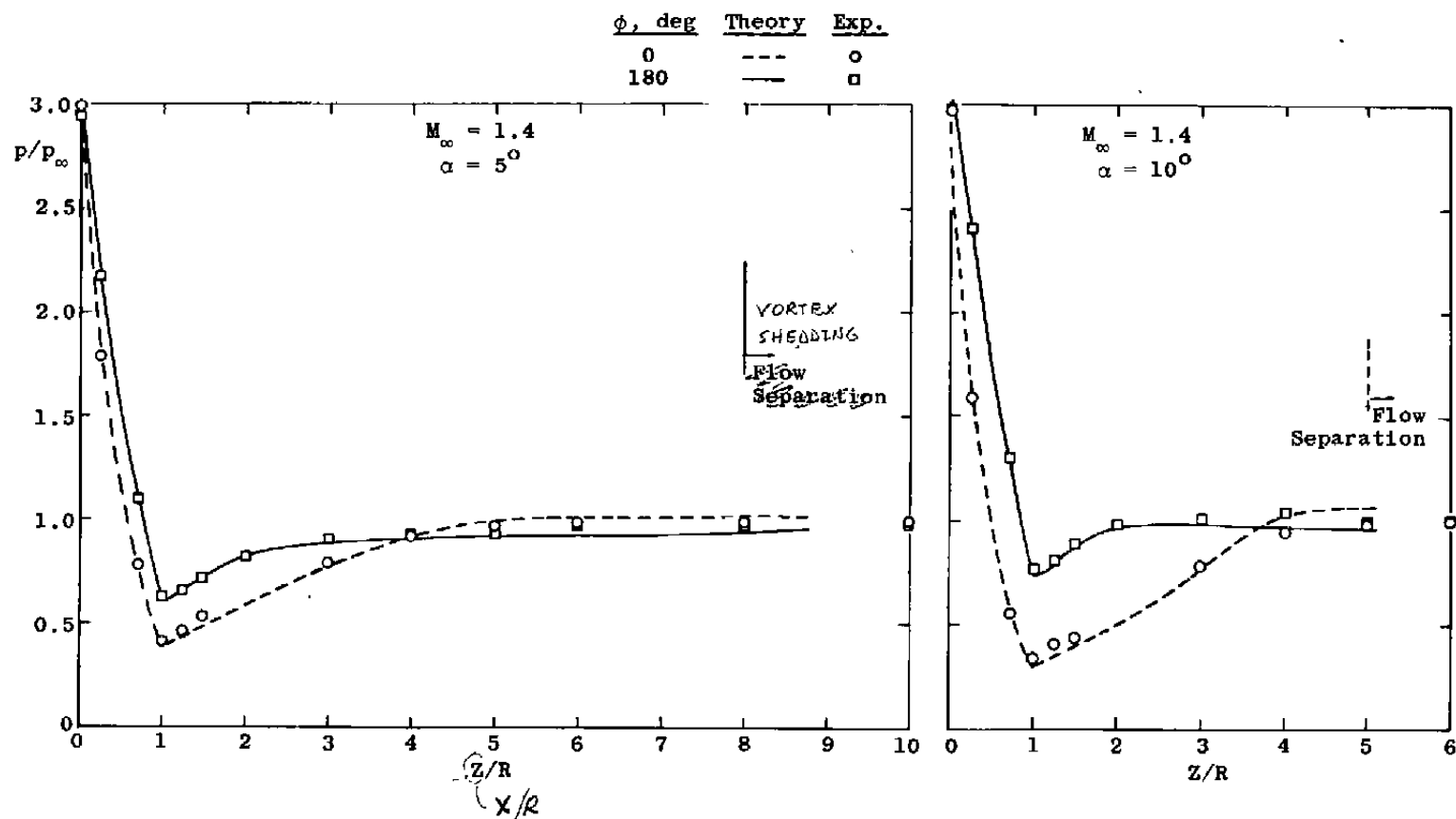
a. $\phi = 0$ and 180 deg

Figure 21. Comparison of surface pressure between theory and
experiments at $M_\infty = 1.4$.
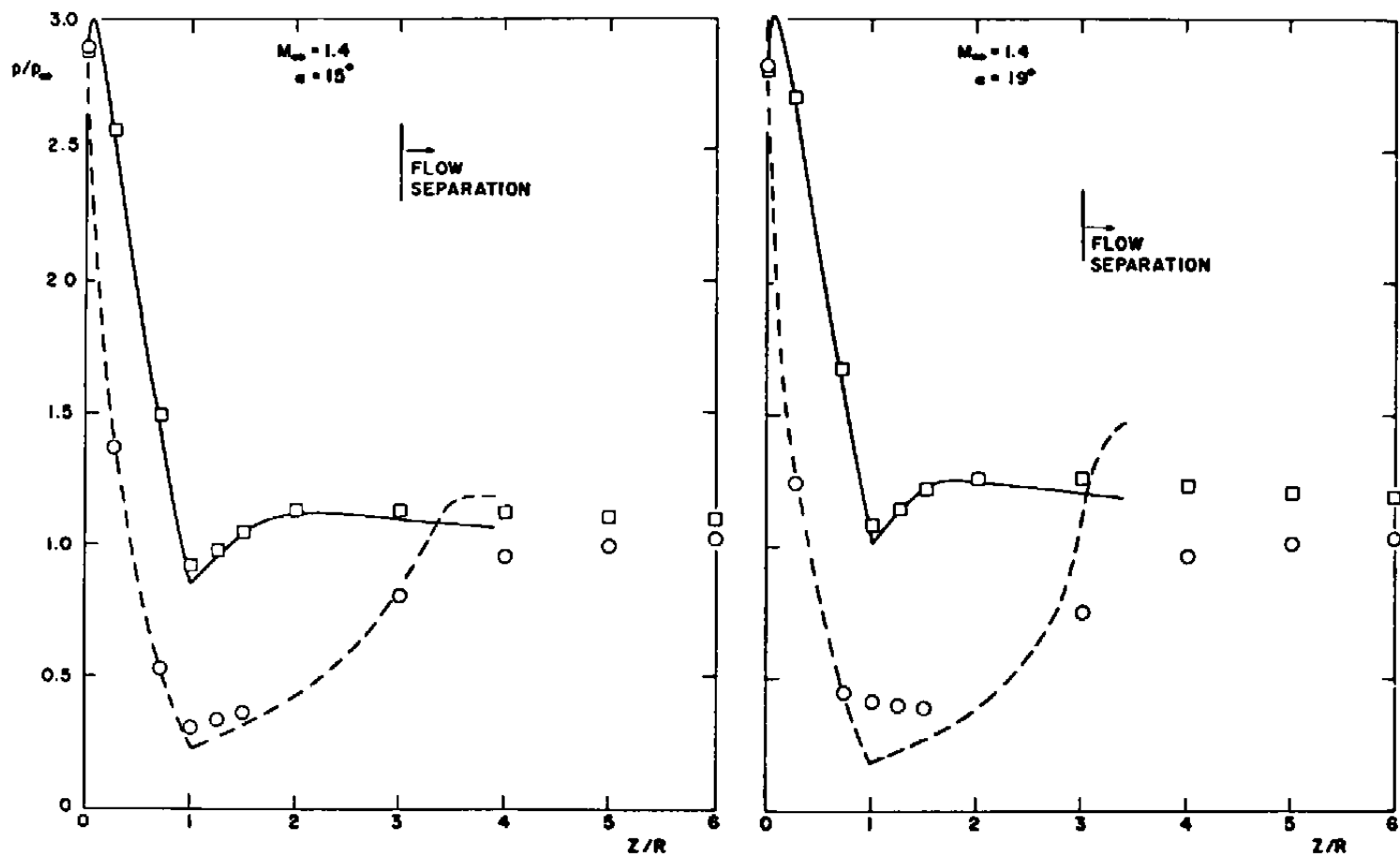
b. $\phi = 0$ and 180 deg
Figure 21. Continued.
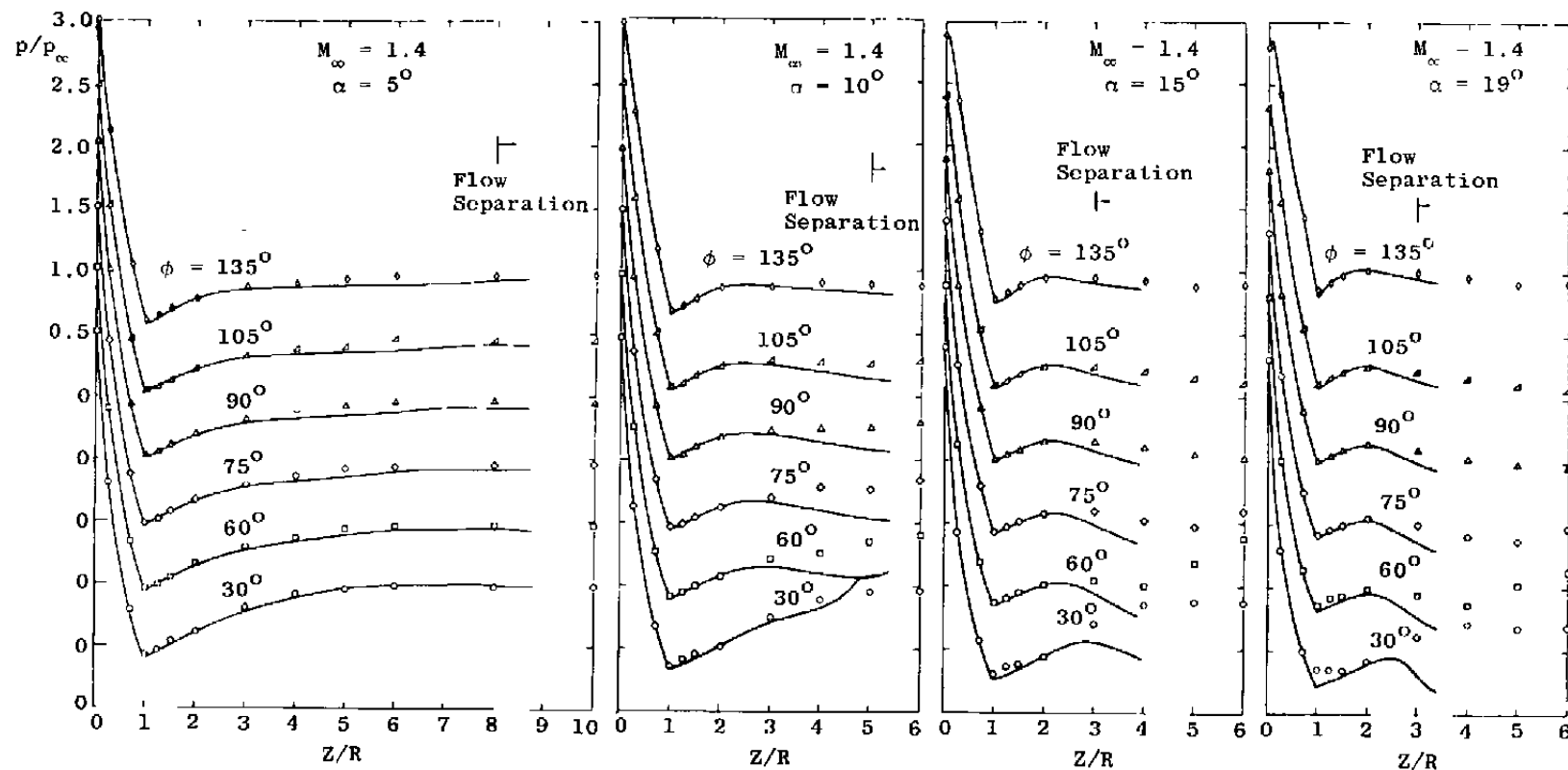
c. ϕ = 30 to 135 deg
Figure 21. Concluded.
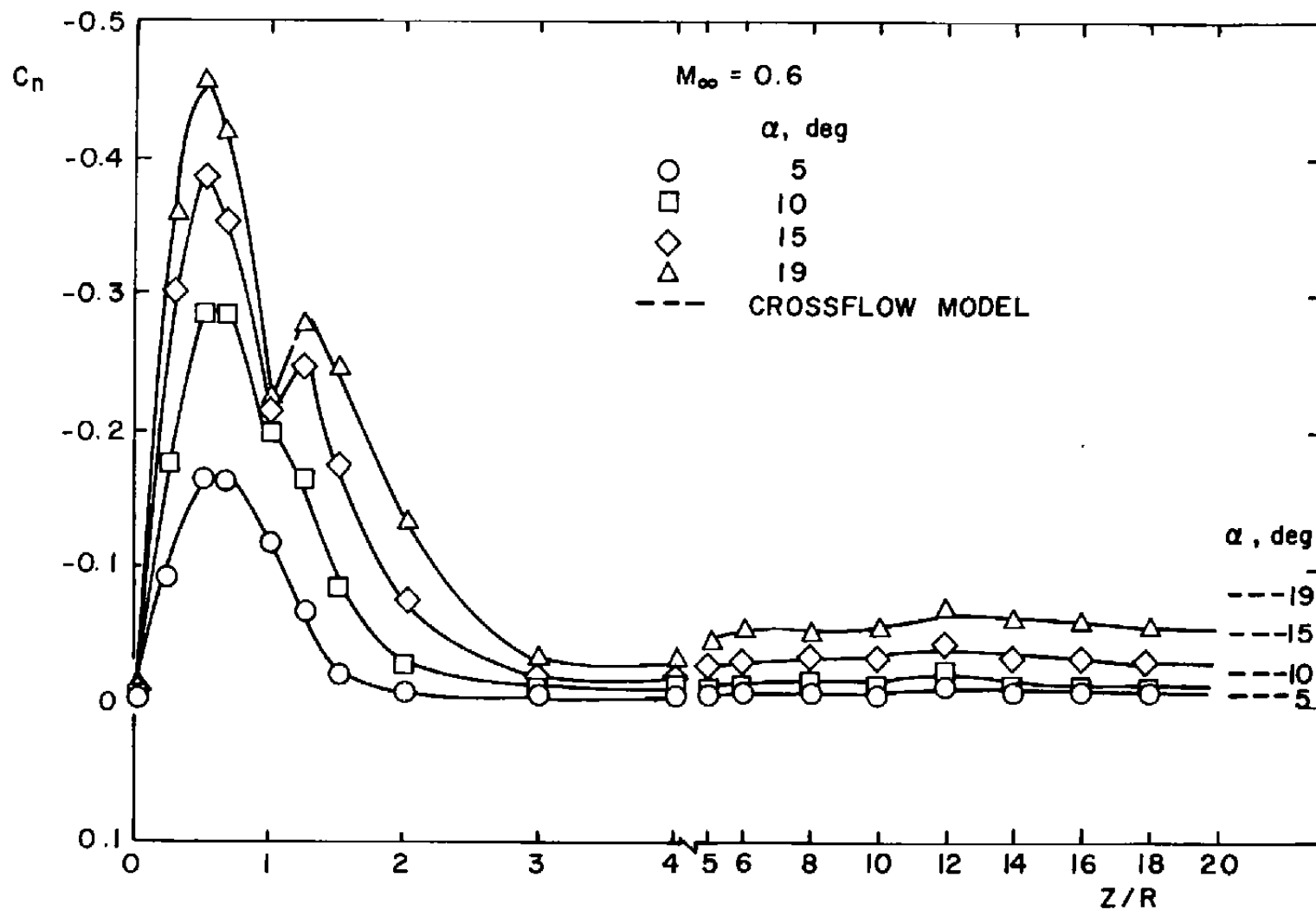
a. $M_\infty = 0.6$

Figure 22. Normal-force distribution over hemisphere-cylinder.
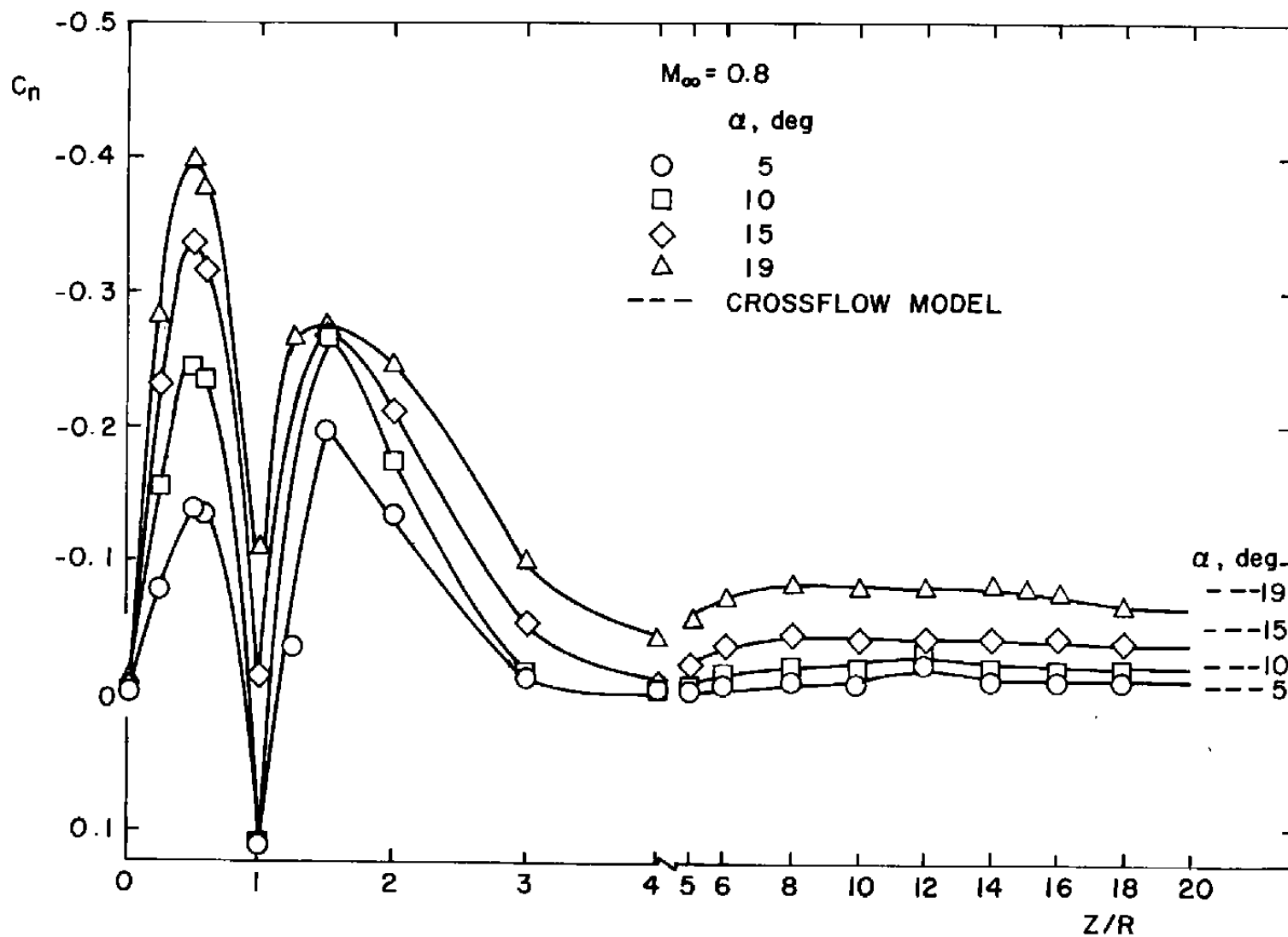
b. $M_\infty = 0.8$
Figure 22. Continued.
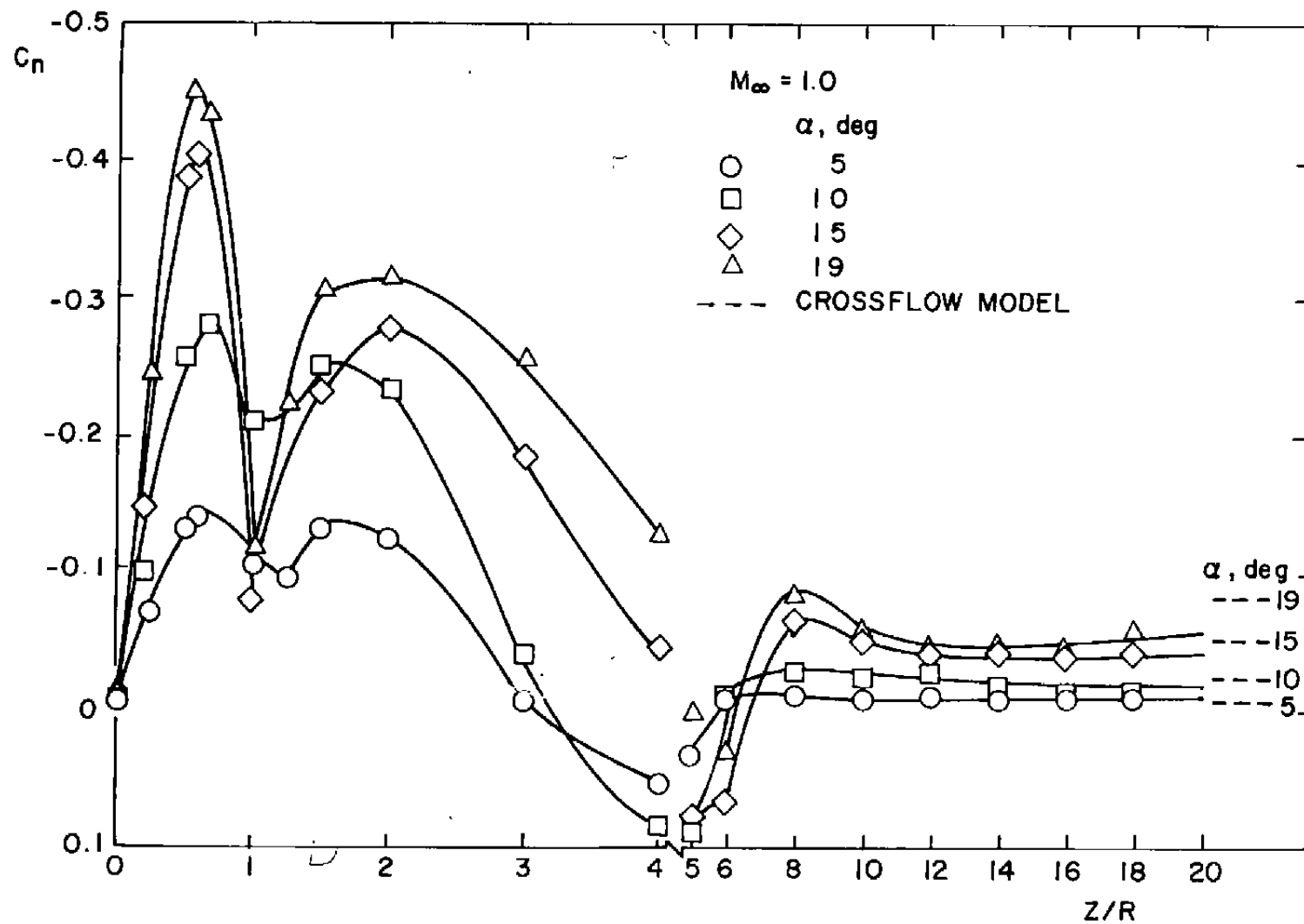
c. $M_\infty = 1.0$
Figure 22. Continued.
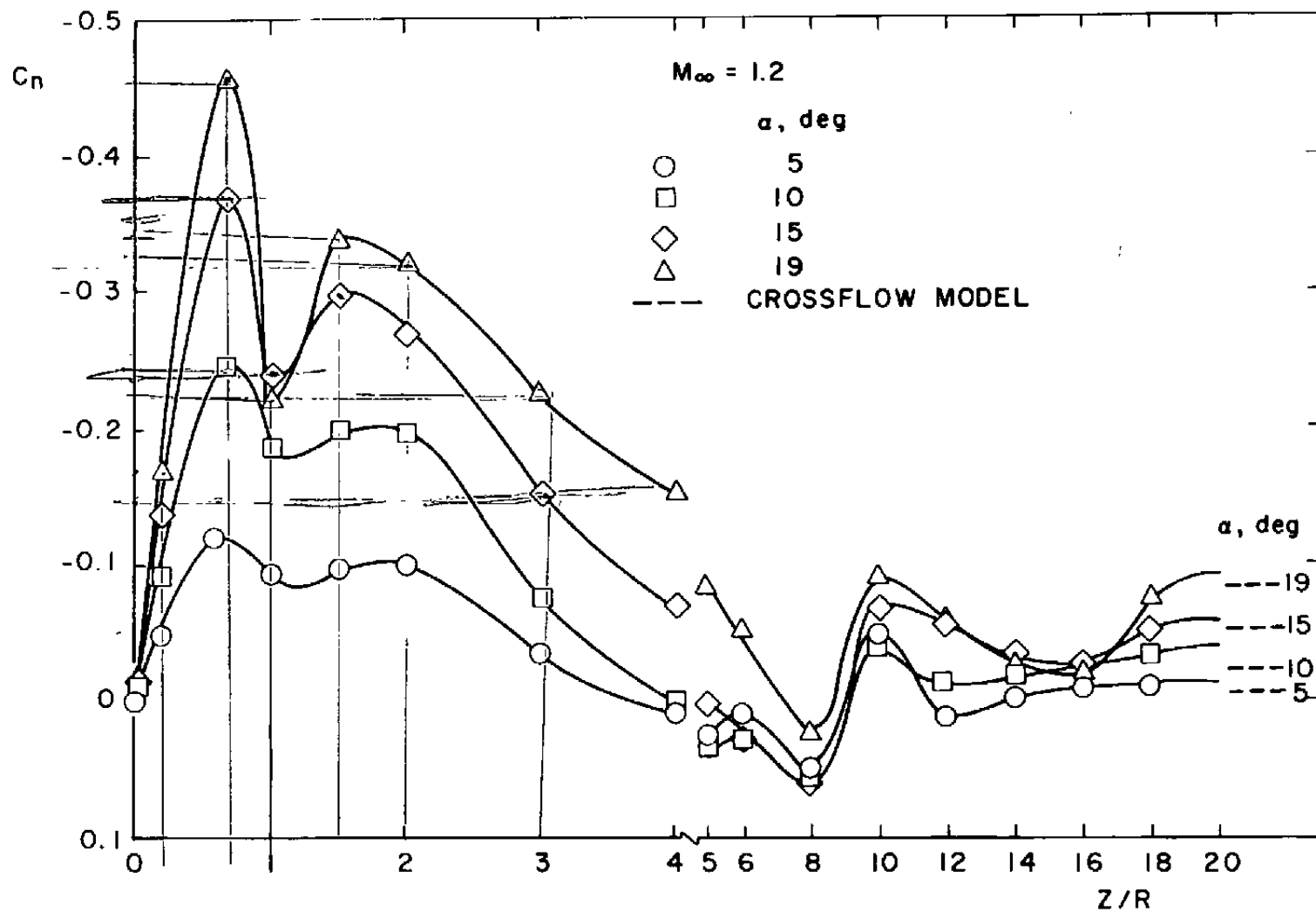
d. $M_\infty = 1.2$

Figure 22. Continued.

e. $M_\infty = 1.4$
Figure 22. Concluded.

C_N

$M_\infty=1.4$

0.6

2.5

2.0

1.5

1.0

0.5

0

0 5 10 15 20

	EXP.	(ANDERSON	THEORY
M_∞	(PRESENT)	& HENSON)	
0.6	△	▲	△
0.8	○	●	○
1.0	□	■	□
1.2	◇	◆	◇
1.4	◠		◠
INCOMPRESSIBLE (SCHINDEL)	◇		

— ⌉ CROSSFLOW
-- ⌋ MODEL

C_A

0.8

0.6

0.4

0.2

0

0 5 10 15 20

α, deg

$(Z/R)_{c.p.}$

.8

$M_\infty=1.4$

0.6

6

4

2

0

0 5 10 15 20

AEDC-TR-76-112
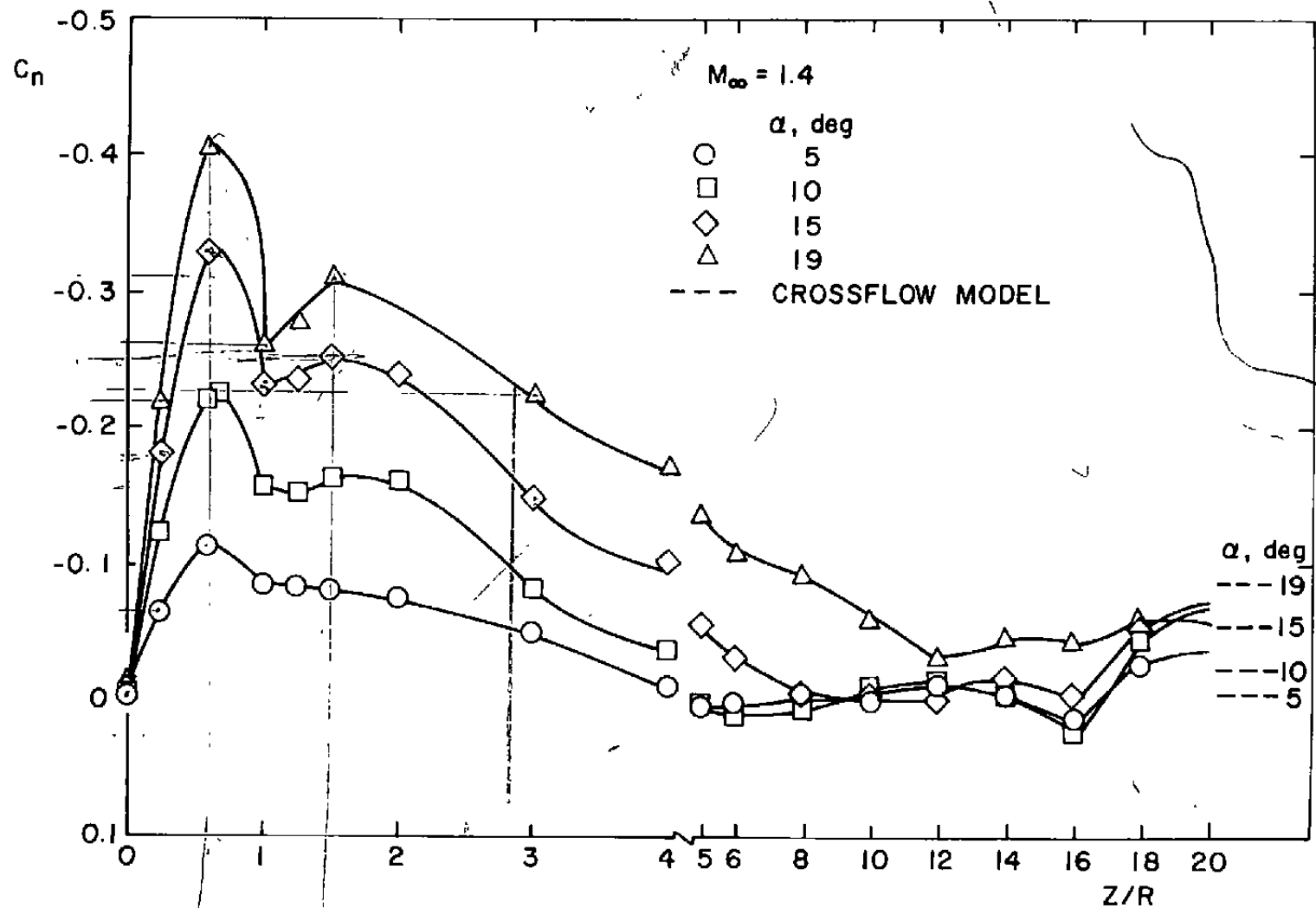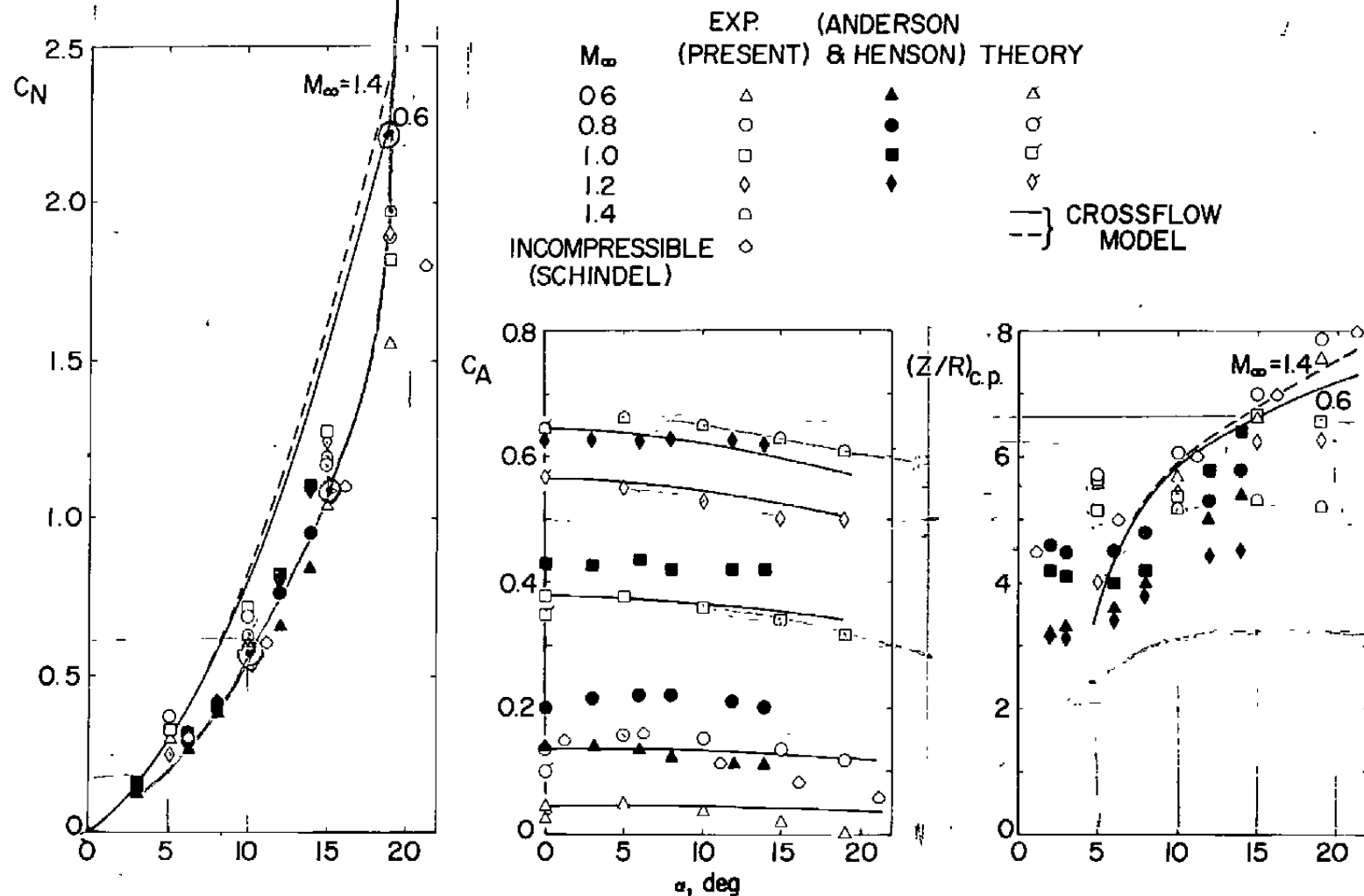
Figure 23. Total normal-force and axial-force coefficients and
center of pressure as a function of incidence.

APPENDIX A
EXPERIMENTAL SURFACE PRESSURE DISTRIBUTION

The results of surface pressure distribution for all cases measured are shown in Fig. A-1 and are preceded by this list of the C_p and p/p_∞ values.

FREESTREAM MACH NO. =0.600   INCIDENCE= 5.00DEG

NO.	PHI=0. CP	P/PF	PHI=30. CP	P/PF	PHI=60. CP	P/PF	PHI=75. CP	P/PF	PHI=90. CP	P/PF	PHI=105. CP	P/PF	PHI=135. CP	P/PF	PHI=180. CP	P/PF
2	1.0891	1.274	1.0860	1.274	1.0877	1.274	1.0838	1.273	1.0849	1.273	1.0829	1.273	1.0817	1.273	1.0841	1.273
3	-0.0954	0.976	-0.0683	0.983	0.0117	1.003	0.0635	1.016	0.1221	1.031	0.1760	1.044	0.2842	1.072	0.3564	1.090
4	-0.9857	0.752	-0.9686	0.756	-0.9357	0.764	-0.8834	0.777	-0.8497	0.786	-0.8062	0.797	-0.7075	0.822	-0.6434	0.838
5	-0.8141	0.795	-0.8026	0.798	-0.7824	0.803	-0.7541	0.810	-0.7247	0.817	-0.7021	0.823	-0.6271	0.842	-0.5800	0.854
6	-0.3694	0.907	-0.3681	0.907	-0.3353	0.916	-0.3095	0.922	-0.3104	0.922	-0.2891	0.927	-0.2542	0.936	-0.2419	0.939
7	-0.1821	0.954	-0.1838	0.954	-0.1857	0.953	-0.1840	0.954	-0.1790	0.955	-0.1784	0.955	-0.1534	0.961	-0.1389	0.965
8	-0.0922	0.977	-0.1022	0.974	-0.1150	0.971	-0.1142	0.971	-0.1188	0.970	-0.1123	0.972	-0.0951	0.976	-0.0783	0.980
9	-0.0345	0.991	-0.0334	0.992	-0.0553	0.986	-0.0593	0.985	-0.0604	0.985	-0.0621	0.984	-0.0396	0.990	-0.0158	0.996
10	-0.0164	0.996	-0.0230	0.994	-0.0351	0.991	-0.0417	0.989	-0.0385	0.990	-0.0435	0.989	-0.0223	0.994	-0.0020	0.999
11	-0.0102	0.997	-0.0157	0.996	-0.0277	0.993	-0.0317	0.992	-0.0354	0.991	-0.0342	0.991	-0.0155	0.996	0.0041	1.001
12	-0.0004	1.000	-0.0047	0.999	-0.0167	0.996	-0.0181	0.995	-0.0208	0.995	-0.0212	0.995	-0.0032	0.999	0.0145	1.004
13	0.0014	1.000	-0.0035	0.999	-0.0118	0.997	-0.0162	0.996	-0.0178	0.996	-0.0206	0.995	0.0023	1.001	0.0194	1.005
14	-0.0035	0.999	-0.0108	0.997	-0.0180	0.995	-0.0231	0.994	-0.0239	0.994	-0.0268	0.993	-0.0069	0.998	0.0096	1.002
15	-0.0244	0.994	-0.0078	0.998	-0.0124	0.997	-0.0156	0.996	-0.0160	0.996	-0.0187	0.995	0.0005	1.000	0.0164	1.004
16	-0.0053	0.999	-0.0102	0.997	-0.0137	0.997	-0.0144	0.996	-0.0160	0.996	-0.0187	0.995	-0.0020	0.999	0.0102	1.003
17	-0.0047	0.999	-0.0145	0.996	-0.0173	0.996	-0.0181	0.995	-0.0196	0.995	-0.0224	0.994	-0.0069	0.998	0.0109	1.003
18	-0.0102	0.997	-0.0230	0.994	-0.0253	0.994	-0.0262	0.993	-0.0275	0.993	-0.0280	0.993	-0.0143	0.996	0.0047	1.001

FREESTREAM MACH NO.=0.600   INCIDENCE= 10.00DEG

NO.	PHI=0.		PHI=30.		PHI=60.		PHI=75.		PHI=90.		PHI=105.		PHI=135.		PHI=180.	
	CP	P/PF	CP	P/PF	CP	P/PF	CP	P/PF	CP	P/PF	CP	P/PF	CP	P/PF	CP	P/PF
2	1.0443	1.263	1.0414	1.262	1.0412	1.262	1.0395	1.262	1.0360	1.261	1.0373	1.261	1.0365	1.261	1.0347	1.261
3	-0.3148	0.921	-0.2565	0.935	-0.1202	0.970	-0.0233	0.994	0.0903	1.023	0.1958	1.049	0.4079	1.103	0.5430	1.137
4	-0.9756	0.754	-0.9837	0.752	-0.9866	0.751	-0.9199	0.768	-0.8482	0.786	-0.7494	0.811	-0.5784	0.854	-0.4359	0.890
5	-0.8338	0.790	-0.8493	0.786	-0.8263	0.792	-0.7826	0.803	-0.7219	0.818	-0.7031	0.823	-0.5583	0.859	-0.4386	0.889
6	-0.5025	0.873	-0.4811	0.879	-0.4364	0.890	-0.3810	0.904	-0.3497	0.912	-0.3170	0.920	-0.2234	0.944	-0.1763	0.956
7	-0.2709	0.932	-0.2841	0.928	-0.2502	0.937	-0.2447	0.938	-0.2354	0.941	-0.2236	0.944	-0.1538	0.961	-0.0909	0.977
8	-0.1187	0.970	-0.1184	0.970	-0.1700	0.957	-0.1802	0.955	-0.1850	0.953	-0.1699	0.957	-0.1099	0.972	-0.0432	0.989
9	-0.0229	0.994	-0.0310	0.992	-0.0999	0.975	-0.1233	0.969	-0.1183	0.970	-0.1180	0.970	-0.0559	0.986	0.0155	1.004
10	-0.0098	0.998	-0.0233	0.994	-0.0741	0.981	-0.0981	0.975	-0.0979	0.975	-0.0980	0.975	-0.0367	0.991	0.0262	1.007
11	-0.0067	0.998	-0.0202	0.995	-0.0631	0.984	-0.0862	0.978	-0.0948	0.976	-0.0881	0.978	-0.0318	0.992	0.0317	1.008
12	0.0006	1.000	-0.0159	0.996	-0.0489	0.988	-0.0688	0.983	-0.0759	0.981	-0.0720	0.982	-0.0178	0.996	0.0427	1.011
13	0.0	1.000	-0.0233	0.994	-0.0385	0.990	-0.0626	0.984	-0.0710	0.982	-0.0702	0.982	-0.0117	0.997	0.0470	1.012
14	-0.0092	0.998	-0.0325	0.992	-0.0403	0.990	-0.0651	0.984	-0.0765	0.981	-0.0776	0.980	-0.0227	0.994	0.0354	1.009
15	-0.0354	0.991	-0.0276	0.993	-0.0330	0.992	-0.0538	0.986	-0.0643	0.984	-0.0677	0.983	-0.0135	0.997	0.0433	1.011
16	-0.0122	0.997	-0.0276	0.993	-0.0323	0.992	-0.0507	0.987	-0.0631	0.984	-0.0677	0.983	-0.0160	0.996	0.0354	1.009
17	-0.0110	0.997	-0.0294	0.993	-0.0348	0.991	-0.0501	0.987	-0.0655	0.983	-0.0696	0.982	-0.0215	0.995	0.0366	1.009
18	-0.0153	0.996	-0.0368	0.991	-0.0403	0.990	-0.0570	0.986	-0.0729	0.982	-0.0770	0.981	-0.0288	0.993	0.0311	1.008

FREESTREAM MACH NO.=0.600   INCIDENCE= 15.00DEG

NO.	PHI=0. CP	P/PF	PHI=30. CP	P/PF	PHI=60. CP	P/PF	PHI=75. CP	P/PF	PHI=90. CP	P/PF	PHI=105. CP	P/PF	PHI=135. CP	P/PF	PHI=180. CP	P/PF
2	0.9681	1.244	0.9627	1.243	0.9597	1.242	0.9568	1.241	0.9539	1.240	0.9535	1.240	0.9527	1.240	0.9510	1.240
3	-0.5226	0.868	-0.4534	0.886	-0.2491	0.937	-0.1223	0.969	0.0389	1.010	0.1919	1.048	0.5079	1.128	0.7151	1.180
4	-0.8629	0.783	-0.9505	0.760	-0.9818	0.753	-0.9599	0.758	-0.8566	0.784	-0.7176	0.819	-0.4349	0.890	-0.2242	0.944
5	-0.7069	0.822	-0.7711	0.806	-0.8154	0.795	-0.8039	0.797	-0.7490	0.811	-0.7176	0.819	-0.4833	0.878	-0.2820	0.929
6	-0.5883	0.852	-0.5752	0.855	-0.5318	0.866	-0.4427	0.888	-0.3808	0.904	-0.3470	0.913	-0.2092	0.947	-0.0920	0.977
7	-0.4140	0.896	-0.3884	0.902	-0.3653	0.908	-0.3554	0.910	-0.3412	0.914	-0.3054	0.923	-0.1599	0.960	-0.0231	0.994
8	-0.1648	0.958	-0.1706	0.957	-0.2807	0.929	-0.2922	0.926	-0.2961	0.925	-0.2647	0.933	-0.1307	0.967	0.0090	1.002
9	0.0038	1.001	-0.0351	0.991	-0.1701	0.957	-0.2254	0.943	-0.2317	0.942	-0.2157	0.946	-0.0823	0.979	0.0595	1.015
10	-0.0035	0.999	-0.0394	0.990	-0.1236	0.969	-0.1870	0.953	-0.1982	0.950	-0.1920	0.952	-0.0634	0.984	0.0684	1.017
11	-0.0071	0.998	-0.0565	0.986	-0.0994	0.975	-0.1653	0.958	-0.1890	0.952	-0.1784	0.955	-0.0591	0.985	0.0727	1.018
12	-0.0029	0.999	-0.0668	0.983	-0.0783	0.980	-0.1406	0.965	-0.1651	0.958	-0.1587	0.960	-0.0433	0.989	0.0837	1.021
13	-0.0084	0.998	-0.0687	0.983	-0.0653	0.984	-0.1245	0.969	-0.1534	0.961	-0.1526	0.962	-0.0360	0.991	0.0886	1.022
14	-0.0345	0.991	-0.0693	0.983	-0.0653	0.984	-0.1177	0.970	-0.1534	0.961	-0.1581	0.960	-0.0482	0.988	0.0764	1.019
15	-0.0668	0.983	-0.0595	0.985	-0.0585	0.985	-0.1009	0.975	-0.1356	0.966	-0.1439	0.964	-0.0372	0.991	0.0855	1.022
16	-0.0430	0.989	-0.0583	0.985	-0.0573	0.986	-0.0941	0.976	-0.1307	0.967	-0.1433	0.964	-0.0403	0.990	0.0770	1.019
17	-0.0442	0.989	-0.0595	0.985	-0.0579	0.985	-0.0898	0.977	-0.1283	0.968	-0.1415	0.964	-0.0445	0.989	0.0764	1.019
18	-0.0534	0.987	-0.0650	0.984	-0.0622	0.984	-0.0941	0.976	-0.1344	0.966	-0.1495	0.962	-0.0536	0.986	0.0702	1.018

FREESTREAM MACH NO.=0.600   INCIDENCE= 19.00DEG

NO.	PHI=0. CP	P/PF	PHI=30. CP	P/PF	PHI=60. CP	P/PF	PHI=75. CP	P/PF	PHI=90. CP	P/PF	PHI=105. CP	P/PF	PHI=135. CP	P/PF	PHI=180. CP	P/PF
2	0.8791	1.222	0.8765	1.221	0.8737	1.220	0.8684	1.219	0.8652	1.218	0.8655	1.218	0.8639	1.218	0.8594	1.217
3	-0.6681	0.827	-0.5983	0.849	-0.3518	0.911	-0.1988	0.950	-0.0108	0.997	0.1795	1.045	0.5713	1.144	0.8345	1.210
4	-0.8103	0.796	-0.8903	0.776	-0.9718	0.755	-0.9668	0.756	-0.8491	0.786	-0.6918	0.826	-0.3210	0.919	-0.0465	0.988
5	-0.6307	0.841	-0.6323	0.841	-0.8693	0.781	-0.8204	0.793	-0.7763	0.804	-0.7148	0.820	-0.4197	0.894	-0.1508	0.962
6	-0.6480	0.837	-0.6185	0.844	-0.5350	0.865	-0.4619	0.884	-0.4613	0.884	-0.4354	0.890	-0.2296	0.942	-0.0106	0.997
7	-0.5386	0.864	-0.5065	0.872	-0.4351	0.890	-0.4508	0.886	-0.4373	0.890	-0.3893	0.902	-0.1793	0.955	0.0393	1.010
8	-0.2233	0.944	-0.2649	0.933	-0.3829	0.904	-0.4137	0.896	-0.4097	0.897	-0.3580	0.910	-0.1500	0.962	0.0623	1.016
9	0.0148	1.004	-0.0565	0.986	-0.2437	0.939	-0.3396	0.914	-0.3480	0.912	-0.3211	0.919	-0.1125	0.972	0.1066	1.027
10	-0.0022	0.999	-0.0831	0.979	-0.1625	0.959	-0.2710	0.932	-0.2985	0.925	-0.2910	0.927	-0.1013	0.974	0.1127	1.028
11	-0.0101	0.997	-0.1254	0.968	-0.1283	0.968	-0.2321	0.942	-0.2770	0.930	-0.2707	0.932	-0.0940	0.976	0.1164	1.029
12	-0.0113	0.997	-0.1333	0.966	-0.1094	0.972	-0.1957	0.951	-0.2568	0.935	-0.2437	0.939	-0.0671	0.983	0.1263	1.032
13	-0.0350	0.991	-0.1033	0.974	-0.0929	0.977	-0.1901	0.952	-0.2392	0.935	-0.2517	0.937	-0.0562	0.986	0.1312	1.033
14	-0.0758	0.981	-0.1058	0.973	-0.0923	0.977	-0.1914	0.952	-0.2543	0.936	-0.2498	0.937	-0.0684	0.983	0.1189	1.030
15	-0.1177	0.970	-0.1021	0.974	-0.0800	0.980	-0.1753	0.956	-0.2433	0.939	-0.2400	0.940	-0.0549	0.986	0.1281	1.032
16	-0.1092	0.972	-0.1015	0.974	-0.0782	0.980	-0.1765	0.956	-0.2439	0.939	-0.2424	0.939	-0.0580	0.985	0.1189	1.030
17	-0.1147	0.971	-0.1003	0.975	-0.0807	0.980	-0.1741	0.956	-0.2476	0.938	-0.2406	0.939	-0.0623	0.984	0.1171	1.030
18	-0.1147	0.971	-0.1009	0.975	-0.0886	0.978	-0.1864	0.953	-0.2654	0.933	-0.2553	0.936	-0.0738	0.981	0.1103	1.028

FREESTREAM MACH NO.=0.70   INCIDENCE=   5.0DEG

	PHI=0.		PHI=90.		PHI=180.	
NO.	CP	P/PF	CP	P/PF	CP	P/PF
2	1.1220	1.385	1.1220	1.385	1.1203	1.384
3	-0.0346	0.988	0.1726	1.059	0.3943	1.135
4	-1.0112	0.653	-0.8987	0.692	-0.6784	0.767
5	-0.8755	0.700	-0.8271	0.716	-0.7007	0.760
6	-0.6074	0.826	-0.4050	0.861	-0.2544	0.913
7	-0.2500	0.914	-0.1830	0.937	-0.1376	0.953
8	-0.0331	0.989	-0.1151	0.961	-0.0773	0.973
9	-0.0258	0.991	-0.0559	0.981	-0.0111	0.996
10	-0.0108	0.996	-0.0338	0.988	0.0015	1.001
11	-0.0044	0.998	-0.0294	0.990	0.0085	1.003
12	0.0045	1.002	-0.0153	0.995	0.0194	1.007
13	0.0074	1.003	-0.0119	0.996	0.0243	1.008
14	0.0030	1.001	-0.0182	0.994	0.0149	1.005
15	-0.0314	0.989	-0.0094	0.997	0.0224	1.008
16	0.0020	1.001	-0.0085	0.997	0.0169	1.006
17	0.0035	1.001	-0.0119	0.996	0.0184	1.006
18	-0.0034	0.999	-0.0192	0.993	0.0129	1.004

FREESTREAM MACH NO.=0.70   INCIDENCE= 10.0DEG

	PHI=0.		PHI=90.		PHI=180.	
NO.	CP	P/PF	CP	P/PF	CP	P/PF
2	1.0797	1.370	1.0752	1.369	1.0744	1.369
3	-0.2376	0.919	0.1456	1.050	0.5809	1.199
4	-0.8235	0.718	-0.8862	0.696	-0.4647	0.841
5	-0.7121	0.756	-0.7927	0.728	-0.5225	0.821
6	-0.6102	0.791	-0.4554	0.844	-0.1920	0.934
7	-0.4604	0.842	-0.2524	0.913	-0.0979	0.966
8	-0.0398	0.986	-0.1976	0.932	-0.0482	0.983
9	-0.0095	0.997	-0.1216	0.958	0.0111	1.004
10	0.0001	1.000	-0.0932	0.968	0.0281	1.010
11	-0.0009	1.000	-0.0878	0.970	0.0350	1.012
12	0.0040	1.001	-0.0693	0.976	0.0464	1.016
13	0.0030	1.001	-0.0625	0.979	0.0513	1.018
14	-0.0063	0.998	-0.0688	0.976	0.0400	1.014
15	-0.0398	0.986	-0.0567	0.981	0.0489	1.017
16	-0.0078	0.997	-0.0552	0.981	0.0429	1.015
17	-0.0063	0.998	-0.0562	0.981	0.0434	1.015
18	-0.0117	0.996	-0.0630	0.978	0.0385	1.013

FREESTREAM MACH NO.=0.70   INCIDENCE= 15.00DEG

	PHI =0.		PHI =90.		PHI=180.	
NO.	CP	P/PF	CP	P/PF	CP	P/PF
2	1.0063	1.345	0.9963	1.342	0.9923	1.340
3	-0.4650	0.841	0.1035	1.036	0.7511	1.258
4	-0.7622	0.739	-0.8708	0.701	-0.2293	0.921
5	-0.6114	0.790	-0.7828	0.731	-0.3295	0.887
6	-0.6447	0.779	-0.4273	0.853	-0.1069	0.963
7	-0.5944	0.796	-0.3575	0.877	-0.0319	0.989
8	-0.0229	0.992	-0.3197	0.890	0.0045	1.002
9	0.0030	1.001	-0.2397	0.918	0.0572	1.020
10	0.0065	1.002	-0.1946	0.933	0.0713	1.024
11	-0.0029	0.999	-0.1777	0.939	0.0777	1.027
12	-0.0024	0.999	-0.1515	0.948	0.0891	1.031
13	-0.0083	0.997	-0.1355	0.954	0.0945	1.032
14	-0.0261	0.991	-0.1345	0.954	0.0821	1.028
15	-0.0216	0.993	-0.1151	0.961	0.0915	1.031
16	-0.0413	0.986	-0.1098	0.962	0.0846	1.029
17	-0.0428	0.985	-0.1059	0.964	0.0841	1.029
18	-0.0497	0.983	-0.1113	0.962	0.0777	1.027

FREESTREAM MACH NO.=0.70   INCIDENCE= 19.0DEG

	PHI =0.		PHI =90.		PHI=180.	
NO.	CP	P/PF	CP	P/PF	CP	P/PF
2	0.9242	1.317	0.9122	1.313	0.9076	1.311
3	-0.6355	0.782	0.0634	1.022	0.8653	1.297
4	-0.6200	0.787	-0.8428	0.711	-0.0450	0.986
5	-0.5617	0.807	-0.7643	0.738	-0.1793	0.939
6	-0.6207	0.787	-0.4024	0.862	-0.0207	0.993
7	-0.6377	0.781	-0.4213	0.855	0.0363	1.012
8	-0.0487	0.983	-0.4307	0.852	0.0585	1.020
9	-0.0125	0.996	-0.3682	0.874	0.1037	1.036
10	-0.0014	1.000	-0.2963	0.898	0.1156	1.040
11	-0.0172	0.994	-0.2629	0.910	0.1220	1.042
12	-0.0226	0.992	-0.2261	0.922	0.1334	1.046
13	-0.0423	0.985	-0.1994	0.932	0.1388	1.048
14	-0.0698	0.976	-0.1936	0.934	0.1255	1.043
15	-0.0428	0.985	-0.1708	0.941	0.1343	1.046
16	-0.1191	0.959	-0.1660	0.943	0.1255	1.043
17	-0.1122	0.962	-0.1640	0.944	0.1235	1.042
18	-0.0994	0.966	-0.1747	0.940	0.1171	1.040

FREESTREAM MACH NO.=0.800   INCIDENCE= 5.00DEG

NO.	PHI=0. CP	P/PF	PHI=30. CP	P/PF	PHI=60. CP	P/PF	PHI=75. CP	P/PF	PHI=90. CP	P/PF	PHI=105. CP	P/PF	PHI=135. CP	P/PF	PHI=180. CP	P/PF
2	1.1649	1.522	1.1646	1.522	1.1656	1.522	1.1647	1.522	1.1632	1.521	1.1608	1.520	1.1614	1.520	1.1626	1.521
3	0.0725	1.032	0.0942	1.042	0.1584	1.071	0.2051	1.092	0.2536	1.114	0.2975	1.133	0.3934	1.176	0.4563	1.204
4	-0.7537	0.662	-0.8327	0.627	-0.9060	0.594	-0.8719	0.609	-0.8085	0.638	-0.7766	0.652	-0.6742	0.698	-0.6181	0.723
5	-0.6639	0.703	-0.6599	0.704	-0.7471	0.665	-0.7841	0.649	-0.8060	0.639	-0.8322	0.627	-0.8574	0.616	-0.8919	0.600
6	-0.6335	0.716	-0.6400	0.713	-0.6849	0.693	-0.6774	0.697	-0.7045	0.684	-0.6680	0.701	-0.6325	0.717	-0.5850	0.738
7	-0.5611	0.749	-0.5834	0.739	-0.5405	0.758	-0.4962	0.778	-0.4512	0.798	-0.3807	0.829	-0.2737	0.877	-0.1968	0.912
8	-0.3500	0.843	-0.3037	0.864	-0.2234	0.900	-0.1989	0.911	-0.1664	0.925	-0.1268	0.943	-0.0918	0.959	-0.0693	0.969
9	-0.0297	0.987	-0.0177	0.992	-0.0407	0.982	-0.0527	0.976	-0.0551	0.975	-0.0599	0.973	-0.0408	0.982	-0.0143	0.994
10	0.0033	1.001	-0.0038	0.998	-0.0166	0.993	-0.0289	0.987	-0.0293	0.987	-0.0365	0.984	-0.0183	0.992	0.0013	1.001
11	-0.0012	0.999	-0.0055	0.998	-0.0153	0.993	-0.0226	0.990	-0.0272	0.988	-0.0277	0.988	-0.0121	0.995	0.0084	1.004
12	0.0012	1.001	-0.0001	1.000	-0.0078	0.997	-0.0113	0.995	-0.0149	0.993	-0.0155	0.993	0.0003	1.000	0.0192	1.009
13	0.0012	1.001	-0.0005	1.000	-0.0057	0.997	-0.0118	0.995	-0.0133	0.994	-0.0150	0.993	0.0037	1.002	0.0225	1.010
14	-0.0045	0.998	-0.0092	0.996	-0.0132	0.994	-0.0193	0.991	-0.0215	0.990	-0.0235	0.989	-0.0059	0.997	0.0125	1.006
15	-0.0735	0.967	-0.0047	0.998	-0.0070	0.997	-0.0118	0.995	-0.0141	0.994	-0.0155	0.993	0.0024	1.001	0.0205	1.009
16	-0.0045	0.998	-0.0059	0.997	-0.0086	0.996	-0.0113	0.995	-0.0145	0.994	-0.0159	0.993	0.0003	1.000	0.0155	1.007
17	-0.0029	0.999	-0.0092	0.996	-0.0112	0.995	-0.0138	0.994	-0.0176	0.992	-0.0180	0.992	-0.0034	0.998	0.0167	1.007
18	-0.0079	0.996	-0.0175	0.992	-0.0187	0.992	-0.0214	0.990	-0.0248	0.989	-0.0243	0.989	-0.0092	0.996	0.0130	1.006

FREESTREAM MACH NO.=0.800   INCIDENCE= 10.000EG

NO.	PHI=0. CP	P/PF	PHI=30. CP	P/PF	PHI=60. CP	P/PF	PHI=75. CP	P/PF	PHI=90. CP	P/PF	PHI=105. CP	P/PF	PHI=135. CP	P/PF	PHI=180. CP	P/PF
2	1.1285	1.506	1.1254	1.504	1.1256	1.504	1.1241	1.504	1.1212	1.502	1.1196	1.502	1.1179	1.501	1.1193	1.501
3	-0.1352	0.939	-0.0904	0.960	0.0488	1.022	0.1323	1.059	0.2250	1.101	0.3193	1.143	0.5046	1.226	0.6317	1.283
4	-0.6874	0.692	-0.7782	0.651	-0.9237	0.586	-0.9100	0.592	-0.8075	0.638	-0.7261	0.675	-0.5388	0.759	-0.4174	0.813
5	-0.5819	0.739	-0.5812	0.740	-0.7155	0.679	-0.8174	0.634	-0.7995	0.642	-0.8122	0.636	-0.7922	0.645	-0.8230	0.631
6	-0.6135	0.725	-0.6129	0.725	-0.6468	0.710	-0.6247	0.720	-0.6421	0.712	-0.6217	0.721	-0.4697	0.790	-0.2659	0.881
7	-0.6049	0.729	-0.6135	0.728	-0.5349	0.760	-0.4622	0.793	-0.4311	0.807	-0.3376	0.849	-0.1709	0.923	-0.1019	0.954
8	-0.4000	0.821	-0.4135	0.815	-0.3306	0.852	-0.2960	0.867	-0.2490	0.888	-0.2068	0.907	-0.1310	0.941	-0.0625	0.972
9	-0.0453	0.980	-0.0550	0.975	-0.1156	0.948	-0.1505	0.933	-0.1484	0.934	-0.1383	0.938	-0.0700	0.969	0.0026	1.001
10	0.0153	1.007	-0.0034	0.998	-0.0574	0.974	-0.0966	0.957	-0.1009	0.955	-0.1010	0.955	-0.0391	0.982	0.0252	1.011
11	0.0054	1.002	-0.0109	0.995	-0.0441	0.980	-0.0764	0.966	-0.0885	0.960	-0.0838	0.962	-0.0291	0.987	0.0348	1.016
12	0.0004	1.000	-0.0138	0.994	-0.0324	0.985	-0.0575	0.974	-0.0684	0.969	-0.0641	0.971	-0.0129	0.994	0.0477	1.021
13	-0.0062	0.997	-0.0233	0.990	-0.0274	0.988	-0.0521	0.977	-0.0630	0.972	-0.0612	0.973	-0.0071	0.997	0.0519	1.023
14	-0.0161	0.993	-0.0308	0.986	-0.0324	0.985	-0.0563	0.975	-0.0704	0.968	-0.0704	0.968	-0.0200	0.991	0.0402	1.018
15	-0.0600	0.973	-0.0237	0.989	-0.0262	0.988	-0.0462	0.979	-0.0601	0.973	-0.0604	0.973	-0.0100	0.996	0.0489	1.022
16	-0.0190	0.991	-0.0229	0.990	-0.0258	0.988	-0.0437	0.980	-0.0597	0.973	-0.0612	0.973	-0.0133	0.994	0.0431	1.019
17	-0.0178	0.992	-0.0237	0.989	-0.0270	0.988	-0.0432	0.981	-0.0605	0.973	-0.0625	0.972	-0.0171	0.992	0.0444	1.020
18	-0.0231	0.990	-0.0312	0.986	-0.0341	0.985	-0.0504	0.977	-0.0675	0.970	-0.0687	0.969	-0.0246	0.989	0.0414	1.019

73

FREESTREAM MACH NO.=0.800   INCIDENCE= 15.00DEG

NO.	PHI=0. CP	P/PF	PHI=30. CP	P/PF	PHI=60. CP	P/PF	PHI=75. CP	P/PF	PHI=90. CP	P/PF	PHI=105. CP	P/PF	PHI=135. CP	P/PF	PHI=180. CP	P/PF
2	1.0563	1.473	1.0553	1.473	1.0529	1.472	1.0486	1.470	1.0461	1.469	1.0440	1.468	1.0431	1.467	1.0446	1.468
3	-0.3570	0.840	-0.2902	0.870	-0.0882	0.960	0.0422	1.019	0.1802	1.081	0.3213	1.144	0.6053	1.271	0.7919	1.355
4	-0.5878	0.737	-0.7341	0.671	-0.8848	0.604	-0.9416	0.578	-0.8955	0.639	-0.6779	0.696	-0.3927	0.824	-0.2037	0.909
5	-0.5287	0.763	-0.5428	0.757	-0.7345	0.671	-0.8818	0.605	-0.8161	0.634	-0.7844	0.649	-0.6433	0.712	-0.4795	0.785
6	-0.5754	0.742	-0.5836	0.739	-0.5635	0.748	-0.6187	0.723	-0.5571	0.750	-0.5066	0.773	-0.2391	0.893	-0.1372	0.939
7	-0.6140	0.725	-0.6096	0.727	-0.4815	0.784	-0.4777	0.785	-0.3834	0.828	-0.3352	0.850	-0.1875	0.916	-0.0563	0.975
8	-0.4250	0.810	-0.4957	0.778	-0.4207	0.812	-0.3846	0.828	-0.3803	0.830	-0.3238	0.855	-0.1632	0.927	-0.0193	0.991
9	-0.0715	0.968	-0.1106	0.950	-0.2441	0.891	-0.2858	0.872	-0.2901	0.870	-0.2722	0.878	-0.1110	0.950	0.0421	1.019
10	0.0150	1.007	-0.0340	0.985	-0.1139	0.949	-0.1968	0.912	-0.2184	0.902	-0.2125	0.905	-0.0735	0.967	0.0836	1.028
11	0.0004	1.000	-0.0551	0.975	-0.0746	0.967	-0.1544	0.931	-0.1846	0.917	-0.1806	0.919	-0.0586	0.974	0.0757	1.034
12	-0.0087	0.996	-0.0712	0.968	-0.0625	0.972	-0.1234	0.945	-0.1521	0.932	-0.1508	0.932	-0.0370	0.983	0.0891	1.040
13	-0.0232	0.990	-0.0745	0.967	-0.0600	0.973	-0.1112	0.950	-0.1385	0.938	-0.1420	0.936	-0.0275	0.988	0.0950	1.043
14	-0.0431	0.981	-0.0699	0.969	-0.0613	0.973	-0.1099	0.951	-0.1422	0.936	-0.1487	0.933	-0.0416	0.981	0.0833	1.037
15	-0.0456	0.980	-0.0576	0.974	-0.0550	0.975	-0.0961	0.957	-0.1265	0.943	-0.1336	0.940	-0.0295	0.987	0.0929	1.042
16	-0.0584	0.974	-0.0551	0.975	-0.0533	0.976	-0.0915	0.959	-0.1236	0.945	-0.1340	0.940	-0.0324	0.985	0.0858	1.038
17	-0.0580	0.974	-0.0555	0.975	-0.0529	0.976	-0.0864	0.961	-0.1220	0.945	-0.1319	0.941	-0.0349	0.984	0.0870	1.039
18	-0.0626	0.972	-0.0600	0.973	-0.0588	0.974	-0.0915	0.959	-0.1294	0.942	-0.1407	0.937	-0.0420	0.981	0.0837	1.037

FREESTREAM MACH NO.=0.800   INCIDENCE= 19.00DEG

NO.	PHI=0.		PHI=30.		PHI=60.		PHI=75.		PHI=90.		PHI=105.		PHI=135.		PHI=180.	
	CP	P/PF	CP	P/PF	CP	P/PF	CP	P/PF	CP	P/PF	CP	P/PF	CP	P/PF	CP	P/PF
2	0.9800	1.439	0.9783	1.438	0.9740	1.436	0.9686	1.434	0.9655	1.433	0.9632	1.432	0.9616	1.431	0.9634	1.432
3	-0.5229	0.766	-0.4496	0.799	-0.2082	0.907	-0.0352	0.984	0.1366	1.061	0.3140	1.141	0.6669	1.299	0.9071	1.406
4	-0.5471	0.755	-0.6596	0.704	-0.8424	0.623	-0.8876	0.602	-0.8008	0.641	-0.6367	0.715	-0.2621	0.883	-0.0243	0.989
5	-0.5223	0.766	-0.5403	0.758	-0.7867	0.648	-0.8274	0.629	-0.7854	0.648	-0.7977	0.643	-0.5226	0.766	-0.2426	0.891
6	-0.5626	0.748	-0.5807	0.740	-0.5335	0.761	-0.5035	0.774	-0.5109	0.771	-0.3089	0.862	-0.1999	0.910	-0.0462	0.979
7	-0.5999	0.731	-0.6080	0.728	-0.4453	0.801	-0.4036	0.819	-0.3796	0.830	-0.3699	0.834	-0.1738	0.922	0.0170	1.008
8	-0.4600	0.794	-0.5291	0.763	-0.4747	0.787	-0.4802	0.785	-0.4573	0.795	-0.3945	0.823	-0.1682	0.925	0.0389	1.017
9	-0.1385	0.938	-0.1762	0.921	-0.3471	0.844	-0.4438	0.801	-0.4394	0.803	-0.3875	0.826	-0.1346	0.940	0.0858	1.038
10	-0.0112	0.995	-0.1091	0.951	-0.1709	0.923	-0.2946	0.868	-0.3356	0.850	-0.3209	0.856	-0.1004	0.955	0.1085	1.049
11	-0.0228	0.990	-0.1414	0.937	-0.1192	0.947	-0.2084	0.907	-0.2760	0.876	-0.2701	0.879	-0.0797	0.964	0.1214	1.054
12	-0.0385	0.983	-0.1526	0.932	-0.1075	0.952	-0.1616	0.928	-0.2270	0.898	-0.2269	0.898	-0.0519	0.977	0.1356	1.061
13	-0.0662	0.970	-0.1381	0.938	-0.1054	0.953	-0.1436	0.936	-0.2024	0.909	-0.2076	0.907	-0.0358	0.984	0.1431	1.064
14	-0.0923	0.959	-0.1323	0.941	-0.1092	0.951	-0.1423	0.936	-0.2020	0.910	-0.2093	0.906	-0.0465	0.979	0.1298	1.058
15	-0.0828	0.963	-0.1174	0.947	-0.1012	0.955	-0.1293	0.942	-0.1835	0.918	-0.1904	0.915	-0.0312	0.986	0.1394	1.062
16	-0.1259	0.944	-0.1095	0.951	-0.0962	0.957	-0.1222	0.945	-0.1822	0.918	-0.1929	0.914	-0.0349	0.984	0.1323	1.059
17	-0.1155	0.948	-0.1016	0.954	-0.0904	0.960	-0.1159	0.948	-0.1806	0.919	-0.1942	0.913	-0.0382	0.983	0.1319	1.059
18	-0.1027	0.954	-0.0962	0.957	-0.0896	0.960	-0.1168	0.948	-0.1917	0.914	-0.2105	0.906	-0.0507	0.977	0.1285	1.058

FREESTREAM MACH NO.=0.90 INCIDENCE= 5.0DEG

NO.	PHI=0. CP	P/PF	PHI=90. CP	P/PF	PHI=180. CP	P/PF
2	1.2145	1.689	1.2096	1.586	1.2080	1.685
3	0.1846	1.105	0.3530	1.200	0.5418	1.307
4	-0.6515	0.608	-0.6465	0.633	-0.4539	0.743
5	-0.5708	0.676	-0.6562	0.528	-0.9418	0.466
6	-0.5850	0.668	-0.6486	0.632	-0.8253	0.532
7	-0.5927	0.664	-0.6193	0.649	-0.7182	0.593
8	-0.0600	0.966	-0.5324	0.698	-0.1045	0.941
9	-0.1588	0.887	-0.0859	0.951	0.0142	1.008
10	0.0321	1.018	-0.0180	0.990	0.0151	1.009
11	0.0369	1.021	-0.0079	0.996	0.0195	1.011
12	0.0211	1.012	0.0005	1.000	0.0291	1.016
13	0.0047	1.003	-0.0057	0.997	0.0280	1.016
14	-0.0059	0.997	-0.0176	0.990	0.0162	1.009
15	-0.0560	0.968	-0.0104	0.994	0.0236	1.013
16	-0.0067	0.996	-0.0104	0.994	0.0191	1.011
17	-0.0026	0.999	-0.0122	0.993	0.0225	1.013
18	-0.0059	0.997	-0.0162	0.991	0.0236	1.013

FREESTREAM MACH NO.=0.90 INCIDENCE= 10.0DEG

NO.	PHI=0. CP	P/PF	PHI=90. CP	P/PF	PHI=180. CP	P/PF
2	1.1781	1.668	1.1730	1.665	1.1702	1.664
3	-0.0167	0.991	0.3284	1.186	0.7048	1.400
4	-0.5952	0.663	-0.6519	0.630	-0.2818	0.840
5	-0.5053	0.713	-0.7010	0.603	-0.8013	0.546
6	-0.5277	0.701	-0.6187	0.649	-0.6655	0.623
7	-0.5557	0.685	-0.6029	0.658	-0.5092	0.711
8	-0.0172	0.990	-0.4178	0.763	-0.0157	0.991
9	-0.2662	0.849	-0.2342	0.867	-0.0074	0.996
10	0.0138	1.008	-0.1317	0.925	0.0224	1.013
11	0.0369	1.021	-0.0877	0.950	0.0397	1.023
12	0.0189	1.011	-0.0565	0.968	0.0552	1.031
•13	-0.0059	0.997	-0.0540	0.969	0.0578	1.033
14	-0.0183	0.990	-0.0649	0.963	0.0438	1.025
15	-0.0147	0.992	-0.0561	0.968	0.0526	1.030
16	-0.0246	0.986	-0.0569	0.968	0.0467	1.026
17	-0.0216	0.988	-0.0565	0.968	0.0497	1.028
18	-0.0253	0.986	-0.0609	0.965	0.0497	1.028

	FREESTREAM MACH NO.=0.90 INCIDENCE= 15.0DEG						FREESTREAM MACH NO.=0.90 INCIDENCE= 19.0DEG					
	PHI=0.		PHI=90.		PHI=180.			PHI=0.		PHI=90.		PHI=180.	
NO.	CP	P/PF	CP	P/PF	CP	P/PF	NO.	CP	P/PF	CP	P/PF	CP	P/PF
2	1.1124	1.631	1.1023	1.625	1.1016	1.625	2	1.0431	1.591	1.0271	1.582	1.0254	1.581
3	-0.2069	0.883	0.2873	1.163	0.8519	1.483	3	-0.3693	0.791	0.2425	1.137	0.9582	1.543
4	-0.54C2	0.694	-0.6553	0.628	-0.0947	0.946	4	-0.5024	0.715	-0.6605	0.625	0.0638	1.031
5	-0.4914	0.721	-0.7216	0.591	-0.6218	0.647	5	-0.4809	0.727	-0.7386	0.581	-0.3752	0.787
6	-0.5177	0.706	-0.6407	0.637	-0.4146	0.765	6	-0.5112	0.710	-0.5856	0.668	-0.0713	0.960
7	-0.5473	0.690	-0.4375	0.752	-0.0714	0.960	7	-0.5436	0.692	-0.3946	0.776	0.0064	1.004
8	0.0107	1.006	-0.4070	0.769	-0.0405	0.977	8	-0.0145	0.992	-0.4336	0.754	0.0114	1.006
9	-0.3220	0.817	-0.4059	0.770	0.0054	1.003	9	-0.3753	0.787	-0.5357	0.696	0.0445	1.025
10	-0.0461	0.974	-0.2871	0.837	0.0457	1.026	10	-0.1027	0.942	-0.4445	0.748	0.0783	1.044
11	0.0149	1.008	-0.2071	0.883	0.0733	1.042	11	-0.0158	0.991	-0.3197	0.819	0.1114	1.063
12	0.0083	1.005	-0.1477	0.916	0.0951	1.054	12	-0.0154	0.991	-0.2285	0.870	0.1371	1.078
13	-0.0253	0.986	-0.1289	0.927	0.1024	1.058	13	-0.0624	0.965	-0.1913	0.892	0.1486	1.084
14	-0.0476	0.973	-0.1379	0.922	0.0877	1.050	14	-0.0195	0.989	-0.1967	0.888	0.1334	1.076
15	0.0149	1.008	-0.1256	0.929	0.0965	1.055	15	-0.0088	0.995	-0.1815	0.897	0.1430	1.081
16	-0.0666	0.962	-0.1260	0.929	0.0899	1.051	16	-0.1181	0.933	-0.1819	0.897	0.1353	1.077
17	-0.0640	0.964	-0.1231	0.930	0.0917	1.052	17	-0.1100	0.938	-0.1801	0.898	0.1356	1.077
18	-0.0669	0.962	-0.1285	0.927	0.0914	1.052	18	-0.1034	0.941	-0.1877	0.894	0.1356	1.077

77

FREESTREAM MACH NO.=1.000   INCIDENCE=   5.00DEG

NO.	PHI=0. CP	P/PF	PHI=30. CP	P/PF	PHI=60. CP	P/PF	PHI=75. CP	P/PF	PHI=90. CP	P/PF	PHI=105. CP	P/PF	PHI=135. CP	P/PF	PHI=180. CP	P/PF
2	1.2698	1.889	1.2696	1.889	1.2685	1.888	1.2700	1.889	1.2699	1.889	1.2684	1.888	1.2648	1.885	1.2651	1.886
3	0.3107	1.217	0.3316	1.232	0.3938	1.276	0.4312	1.302	0.4738	1.332	0.5151	1.361	0.5929	1.415	0.6441	1.451
4	-0.5821	0.593	-0.5704	0.601	-0.5235	0.634	-0.4814	0.663	-0.4454	0.688	-0.4065	0.715	-0.3282	0.770	-0.2774	0.806
5	-0.9300	0.349	-0.9250	0.353	-0.8907	0.377	-0.8609	0.397	-0.8363	0.415	-0.8075	0.435	-0.7597	0.468	-0.7207	0.496
6	-0.8318	0.418	-0.8228	0.424	-0.8132	0.431	-0.7881	0.448	-0.7649	0.465	-0.7387	0.483	-0.6860	0.520	-0.6496	0.545
7	-0.8099	0.433	-0.7872	0.449	-0.7438	0.479	-0.7118	0.502	-0.6808	0.523	-0.6513	0.544	-0.5880	0.588	-0.5429	0.620
8	-0.6423	0.550	-0.6296	0.559	-0.5864	0.590	-0.5552	0.611	-0.5306	0.629	-0.4960	0.653	-0.4397	0.692	-0.3976	0.722
9	-0.2351	0.835	-0.2369	0.834	-0.2912	0.796	-0.3178	0.778	-0.3036	0.787	-0.3015	0.789	-0.2630	0.816	-0.2203	0.846
10	-0.0741	0.948	-0.0744	0.948	-0.1070	0.925	-0.1387	0.903	-0.1546	0.892	-0.1797	0.874	-0.1801	0.874	-0.1620	0.887
11	-0.0063	0.996	-0.0096	0.993	-0.0300	0.979	-0.0611	0.957	-0.0716	0.950	-0.0812	0.943	-0.0646	0.955	-0.0688	0.952
12	0.0518	1.036	0.0517	1.036	0.0432	1.030	0.0299	1.021	0.0246	1.017	0.0270	1.019	0.0601	1.042	0.0725	1.051
13	0.0515	1.036	0.0507	1.035	0.0439	1.031	0.0420	1.029	0.0449	1.031	0.0447	1.031	0.0611	1.043	0.0778	1.054
14	0.0066	1.005	0.0013	1.001	-0.0051	0.996	-0.0082	0.994	-0.0066	0.995	-0.0062	0.996	0.0087	1.006	0.0264	1.018
15	-0.0020	0.999	-0.0106	0.993	-0.0134	0.991	-0.0213	0.985	-0.0217	0.985	-0.0216	0.985	0.0017	1.001	0.0170	1.012
16	-0.0090	0.994	-0.0115	0.992	-0.0141	0.990	-0.0149	0.990	-0.0168	0.988	-0.0156	0.989	-0.0032	0.998	0.0097	1.007
17	-0.0100	0.993	-0.0181	0.987	-0.0187	0.987	-0.0246	0.983	-0.0263	0.982	-0.0270	0.981	-0.0079	0.994	0.0107	1.007
18	-0.0087	0.994	-0.0175	0.988	-0.0194	0.986	-0.0199	0.986	-0.0237	0.983	-0.0193	0.986	-0.0076	0.995	0.0123	1.009

FREESTREAM MACH NO.=1.000   INCIDENCE= 10.000EG

	PHI=0.		PHI=30.		PHI=60.		PHI=75.		PHI=90.		PHI=105.		PHI=135.		PHI=180.	
NO.	CP	P/PF	CP	P/PF	CP	P/PF	CP	P/PF	CP	P/PF	CP	P/PF	CP	P/PF	CP	P/PF
2	1.2356	1.865	1.2345	1.864	1.2343	1.864	1.2338	1.864	1.2316	1.862	1.2301	1.861	1.2267	1.859	1.2272	1.859
3	0.1216	1.085	0.1607	1.112	0.2877	1.201	0.3675	1.257	0.4455	1.312	0.5262	1.368	0.6876	1.481	0.7926	1.555
4	-0.7152	0.499	-0.6877	0.519	-0.5995	0.580	-0.5239	0.633	-0.4555	0.681	-0.3811	0.733	-0.2086	0.854	-0.1207	0.916
5	-1.0044	0.297	-1.0042	0.297	-0.9446	0.339	-0.8924	0.375	-0.8431	0.410	-0.7884	0.448	-0.6746	0.528	-0.5995	0.580
6	-0.9203	0.356	-0.9126	0.361	-0.8766	0.386	-0.8251	0.422	-0.7736	0.458	-0.7184	0.497	-0.5921	0.586	-0.5041	0.647
7	-0.9118	0.362	-0.8685	0.392	-0.8026	0.438	-0.7512	0.474	-0.6947	0.514	-0.6359	0.555	-0.4981	0.651	-0.3892	0.728
8	-0.6904	0.517	-0.7258	0.492	-0.6525	0.543	-0.6008	0.579	-0.5586	0.609	-0.4944	0.654	-0.3499	0.755	-0.2527	0.823
9	-0.2269	0.841	-0.2083	0.854	-0.4305	0.699	-0.4515	0.684	-0.4205	0.706	-0.3866	0.729	-0.2549	0.822	-0.1559	0.891
10	-0.0362	0.975	-0.0442	0.969	-0.1511	0.894	-0.2348	0.836	-0.3186	0.777	-0.3596	0.748	-0.2340	0.836	-0.1445	0.899
11	0.0175	1.012	0.0116	1.008	-0.0531	0.963	-0.1044	0.927	-0.1341	0.906	-0.1582	0.889	-0.1497	0.881	-0.1288	0.910
12	0.0577	1.040	0.0410	1.029	0.0126	1.009	-0.0082	0.994	-0.0187	0.987	-0.0213	0.985	0.0462	1.032	0.0954	1.067
13	0.0560	1.039	0.0080	1.006	0.0143	1.010	0.0045	1.003	-0.0049	0.997	-0.0021	0.999	0.0541	1.038	0.1084	1.076
14	0.0016	1.001	-0.0442	0.969	-0.0257	0.982	-0.0451	0.968	-0.0605	0.958	-0.0575	0.960	-0.0022	0.998	0.0546	1.038
15	-0.0429	0.970	-0.0306	0.979	-0.0311	0.978	-0.0515	0.964	-0.0693	0.951	-0.0706	0.951	-0.0076	0.995	0.0479	1.034
16	-0.0203	0.986	-0.0280	0.980	-0.0307	0.979	-0.0417	0.971	-0.0634	0.956	-0.0649	0.955	-0.0135	0.991	0.0392	1.027
17	-0.0223	0.984	-0.0287	0.980	-0.0344	0.976	-0.0484	0.966	-0.0700	0.951	-0.0720	0.950	-0.0188	0.987	0.0398	1.028
18	-0.0173	0.988	-0.0303	0.979	-0.0324	0.977	-0.0414	0.971	-0.0647	0.955	-0.0663	0.954	-0.0178	0.988	0.0422	1.030

FREESTREAM MACH NO.=1.000   INCIDENCE= 15.00DEG

	PHI=0.		PHI=30.		PHI=60.		PHI=75.		PHI=90.		PHI=105.		PHI=135.		PHI=180.	
NO.	CP	P/PF	CP	P/PF	CP	P/PF	CP	P/PF	CP	P/PF	CP	P/PF	CP	P/PF	CP	P/PF
2	1.1724	1.821	1.1709	1.820	1.1692	1.818	1.1676	1.817	1.1623	1.814	1.1628	1.814	1.1601	1.812	1.1644	1.815
3	-0.0596	0.959	-0.0057	0.996	0.1608	1.113	0.2801	1.196	0.4045	1.283	0.5256	1.368	0.7682	1.538	0.9350	1.655
4	-0.6836	0.521	-0.7731	0.459	-0.6770	0.526	-0.5677	0.603	-0.4607	0.678	-0.3503	0.755	-0.0997	0.930	0.0600	1.042
5	-0.6373	0.554	-0.6522	0.543	-0.7016	0.509	-0.7402	0.482	-0.7946	0.444	-0.7538	0.472	-0.5857	0.590	-0.4307	0.699
6	-0.6746	0.528	-0.6636	0.535	-0.6795	0.524	-0.7155	0.499	-0.6857	0.520	-0.6246	0.563	-0.4792	0.665	-0.3113	0.782
7	-0.6931	0.515	-0.6780	0.525	-0.6565	0.540	-0.6124	0.571	-0.5877	0.589	-0.5417	0.621	-0.3902	0.727	-0.1808	0.873
8	-0.6457	0.549	-0.6676	0.533	-0.5469	0.617	-0.5018	0.649	-0.4587	0.679	-0.4015	0.719	-0.2345	0.836	-0.0774	0.946
9	-0.4007	0.720	-0.4219	0.705	-0.5244	0.633	-0.5265	0.631	-0.4829	0.662	-0.4161	0.709	-0.2221	0.845	-0.0354	0.975
10	-0.1587	0.889	-0.1852	0.870	-0.3874	0.729	-0.5335	0.627	-0.5206	0.636	-0.4454	0.688	-0.2347	0.836	-0.0584	0.961
11	-0.0136	0.990	-0.1000	0.930	-0.1409	0.901	-0.2476	0.827	-0.4359	0.695	-0.4618	0.677	-0.2496	0.825	-0.0578	0.960
12	0.0561	1.039	-0.0749	0.948	-0.0638	0.955	-0.0836	0.941	-0.1247	0.913	-0.1821	0.873	-0.2118	0.852	-0.0428	0.970
13	0.0358	1.025	-0.0799	0.944	-0.0287	0.980	-0.0330	0.977	-0.0653	0.954	-0.0631	0.956	0.0392	1.027	0.1595	1.112
14	-0.0405	0.972	-0.0713	0.950	-0.0568	0.960	-0.0803	0.944	-0.1313	0.908	-0.1295	0.909	-0.0195	0.986	0.1128	1.079
15	-0.0475	0.967	-0.0587	0.959	-0.0624	0.956	-0.0866	0.939	-0.1355	0.905	-0.1412	0.901	-0.0261	0.982	0.0918	1.064
16	-0.0624	0.956	-0.0630	0.956	-0.0651	0.954	-0.0826	0.942	-0.1339	0.906	-0.1368	0.904	-0.0347	0.976	0.0842	1.059
17	-0.0631	0.956	-0.0630	0.956	-0.0654	0.954	-0.0843	0.941	-0.1362	0.905	-0.1399	0.902	-0.0404	0.972	0.0808	1.057
18	-0.0674	0.953	-0.0680	0.952	-0.0684	0.952	-0.0826	0.942	-0.1336	0.906	-0.1389	0.903	-0.0401	0.972	0.0855	1.060

FREESTREAM MACH NO.=1.000   INCIDENCE= 19.00 DEG

	PHI=0.		PHI=30.		PHI=60.		PHI=75.		PHI=90.		PHI=105.		PHI=135.		PHI=180.	
NO.	CP	P/PF	CP	P/PF	CP	P/PF	CP	P/PF	CP	P/PF	CP	P/PF	CP	P/PF	CP	P/PF
2	1.1044	1.773	1.1020	1.771	1.0975	1.768	1.0969	1.768	1.0990	1.769	1.0907	1.763	1.0882	1.762	1.0909	1.764
3	-0.2149	0.850	-0.1493	0.895	0.0592	1.041	0.2035	1.142	0.3600	1.252	0.5111	1.358	0.8180	1.573	1.0314	1.722
4	-0.5487	0.616	-0.7232	0.494	-0.7304	0.489	-0.6025	0.578	-0.4725	0.669	-0.3343	0.766	-0.0237	0.983	0.1880	1.132
5	-0.5373	0.624	-0.6415	0.551	-0.6884	0.518	-0.6980	0.511	-0.7353	0.485	-0.7228	0.494	-0.4915	0.656	-0.2899	0.797
6	-0.5527	0.613	-0.6390	0.553	-0.6749	0.528	-0.6844	0.521	-0.6373	0.554	-0.5856	0.590	-0.3626	0.746	-0.1029	0.928
7	-0.5652	0.604	-0.6445	0.549	-0.6238	0.563	-0.5849	0.591	-0.5641	0.605	-0.4725	0.669	-0.2163	0.849	0.0436	1.031
8	-0.5700	0.601	-0.6390	0.553	-0.5413	0.621	-0.4995	0.650	-0.4477	0.687	-0.3750	0.738	-0.1531	0.893	0.0491	1.034
9	-0.4904	0.657	-0.4524	0.683	-0.6188	0.567	-0.6196	0.566	-0.5636	0.605	-0.4690	0.672	-0.1968	0.862	0.0531	1.037
10	-0.2638	0.815	-0.2677	0.813	-0.4807	0.664	-0.7215	0.495	-0.6563	0.541	-0.5370	0.624	-0.2275	0.841	0.0256	1.018
11	-0.0689	0.952	-0.2432	0.830	-0.2552	0.821	-0.2997	0.790	-0.6147	0.570	-0.5762	0.597	-0.2534	0.823	0.0176	1.012
12	0.0602	1.042	-0.2148	0.850	-0.1638	0.885	-0.1838	0.871	-0.2448	0.829	-0.4127	0.711	-0.2488	0.826	0.0239	1.017
13	0.0253	1.018	-0.1458	0.898	-0.0551	0.961	-0.0568	0.960	-0.1042	0.927	-0.1309	0.908	0.0167	1.012	0.1935	1.135
14	-0.0729	0.949	-0.0848	0.941	-0.0681	0.952	-0.0746	0.948	-0.1762	0.877	-0.1939	0.864	-0.0414	0.971	0.1665	1.117
15	-0.0592	0.959	-0.0736	0.948	-0.0744	0.948	-0.0910	0.936	-0.1399	0.860	-0.2166	0.848	-0.0577	0.960	0.1442	1.101
16	-0.0955	0.933	-0.0805	0.944	-0.0781	0.945	-0.0917	0.936	-0.1963	0.863	-0.2180	0.847	-0.0703	0.951	0.1275	1.089
17	-0.0928	0.935	-0.0854	0.940	-0.0831	0.942	-0.0954	0.933	-0.1917	0.866	-0.2190	0.847	-0.0739	0.948	0.1259	1.088
18	-0.0968	0.932	-0.1010	0.929	-0.0964	0.933	-0.1077	0.925	-0.1897	0.867	-0.2186	0.847	-0.0709	0.950	0.1302	1.091

FREESTREAM MACH NO.=1.10   INCIDENCE= 5.0DEG

NO.	PHI=0.		PHI=90.		PHI=180.	
	CP	P/PF	CP	P/PF	CP	P/PF
2	1.3321	2.128	1.3297	2.126	1.3314	2.128
3	0.4282	1.363	0.5811	1.492	0.7443	1.630
4	-0.4058	0.656	-0.2789	0.764	-0.1209	0.898
5	-0.7310	0.381	-0.6423	0.456	-0.5304	0.551
6	-0.6360	0.461	-0.5823	0.507	-0.4681	0.604
7	-0.6175	0.477	-0.5022	0.575	-0.3756	0.682
8	-0.4637	0.607	-0.3708	0.686	-0.2454	0.792
9	-0.1273	0.892	-0.1712	0.855	-0.0892	0.924
10	-0.0215	0.982	-0.0790	0.933	-0.0431	0.963
11	-0.0203	0.983	-0.0631	0.947	-0.0242	0.980
12	-0.0308	0.974	-0.0732	0.938	-0.0149	0.987
13	-0.0169	0.986	-0.1007	0.915	-0.0214	0.982
14	-0.0030	0.997	-0.0378	0.968	0.0570	1.048
15	-0.0231	0.980	-0.0411	0.965	0.0043	1.004
16	-0.0716	0.939	-0.0659	0.944	-0.0570	0.952
17	0.0520	1.044	-0.0054	0.995	0.0496	1.042
18	0.0214	1.018	0.0206	1.023	0.0766	1.065

FREESTREAM MACH NO.=1.10   INCIDENCE= 10.0DEG

NO.	PHI=0.		PHI=90.		PHI=180.	
	CP	P/PF	CP	P/PF	CP	P/PF
2	1.2998	2.101	1.2955	2.097	1.2948	2.097
3	0.2532	1.214	0.5571	1.472	0.8837	1.748
4	-0.5274	0.563	-0.2833	0.760	0.0289	1.024
5	-0.8041	0.319	-0.6435	0.455	-0.4143	0.649
6	-0.7240	0.387	-0.5845	0.505	-0.3339	0.717
7	-0.7046	0.403	-0.5126	0.566	-0.2325	0.803
8	-0.5329	0.549	-0.3936	0.667	-0.1130	0.904
9	-0.1091	0.908	-0.2700	0.771	-0.0237	0.980
10	-0.0024	0.998	-0.2572	0.782	-0.0164	0.986
11	-0.0036	0.997	-0.1598	0.865	-0.0235	0.980
12	0.0029	1.002	-0.1467	0.876	-0.0167	0.986
13	0.0059	1.005	-0.1467	0.876	-0.0055	0.995
14	-0.0098	0.992	-0.0893	0.924	0.0859	1.073
15	-0.0061	0.995	-0.0870	0.931	0.0422	1.036
16	-0.0937	0.921	-0.1107	0.906	-0.0127	0.989
17	0.0448	1.038	-0.0283	0.976	0.0608	1.051
18	0.0041	1.003	-0.0140	0.988	0.0974	1.082

FREESTREAM MACH NO.=1.10   INCIDENCE= 15.0 DEG

NO.	PHI=0. CP	P/PF	PHI=90. CP	P/PF	PHI=180. CP	P/PF
2	1.2426	2.052	1.2307	2.042	1.2342	2.045
3	0.0867	1.073	0.5135	1.435	1.0136	1.859
4	-0.6353	0.462	-0.2959	0.749	0.1871	1.158
5	-0.6173	0.477	-0.6550	0.445	-0.2727	0.769
6	-0.6548	0.445	-0.5724	0.515	-0.1694	0.857
7	-0.6492	0.450	-0.5062	0.571	-0.0567	0.952
8	-0.5464	0.537	-0.3717	0.695	0.0377	1.032
9	-0.2264	0.808	-0.3846	0.674	0.0670	1.057
10	-0.0351	0.970	-0.4397	0.628	0.0574	1.049
11	0.0189	1.016	-0.4795	0.594	0.0435	1.037
12	0.0411	1.035	-0.3102	0.737	0.0348	1.029
13	0.0090	1.008	-0.2030	0.828	-0.0012	0.999
14	-0.0524	0.956	-0.1633	0.862	0.1130	1.096
15	-0.0669	0.943	-0.1424	0.879	0.1033	1.087
16	-0.1117	0.905	-0.1684	0.840	0.0627	1.053
17	-0.0015	0.999	-0.1746	0.852	0.0276	1.023
18	-0.0277	0.977	-0.0974	0.918	0.1300	1.110

FREESTREAM MACH NO.=1.10   INCIDENCE= 19.0 DEG

NO.	PHI=0. CP	P/PF	PHI=90. CP	P/PF	PHI=180. CP	P/PF
2	1.1800	1.999	1.1660	1.988	1.1664	1.988
3	-0.0527	0.955	0.4716	1.399	1.1018	1.933
4	-0.5199	0.560	-0.3054	0.741	0.3074	1.260
5	-0.5037	0.573	-0.6475	0.452	-0.1474	0.875
6	-0.5277	0.553	-0.5338	0.548	-0.0023	0.998
7	-0.5411	0.542	-0.4783	0.595	0.1242	1.105
8	-0.5300	0.551	-0.3457	0.707	0.1563	1.132
9	-0.3409	0.711	-0.4416	0.626	0.1549	1.131
10	-0.0555	0.953	-0.5350	0.547	0.1309	1.111
11	0.0263	1.022	-0.6007	0.491	0.1123	1.095
12	0.0845	1.072	-0.5276	0.553	0.1042	1.088
13	-0.0018	0.998	-0.1968	0.833	0.0434	1.037
14	-0.1014	0.914	-0.2057	0.826	0.1172	1.099
15	-0.1057	0.910	-0.1772	0.850	0.1699	1.144
16	-0.1242	0.895	-0.2616	0.778	0.1309	1.111
17	-0.0465	0.961	-0.3231	0.726	0.1011	1.086
18	-0.0558	0.953	-0.1693	0.907	0.1575	1.133

FREESTREAM MACH NO.=1.200   INCIDENCE=   5.00DEG

NO.	PHI=0. CP	P/PF	PHI=30. CP	P/PF	PHI=60. CP	P/PF	PHI=75. CP	P/PF	PHI=90. CP	P/PF	PHI=105. CP	P/PF	PHI=135. CP	P/PF	PHI=180. CP	P/PF
2	1.3881	2.399	1.3859	2.397	1.3856	2.397	1.3889	2.400	1.3848	2.396	1.3870	2.398	1.3853	2.396	1.3834	2.394
3	0.4960	1.500	0.5138	1.518	0.5710	1.576	0.6056	1.610	0.6473	1.652	0.6824	1.688	0.7572	1.763	0.8032	1.810
4	-0.2979	0.700	-0.2920	0.706	-0.2552	0.743	-0.2207	0.778	-0.1822	0.816	-0.1498	0.849	-0.0868	0.913	-0.0430	0.957
5	-0.6021	0.393	-0.6032	0.392	-0.5725	0.423	-0.5493	0.445	-0.5236	0.472	-0.4983	0.498	-0.4547	0.542	-0.4262	0.570
6	-0.5277	0.468	-0.5356	0.460	-0.5343	0.461	-0.5089	0.487	-0.4826	0.514	-0.4570	0.539	-0.4098	0.587	-0.3829	0.614
7	-0.4991	0.497	-0.4948	0.501	-0.4673	0.529	-0.4467	0.550	-0.4188	0.578	-0.3961	0.601	-0.3435	0.654	-0.3116	0.686
8	-0.3987	0.598	-0.4079	0.589	-0.3684	0.629	-0.3432	0.654	-0.3206	0.677	-0.2947	0.703	-0.2441	0.754	-0.2129	0.785
9	-0.1706	0.828	-0.1801	0.818	-0.1980	0.800	-0.2007	0.798	-0.1844	0.814	-0.1813	0.817	-0.1369	0.862	-0.1067	0.892
10	-0.0525	0.947	-0.0587	0.941	-0.0968	0.902	-0.1304	0.869	-0.1189	0.880	-0.1255	0.873	-0.0913	0.908	-0.0729	0.927
11	-0.0216	0.978	-0.0204	0.979	-0.0492	0.950	-0.0638	0.936	-0.0793	0.920	-0.0855	0.914	-0.0720	0.927	-0.0605	0.939
12	-0.0134	0.986	-0.0163	0.984	-0.0294	0.970	-0.0369	0.963	-0.0380	0.962	-0.0505	0.949	-0.0424	0.957	-0.0269	0.973
13	0.1319	1.133	0.1268	1.128	0.0963	1.097	0.0774	1.078	0.0680	1.069	0.0778	1.078	0.0499	1.050	0.0171	1.017
14	0.0379	1.038	0.0276	1.028	0.0289	1.029	0.0345	1.035	0.0461	1.046	0.0553	1.056	0.1050	1.106	0.1259	1.127
15	0.0512	1.052	0.0253	1.026	0.0194	1.020	0.0312	1.031	0.0197	1.020	0.0126	1.013	0.0098	1.010	0.0182	1.018
16	-0.0211	0.979	-0.0370	0.963	-0.0486	0.951	-0.0422	0.957	-0.0520	0.948	-0.0404	0.959	-0.0330	0.967	-0.0293	0.970
17	-0.0460	0.954	-0.0587	0.941	-0.0557	0.944	-0.0564	0.943	-0.0520	0.948	-0.0520	0.948	-0.0517	0.948	-0.0254	0.974
18	-0.0809	0.918	-0.0880	0.911	-0.0888	0.910	-0.0848	0.915	-0.0927	0.907	-0.0970	0.902	-0.0749	0.925	-0.0529	0.947

FREESTREAM MACH NO. =1.200   INCIDENCE= 10.00DEG

NO.	PHI=0. CP	P/PF	PHI=30. CP	P/PF	PHI=60. CP	P/PF	PHI=75. CP	P/PF	PHI=90. CP	P/PF	PHI=105. CP	P/PF	PHI=135. CP	P/PF	PHI=180. CP	P/PF
2	1.3581	2.369	1.3549	2.366	1.3531	2.364	1.3544	2.365	1.3526	2.363	1.3521	2.363	1.3503	2.361	1.3494	2.360
3	0.3291	1.332	0.3644	1.367	0.4722	1.476	0.5459	1.550	0.6246	1.630	0.6961	1.702	0.8465	1.853	0.9405	1.948
4	-0.4115	0.585	-0.3940	0.603	-0.3186	0.679	-0.2540	0.744	-0.1781	0.820	-0.1209	0.878	0.0302	1.030	0.1055	1.106
5	-0.6740	0.321	-0.6697	0.325	-0.6139	0.381	-0.5698	0.426	-0.5231	0.473	-0.4780	0.518	-0.3796	0.617	-0.3144	0.683
6	-0.6035	0.392	-0.5993	0.396	-0.5767	0.419	-0.5321	0.464	-0.4829	0.513	-0.4362	0.560	-0.3277	0.670	-0.2605	0.737
7	-0.5775	0.418	-0.5633	0.432	-0.5164	0.479	-0.4735	0.523	-0.4239	0.573	-0.3757	0.621	-0.2662	0.732	-0.1823	0.816
8	-0.4626	0.534	-0.4890	0.507	-0.4242	0.572	-0.3877	0.609	-0.3335	0.664	-0.2832	0.715	-0.1734	0.825	-0.0921	0.907
9	-0.1476	0.851	-0.1940	0.804	-0.2971	0.701	-0.2794	0.718	-0.2471	0.751	-0.2200	0.778	-0.1237	0.875	-0.0293	0.970
10	-0.0217	0.978	-0.0458	0.954	-0.1789	0.820	-0.2719	0.726	-0.2536	0.744	-0.2272	0.771	-0.1142	0.885	-0.0243	0.976
11	-0.0056	0.994	-0.0277	0.972	-0.0926	0.907	-0.1393	0.860	-0.1989	0.800	-0.2165	0.782	-0.1227	0.876	-0.0370	0.963
12	-0.0047	0.995	-0.0279	0.972	-0.0684	0.931	-0.0960	0.903	-0.1194	0.880	-0.1302	0.869	-0.1177	0.881	-0.0240	0.976
13	0.1098	1.111	0.0582	1.059	0.0563	1.057	0.0440	1.044	0.0501	1.051	-0.0312	0.969	-0.0409	0.959	0.0152	1.015
14	0.0696	1.070	-0.0036	0.996	0.0137	1.014	-0.0075	0.992	-0.0213	0.979	-0.0143	0.986	0.0590	1.059	0.1392	1.140
15	0.0467	1.047	-0.0048	0.995	0.0025	1.003	0.0058	1.006	-0.0047	0.995	-0.0069	0.993	0.0215	1.022	0.0656	1.066
16	-0.0267	0.973	-0.0429	0.957	-0.0498	0.950	-0.0670	0.932	-0.0821	0.917	-0.0798	0.920	-0.0313	0.968	0.0267	1.027
17	-0.0690	0.930	-0.0772	0.922	-0.0793	0.920	-0.0842	0.915	-0.1008	0.898	-0.1201	0.879	-0.0899	0.909	-0.0264	0.973
18	-0.1039	0.895	-0.1074	0.892	-0.1036	0.896	-0.1029	0.896	-0.1290	0.870	-0.1341	0.865	-0.0667	0.933	-0.0069	0.993

FREESTREAM MACH NO.=1.200   INCIDENCE= 15.00DEG

NO.	PHI=0.		PHI=30.		PHI=60.		PHI=75.		PHI=90.		PHI=105.		PHI=135.		PHI=180.	
	CP	P/PF	CP	P/PF	CP	P/PF	CP	P/PF	CP	P/PF	CP	P/PF	CP	P/PF	CP	P/PF
2	1.3023	2.312	1.3004	2.311	1.2981	2.308	1.2975	2.308	1.2936	2.304	1.2954	2.306	1.2927	2.303	1.2919	2.302
3	0.1654	1.167	0.2149	1.217	0.3636	1.367	0.4682	1.472	0.5584	1.593	0.6990	1.705	0.9191	1.926	1.0687	2.077
4	-0.5169	0.473	-0.4894	0.507	-0.3821	0.615	-0.2905	0.707	-0.1898	0.809	-0.0899	0.909	0.1277	1.129	0.2614	1.263
5	-0.6693	0.325	-0.6200	0.375	-0.6329	0.362	-0.5904	0.405	-0.5269	0.469	-0.4477	0.549	-0.3031	0.694	-0.1800	0.819
6	-0.6561	0.339	-0.6130	0.382	-0.5696	0.426	-0.5357	0.460	-0.4771	0.519	-0.3936	0.603	-0.2420	0.756	-0.1098	0.889
7	-0.6398	0.355	-0.6077	0.387	-0.5390	0.457	-0.4869	0.509	-0.4260	0.571	-0.3431	0.654	-0.1743	0.824	-0.0241	0.976
8	-0.4597	0.537	-0.4855	0.511	-0.4659	0.530	-0.4060	0.591	-0.3431	0.654	-0.2664	0.731	-0.0921	0.907	0.0488	1.049
9	-0.1650	0.834	-0.2582	0.740	-0.4109	0.586	-0.3940	0.603	-0.3256	0.672	-0.2566	0.741	-0.0925	0.907	0.0634	1.064
10	-0.0216	0.978	-0.1109	0.888	-0.3762	0.621	-0.4506	0.546	-0.3910	0.606	-0.3073	0.690	-0.1168	0.882	0.0484	1.049
11	0.0207	1.021	-0.0775	0.922	-0.1721	0.827	-0.3757	0.621	-0.4329	0.564	-0.3380	0.659	-0.1417	0.857	0.0313	1.032
12	0.0342	1.034	-0.0951	0.904	-0.1192	0.880	-0.1459	0.853	-0.3412	0.656	-0.3735	0.624	-0.1376	0.861	0.0375	1.038
13	0.1129	1.114	-0.0344	0.965	-0.0046	0.995	-0.0487	0.951	-0.0937	0.906	-0.1503	0.848	-0.1640	0.835	0.0154	1.016
14	0.0298	1.030	-0.0479	0.952	-0.0002	1.000	-0.0212	0.979	-0.0966	0.903	-0.0888	0.910	0.0505	1.051	0.2098	1.211
15	0.0201	1.020	-0.0373	0.962	-0.0286	0.971	-0.0363	0.963	-0.0725	0.927	-0.0859	0.913	0.0315	1.032	0.1571	1.158
16	-0.0654	0.934	-0.0631	0.936	-0.0705	0.929	-0.0991	0.900	-0.1639	0.835	-0.1619	0.837	-0.0503	0.949	0.0767	1.077
17	-0.0892	0.910	-0.0951	0.904	-0.0971	0.902	-0.1011	0.898	-0.1665	0.832	-0.1864	0.812	-0.1007	0.898	0.0410	1.041
18	-0.1047	0.894	-0.1109	0.888	-0.1012	0.898	-0.1074	0.892	-0.1586	0.840	-0.1675	0.831	-0.0729	0.927	0.0658	1.066

FREESTREAM MACH NO.=1.200   INCIDENCE= 19.00DEG

Z/R	NO.	PHI=0. CP	P/PF	PHI=30. CP	P/PF	PHI=60. CP	P/PF	PHI=75. CP	P/PF	PHI=90. CP	P/PF	PHI=105. CP	P/PF	PHI=135. CP	P/PF	PHI=180. CP	P/PF
0.	2	1.2371	2.247	1.2350	2.245	1.2312	2.241	1.2287	2.239	1.2258	2.236	1.2238	2.234	1.2246	2.234	1.2215	2.231
.271	3	0.0416	1.042	0.0787	1.079	0.2746	1.277	0.4004	1.404	0.5473	1.552	0.6816	1.687	0.9672	1.975	1.1564	2.166
.708	4	-0.5689	0.427	-0.5559	0.440	-0.4290	0.568	-0.3218	0.676	-0.1993	0.799	-0.0808	0.919	0.2036	1.205	0.3794	1.382
1.0	5	-0.5125	0.483	-0.5361	0.460	-0.5434	0.452	-0.5704	0.425	-0.5266	0.469	-0.4384	0.558	-0.2360	0.762	-0.0681	0.931
1.25	6	-0.5455	0.450	-0.5476	0.448	-0.5265	0.469	-0.5002	0.496	-0.4598	0.537	-0.3713	0.626	-0.1504	0.848	0.0306	1.031
1.5	7	-0.5640	0.431	-0.5612	0.434	-0.5141	0.482	-0.4669	0.529	-0.4092	0.588	-0.3206	0.677	-0.0806	0.919	0.1258	1.127
2.0	8	-0.4750	0.521	-0.5062	0.490	-0.4415	0.555	-0.3839	0.613	-0.3285	0.669	-0.2547	0.743	-0.0248	0.975	0.1634	1.165
3.0	9	-0.2412	0.757	-0.3175	0.680	-0.5070	0.489	-0.4678	0.528	-0.3869	0.610	-0.2916	0.706	-0.0608	0.939	0.1399	1.141
4.0	10	-0.0501	0.949	-0.2073	0.791	-0.5233	0.473	-0.5565	0.439	-0.4599	0.536	-0.3541	0.643	-0.0880	0.911	0.1234	1.124
5.0	11	0.0180	1.018	-0.2507	0.747	-0.3127	0.685	-0.4464	0.550	-0.5146	0.481	-0.4039	0.593	-0.1232	0.876	0.1036	1.104
6.0	12	0.0324	1.033	-0.2266	0.772	-0.2533	0.745	-0.2499	0.748	-0.4329	0.564	-0.4315	0.565	-0.1179	0.881	0.1084	1.109
8.0	13	0.0832	1.084	-0.1202	0.879	-0.0533	0.946	-0.1117	0.887	-0.1830	0.816	-0.3093	0.688	-0.1574	0.841	0.0827	1.083
10.0	14	-0.0390	0.961	-0.0598	0.940	-0.0270	0.973	-0.0197	0.980	-0.0850	0.914	-0.1486	0.850	0.0718	1.072	0.2238	1.226
12.0	15	-0.0475	0.952	-0.0627	0.937	-0.0752	0.924	-0.0744	0.925	-0.1458	0.853	-0.1874	0.811	-0.0263	0.973	0.1579	1.159
14.0	16	-0.0531	0.946	-0.0563	0.943	-0.0755	0.924	-0.1087	0.890	-0.2575	0.740	-0.2627	0.735	-0.0558	0.944	0.1163	1.117
16.0	17	-0.1092	0.890	-0.0997	0.900	-0.0964	0.903	-0.0966	0.903	-0.2403	0.758	-0.2826	0.715	-0.1273	0.872	0.0629	1.063
18.0	18	-0.1406	0.858	-0.1199	0.879	-0.1047	0.894	-0.1226	0.876	-0.2360	0.762	-0.2432	0.755	-0.0558	0.944	0.1317	1.133

FREESTREAM MACH NO.=1.30 INCIDENCE= 5.0 DEG						FREESTREAM MACH NO.=1.30 INCIDENCE= 10.0 DEG					
PHI=0.		PHI=90.		PHI=180.		PHI=0.		PHI=90.		PHI=180.	
NO.	CP	P/PF	CP	P/PF	CP	P/PF	NO.	CP	P/PF	CP	P/PF	CP	P/PF
2	1.4361 2.699	1.4357 2.698	1.4326 2.695		2	1.4043 2.661	1.3994 2.655	1.3971 2.653
3	0.5446 1.644	0.7006 1.829	0.8570 2.014		3	0.3890 1.460	0.6792 1.803	0.9966 2.179
4	-0.2229 0.736	-0.1069 0.874	0.0243 1.029		4	-0.3215 0.620	-0.1062 0.874	0.1776 1.210
5	-0.5122 0.394	-0.4294 0.492	-0.3385 0.600		5	-0.5657 0.331	-0.4296 0.492	-0.2250 0.734
6	-0.4540 0.463	-0.4015 0.525	-0.3052 0.639		6	-0.5047 0.403	-0.4013 0.525	-0.1874 0.778
7	-0.4159 0.508	-0.3520 0.584	-0.2470 0.708		7	-0.4790 0.433	-0.3539 0.581	-0.1263 0.851
8	0.1334 1.158	-0.2707 0.680	-0.1670 0.802		8	0.1166 1.138	-0.2836 0.665	-0.0566 0.933
9	-0.1699 0.799	-0.1662 0.803	-0.0899 0.894		9	-0.1635 0.807	-0.2154 0.745	-0.0075 0.991
10	-0.0602 0.929	-0.1095 0.870	-0.0551 0.935		10	-0.0422 0.950	-0.2168 0.744	-0.0147 0.983
11	-0.0297 0.965	-0.0736 0.913	-0.0354 0.958		11	-0.0109 0.987	-0.2055 0.757	-0.0048 0.994
12	-0.0072 0.991	-0.0460 0.946	-0.0252 0.970		12	0.0098 1.012	-0.1395 0.835	0.0038 1.004
13	-0.0055 0.993	-0.0240 0.972	-0.0129 0.985		13	-0.0027 0.997	-0.0870 0.897	-0.0008 0.999
14	-0.0066 0.992	-0.0319 0.962	0.0188 1.022		14	-0.0021 0.998	-0.0881 0.896	0.0183 1.022
15	0.1371 1.162	0.0827 1.098	-0.0063 0.993		15	0.1231 1.146	0.0143 1.017	0.0289 1.034
16	0.0598 1.071	0.0508 1.060	0.1209 1.143		16	0.0466 1.055	0.0067 1.008	0.1511 1.179
17	0.0704 1.083	0.0333 1.039	0.0616 1.073		17	0.0480 1.057	0.0160 1.019	0.0807 1.095
18	0.0079 1.009	0.0248 1.029	0.0533 1.063		18	-0.0354 0.958	-0.0150 0.982	0.1092 1.129

	FREESTREAM MACH NO.=1.30 INCIDENCE= 15.0 DEG						FREESTREAM MACH NO.=1.30 INCIDENCE= 19.0 DEG				
	PHI=0.		PHI=90.		PHI=180.			PHI=0.		PHI=90.		PHI=180.
NO.	CP	P/PF	CP	P/PF	CP	P/PF	NO.	CP	P/PF	CP	P/PF	CP	P/PF
2	1.3518	2.599	1.3380	2.583	1.3368	2.581	2	1.2894	2.525	1.2740	2.507	1.2708	2.503
3	0.2291	1.271	0.6372	1.754	1.1221	2.327	3	0.1159	1.137	0.5944	1.703	1.2071	2.428
4	-0.4159	0.508	-0.1179	0.861	0.3233	1.382	4	-0.4864	0.425	-0.1259	0.851	0.4410	1.522
5	-0.5860	0.307	-0.4369	0.483	-0.1092	0.871	5	-0.4898	0.421	-0.4354	0.485	0.0017	1.002
6	-0.5386	0.339	-0.4005	0.526	-0.0527	0.938	6	-0.5176	0.388	-0.3935	0.534	0.0718	1.085
7	-0.5373	0.364	-0.3598	0.574	0.0144	1.017	7	-0.5164	0.389	-0.3558	0.579	0.1428	1.169
8	0.0551	1.065	-0.3030	0.642	0.0705	1.083	8	-0.0157	0.981	-0.3050	0.639	0.1784	1.211
9	-0.1547	0.817	-0.2933	0.653	0.0880	1.104	9	-0.1983	0.765	-0.3406	0.597	0.1659	1.196
10	-0.0218	0.974	-0.3475	0.589	0.0666	1.079	10	-0.0340	0.960	-0.3970	0.530	0.1428	1.169
11	0.0149	1.018	-0.3780	0.553	0.0618	1.073	11	0.0165	1.020	-0.4445	0.474	0.1369	1.162
12	0.0320	1.038	-0.3924	0.536	0.0609	1.072	12	0.0293	1.035	-0.4391	0.481	0.1343	1.159
13	0.0269	1.032	-0.1560	0.815	0.0364	1.043	13	-0.0052	0.994	-0.3073	0.636	0.1132	1.134
14	-0.0059	0.993	-0.1786	0.789	0.0227	1.027	14	-0.0710	0.916	-0.1145	0.865	0.0824	1.097
15	0.0617	1.073	-0.1224	0.855	0.0726	1.086	15	-0.0018	0.998	-0.1433	0.830	0.0861	1.102
16	0.0192	1.023	-0.0690	0.918	0.2286	1.270	16	-0.0326	0.961	-0.0670	0.921	0.1249	1.148
17	-0.0107	0.987	-0.0410	0.951	0.1813	1.214	17	-0.0508	0.940	-0.1125	0.867	0.1996	1.236
18	-0.0469	0.945	-0.1246	0.853	0.1277	1.151	18	-0.0480	0.943	-0.1876	0.778	0.1457	1.172

FREESTREAM MACH NO.=1.400   INCIDENCE=   5.00DEG

	PHI=0.		PHI=30.		PHI=60.		PHI=75.		PHI=90.		PHI=105.		PHI=135.		PHI=180.	
NO.	CP	P/PF	CP	P/PF	CP	P/PF	CP	P/PF	CP	P/PF	CP	P/PF	CP	P/PF	CP	P/PF
2	1.4760	3.025	1.4743	3.023	1.4808	3.032	1.4714	3.019	1.4834	3.035	1.4702	3.017	1.4747	3.023	1.4784	3.028
3	0.5803	1.796	0.5889	1.808	0.6487	1.890	0.6873	1.943	0.7367	2.011	0.7559	2.037	0.8270	2.135	0.8908	2.222
4	-0.1581	0.783	-0.1556	0.787	-0.1169	0.840	-0.0897	0.877	-0.0448	0.939	-0.0310	0.957	0.0349	1.048	0.0816	1.112
5	-0.4281	0.413	-0.4241	0.418	-0.3975	0.455	-0.3767	0.483	-0.3516	0.518	-0.3406	0.533	-0.2949	0.595	-0.2587	0.645
6	-0.3939	0.460	-0.3939	0.460	-0.3764	0.484	-0.3567	0.511	-0.3290	0.549	-0.3160	0.566	-0.2663	0.635	-0.2364	0.676
7	-0.3403	0.533	-0.3432	0.529	-0.3340	0.542	-0.3142	0.569	-0.2877	0.605	-0.2760	0.621	-0.2215	0.696	-0.1917	0.737
8	-0.2800	0.616	-0.2852	0.609	-0.2551	0.650	-0.2423	0.668	-0.2209	0.697	-0.2048	0.712	-0.1627	0.777	-0.1357	0.814
9	-0.1513	0.792	-0.1451	0.801	-0.1585	0.783	-0.1539	0.789	-0.1353	0.814	-0.1363	0.813	-0.0943	0.871	-0.0418	0.943
10	-0.0578	0.921	-0.0623	0.915	-0.1017	0.860	-0.1048	0.856	-0.0830	0.886	-0.0958	0.869	-0.0760	0.896	-0.0324	0.956
11	-0.0260	0.964	-0.0321	0.956	-0.0457	0.937	-0.0606	0.917	-0.0605	0.917	-0.0817	0.888	-0.0486	0.933	-0.0293	0.960
12	-0.0102	0.986	-0.0147	0.980	-0.0268	0.963	-0.0459	0.937	-0.0388	0.947	-0.0330	0.955	-0.0332	0.954	-0.0273	0.963
13	-0.0111	0.985	-0.0189	0.974	-0.0256	0.965	-0.0385	0.947	-0.0288	0.960	-0.0387	0.947	-0.0268	0.963	0.0036	1.005
14	-0.0055	0.992	-0.0153	0.979	-0.0237	0.967	-0.0334	0.954	-0.0413	0.943	-0.0409	0.944	-0.0229	0.969	-0.0082	0.989
15	-0.0075	0.990	-0.0119	0.984	-0.0172	0.976	-0.0221	0.970	-0.0249	0.966	-0.0333	0.954	0.0001	1.000	0.0221	1.030
16	-0.0091	0.988	-0.0186	0.974	-0.0194	0.973	-0.0255	0.965	-0.0237	0.967	-0.0256	0.965	-0.0108	0.985	-0.0133	0.982
17	0.0758	1.104	0.0561	1.077	0.0589	1.081	0.0624	1.086	0.0483	1.066	0.0378	1.052	0.0759	1.104	0.0095	1.013
18	0.0539	1.074	0.0390	1.054	0.0459	1.063	0.0494	1.068	0.0597	1.082	0.0480	1.066	0.0773	1.106	0.1050	1.144

FREESTREAM MACH NO.=1.400   INCIDENCE= 10.00DEG

	PHI=0.		PHI=30.		PHI=60.		PHI=75.		PHI=90.		PHI=105.		PHI=135.		PHI=180.	
NO.	CP	P/PF	CP	P/PF	CP	P/PF	CP	P/PF	CP	P/PF	CP	P/PF	CP	P/PF	CP	P/PF
2	1.4441	2.981	1.4418	2.978	1.4387	2.974	1.4359	2.970	1.4368	2.971	1.4441	2.981	1.4376	2.972	1.4392	2.975
3	0.4319	1.593	0.4554	1.625	0.5514	1.757	0.6174	1.847	0.7086	1.972	0.7760	2.065	0.9176	2.259	1.0236	2.404
4	-0.2552	0.650	-0.2404	0.670	-0.1719	0.764	-0.1186	0.837	-0.0575	0.921	0.0001	1.000	0.1218	1.167	0.2205	1.303
5	-0.4857	0.334	-0.4717	0.353	-0.4287	0.412	-0.3924	0.462	-0.3648	0.499	-0.3157	0.567	-0.2333	0.680	-0.1690	0.768
6	-0.4359	0.402	-0.4310	0.409	-0.4092	0.439	-0.3724	0.489	-0.3440	0.528	-0.2932	0.598	-0.2044	0.720	-0.1387	0.810
7	-0.4114	0.436	-0.4016	0.449	-0.3693	0.493	-0.3342	0.541	-0.3026	0.585	-0.2542	0.651	-0.1624	0.777	-0.0822	0.887
8	-0.3150	0.568	-0.3546	0.513	-0.3100	0.575	-0.2746	0.623	-0.2412	0.669	-0.1943	0.733	-0.0978	0.866	-0.0156	0.979
9	-0.1573	0.784	-0.1834	0.748	-0.2109	0.711	-0.2202	0.698	-0.2003	0.725	-0.1544	0.788	-0.0869	0.881	0.0084	1.012
10	-0.0398	0.945	-0.0803	0.890	-0.1741	0.761	-0.1975	0.729	-0.1899	0.739	-0.1638	0.775	-0.0677	0.907	0.0276	1.038
11	-0.0122	0.983	-0.0355	0.951	-0.1078	0.852	-0.1678	0.770	-0.1829	0.749	-0.1745	0.761	-0.0800	0.890	0.0011	1.002
12	0.0018	1.002	-0.0288	0.960	-0.0722	0.901	-0.1162	0.841	-0.1531	0.790	-0.1581	0.783	-0.0881	0.879	-0.0048	0.993
13	0.0094	1.013	-0.0388	0.947	-0.0507	0.930	-0.0825	0.887	-0.1083	0.851	-0.1188	0.837	-0.0660	0.909	-0.0067	0.991
14	-0.0004	0.999	-0.0702	0.904	-0.0510	0.930	-0.0672	0.908	-0.0897	0.877	-0.0967	0.867	-0.0573	0.921	0.0180	1.025
15	0.0100	1.014	-0.0665	0.909	-0.0394	0.946	-0.0513	0.930	-0.0824	0.887	-0.0797	0.891	-0.0268	0.963	0.0208	1.029
16	0.0193	1.026	-0.0265	0.964	-0.0292	0.960	-0.0484	0.934	-0.0730	0.900	-0.0854	0.883	-0.0263	0.964	0.0177	1.024
17	0.0798	1.109	0.0367	1.050	0.0462	1.063	0.0655	1.090	0.0208	1.029	0.0773	1.106	-0.0204	0.972	0.0290	1.040
18	0.0350	1.048	0.0177	1.024	0.0177	1.024	0.0156	1.021	-0.0070	0.990	-0.0011	0.998	0.0598	1.082	0.1605	1.220

FREESTREAM MACH NO.=1.400   INCICENCE= 15.00DEG

NO.	PHI=0. CP	P/PF	PHI=30. CP	P/PF	PHI=60. CP	P/PF	PHI=75. CP	P/PF	PHI=90. CP	P/PF	PHI=105. CP	P/PF	PHI=135. CP	P/PF	PHI=180. CP	P/PF
2	1.3881	2.904	1.3838	2.899	1.3778	2.890	1.3809	2.895	1.3708	2.881	1.3826	2.897	1.3780	2.891	1.3769	2.889
3	0.2720	1.373	0.3106	1.426	0.4561	1.626	0.5525	1.758	0.6651	1.913	0.7798	2.070	0.9952	2.365	1.1535	2.583
4	-0.3456	0.526	-0.3186	0.563	-0.2245	0.692	-0.1508	0.793	-0.0668	0.908	0.0246	1.034	0.2347	1.322	0.3656	1.502
5	-0.5094	0.301	-0.5091	0.302	-0.4597	0.369	-0.4101	0.437	-0.3718	0.490	-0.2956	0.594	-0.1611	0.779	-0.0539	0.926
6	-0.4820	0.339	-0.4667	0.360	-0.4368	0.401	-0.3854	0.471	-0.3446	0.527	-0.2647	0.637	-0.1259	0.827	-0.0143	0.980
7	-0.4676	0.358	-0.4537	0.378	-0.4037	0.446	-0.3540	0.514	-0.3112	0.573	-0.2307	0.683	-0.0818	0.888	0.0380	1.052
8	-0.3450	0.527	-0.4042	0.445	-0.3576	0.509	-0.3043	0.583	-0.2644	0.637	-0.1896	0.740	-0.0373	0.949	0.0987	1.135
9	-0.1379	0.811	-0.2162	0.703	-0.3300	0.547	-0.2941	0.596	-0.2594	0.644	-0.1832	0.749	-0.0298	0.959	0.0983	1.135
10	-0.0306	0.958	-0.1044	0.857	-0.3012	0.504	-0.3414	0.532	-0.2963	0.593	-0.2158	0.704	-0.0509	0.930	0.0911	1.125
11	-0.0036	0.995	-0.0868	0.881	-0.2282	0.687	-0.3788	0.480	-0.3378	0.537	-0.2505	0.656	-0.0834	0.886	0.0760	1.104
12	0.0209	1.029	-0.0882	0.879	-0.1575	0.784	-0.2927	0.598	-0.3590	0.507	-0.2794	0.617	-0.0730	0.900	0.0732	1.100
13	0.0156	1.021	-0.1450	0.801	-0.1030	0.859	-0.1147	0.843	-0.2517	0.655	-0.3031	0.584	-0.1066	0.854	0.0538	1.074
14	-0.0196	0.973	-0.1380	0.811	-0.0923	0.873	-0.0915	0.874	-0.1818	0.751	-0.1677	0.770	-0.1259	0.827	0.0271	1.037
15	0.0925	1.072	-0.0630	0.914	-0.0606	0.917	-0.0770	0.894	-0.1629	0.777	-0.1747	0.760	-0.0582	0.920	0.0512	1.070
16	-0.0531	0.927	-0.0515	0.929	-0.0516	0.929	-0.0651	0.911	-0.1236	0.830	-0.1657	0.773	-0.0554	0.924	0.0554	1.076
17	-0.0362	0.950	-0.0056	0.992	-0.0146	0.980	-0.0541	0.926	-0.0005	0.999	-0.1309	0.820	-0.0534	0.927	0.0605	1.083
18	-0.0052	0.993	0.0056	1.008	0.0060	1.008	-0.0036	0.995	-0.0743	0.898	-0.0783	0.893	0.0700	1.096	0.1653	1.227

FREESTREAM MACH NO.=1.400   INCIDENCE= 19.00DEG

NO.	PHI=0. CP	P/PF	PHI=30. CP	P/PF	PHI=60. CP	P/PF	PHI=75. CP	P/PF	PHI=90. CP	P/PF	PHI=105. CP	P/PF	PHI=135. CP	P/PF	PHI=180. CP	P/PF
2	1.3363	2.833	1.3243	2.817	1.3190	2.810	1.3186	2.809	1.3039	2.785	1.3199	2.811	1.3102	2.798	1.3170	2.807
3	0.1744	1.239	0.2113	1.290	0.3670	1.504	0.4932	1.677	0.6261	1.859	0.7745	2.063	1.0465	2.436	1.2420	2.704
4	-0.4078	0.440	-0.3732	0.488	-0.2655	0.636	-0.1803	0.753	-0.C807	0.889	0.0387	1.053	0.3108	1.426	0.4883	1.670
5	-0.4297	0.410	-0.4761	0.347	-0.4689	0.357	-0.4251	0.417	-0.3779	0.482	-0.2817	0.614	-0.0991	0.864	0.0565	1.078
6	-0.4407	0.395	-0.4756	0.347	-0.4265	0.415	-0.3958	0.457	-0.3458	0.526	-0.2435	0.666	-0.0529	0.927	0.1045	1.143
7	-0.4458	0.388	-0.4807	0.340	-0.4151	0.430	-0.3673	0.496	-0.3144	0.569	-0.2121	0.709	-0.0117	0.984	0.1597	1.219
8	-0.3500	0.520	-0.4290	0.411	-0.3727	0.489	-0.3291	0.548	-0.2759	0.621	-0.1837	0.748	0.0181	1.025	0.1892	1.260
9	-0.1819	0.750	-0.2871	0.606	-0.4070	0.442	-0.3622	0.503	-0.3140	0.569	-0.2062	0.717	0.0072	1.010	0.1850	1.254
10	-0.0278	0.962	-0.2065	0.717	-0.4659	0.361	-0.4294	0.411	-0.3639	0.501	-0.2492	0.658	-0.0215	0.971	0.1697	1.233
11	0.0085	1.012	-0.2339	0.679	-0.3515	0.518	-0.4555	0.375	-0.3993	0.452	-0.2851	0.609	-0.0596	0.918	0.1483	1.203
12	0.0226	1.031	-0.2272	0.688	-0.2719	0.627	-0.3855	0.471	-0.4185	0.426	-0.3126	0.571	-0.0529	0.927	0.1379	1.189
13	-0.0481	0.934	-0.2712	0.628	-0.1911	0.738	-0.2075	0.715	-0.3363	0.539	-0.3412	0.532	-0.0778	0.893	0.1278	1.175
14	-0.0627	0.914	-0.1847	0.747	-0.1332	0.817	-0.1309	0.820	-0.1705	0.766	-0.3148	0.568	-0.1080	0.852	0.1244	1.171
15	-0.0109	0.985	-0.1175	0.839	-0.0939	0.871	-0.0978	0.866	-0.0924	0.873	-0.2628	0.639	-0.1041	0.857	0.1185	1.163
16	-0.0996	0.863	-0.0959	0.868	-0.0730	0.900	-0.0839	0.885	-0.1367	0.812	-0.2345	0.678	-0.0602	0.917	0.0949	1.130
17	-0.0830	0.886	-0.0685	0.906	-0.0739	0.899	-0.0910	0.875	-0.1730	0.763	-0.2277	0.689	-0.0716	0.902	0.1216	1.167
18	-0.0061	0.992	0.0054	1.007	0.0072	1.010	0.0133	1.018	-0.1354	0.814	-0.0560	0.923	-0.0551	0.924	0.1326	1.182

FREE STREAM MACH NO.=1.50   INCIDENCE=   5.0DEG | FREE STREAM MACH NO.=1.50   INCIDENCE= 10.0DEG

	PHI =0.		PHI =90.		PHI =180.			PHI =0.		PHI =90.		PHI =180.	
NO.	CP	P/PF	CP	P/PF	CP	P/PF	NO.	CP	P/PF	CP	P/PF	CP	P/PF
2	1.5274	3.406	1.5180	3.391	1.5123	3.382	2	1.4851	3.339	1.4800	3.331	1.4790	3.329
3	0.6113	1.963	0.7500	2.181	0.9408	2.482	3	0.4644	1.731	0.7211	2.136	1.0827	2.705
4	-0.1186	0.813	0.0020	1.003	0.1280	1.202	4	-0.2014	0.683	-0.0301	0.953	0.2632	1.415
5	-0.3668	0.422	-0.3021	0.524	-0.2052	0.677	5	-0.4128	0.350	-0.3252	0.488	-0.1156	0.818
6	-0.3543	0.442	-0.2751	0.567	-0.1753	0.724	6	-0.3751	0.409	-0.3153	0.503	-0.0269	0.958
7	-0.3045	0.520	-0.2511	0.605	-0.1559	0.754	7	-0.3604	0.432	-0.2711	0.573	-0.0558	0.912
8	-0.2446	0.615	-0.1803	0.716	-0.0795	0.875	8	-0.2977	0.531	-0.2221	0.650	0.0007	1.001
9	-0.1425	0.776	-0.1002	0.842	-0.0277	0.956	9	-0.1579	0.751	-0.1905	0.700	0.0232	1.037
10	-0.0619	0.903	-0.0451	0.929	-0.0364	0.943	10	-0.0517	0.919	-0.1652	0.740	0.0536	1.084
11	-0.0409	0.936	-0.0352	0.945	-0.0648	0.898	11	-0.0197	0.969	-0.1412	0.778	0.0035	1.006
12	0.0026	1.004	-0.0301	0.953	-0.0147	0.977	12	0.0082	1.013	-0.1600	0.748	-0.0055	0.991
13	-0.0016	0.997	-0.0200	0.969	-0.0150	0.976	13	0.0060	1.009	-0.1150	0.819	0.0088	1.014
14	-0.0086	0.986	-0.0403	0.937	-0.0013	0.998	14	0.0029	1.005	-0.0802	0.874	-0.0038	0.994
15	-0.0130	0.980	-0.0711	0.888	0.0020	1.003	15	-0.0049	0.992	-0.1403	0.779	0.0185	1.029
16	-0.0114	0.982	-0.0905	0.857	0.0075	1.012	16	-0.0085	0.987	-0.1211	0.809	0.0366	1.058
17	-0.0097	0.985	0.0500	1.079	0.0140	1.022	17	-0.0104	0.984	0.0200	1.031	0.0461	1.073
18	-0.0066	0.990	0.0613	1.097	-0.0033	0.995	18	0.0057	1.009	0.0031	1.005	0.0249	1.039

FREESTREAM MACH NO.=1.50   INCIDENCE= 15.0DEG

NO.	PHI=0. CP	P/PF	PHI=90. CP	P/PF	PHI=180. CP	P/PF
2	1.4317	3.255	1.4250	3.244	1.4210	3.238
3	0.3154	1.497	0.6752	2.063	1.2088	2.904
4	-0.2826	0.555	-0.0522	0.918	0.4051	1.638
5	-0.4416	0.304	-0.3301	0.480	-0.0030	0.995
6	-0.4127	0.350	-0.3103	0.511	0.0137	1.022
7	-0.4081	0.357	-0.2811	0.557	0.0711	1.112
8	-0.3453	0.456	-0.2305	0.637	0.1238	1.195
9	-0.1524	0.760	-0.2202	0.653	0.0602	1.095
10	-0.0283	0.955	-0.2512	0.604	0.0951	1.150
11	0.0024	1.004	-0.2907	0.542	0.0867	1.137
12	0.0241	1.038	-0.3514	0.447	0.0588	1.093
13	0.0194	1.031	-0.3002	0.527	0.0641	1.101
14	-0.0113	0.982	-0.1932	0.696	0.0415	1.065
15	-0.0445	0.930	-0.1811	0.715	0.0440	1.069
16	-0.0662	0.896	-0.1407	0.778	0.0789	1.124
17	-0.0381	0.940	0.0101	1.016	0.0683	1.108
18	-0.0621	0.902	-0.0404	0.936	0.0716	1.113

FREESTREAM MACH NO.=1.50   INCIDENCE= 19.0DEG

NO.	PHI=0. CP	P/PF	PHI=90. CP	P/PF	PHI=180. CP	P/PF
2	1.3769	3.169	1.3600	3.142	1.3543	3.133
3	0.2147	1.338	0.6351	2.000	1.2882	3.029
4	-0.3490	0.450	-0.0600	0.906	0.5334	1.840
5	-0.3938	0.380	-0.3312	0.478	0.1015	1.160
6	-0.4018	0.367	-0.3004	0.527	0.0610	1.096
7	-0.4047	0.363	-0.2913	0.541	0.1836	1.289
8	-0.3817	0.399	-0.2451	0.614	0.2279	1.359
9	-0.1802	0.716	-0.3007	0.526	0.1133	1.178
10	-0.0119	0.981	-0.3314	0.478	0.1619	1.255
11	0.0149	1.023	-0.3753	0.409	0.1915	1.302
12	0.0088	1.014	-0.4106	0.353	0.1315	1.207
13	-0.0588	0.907	-0.3431	0.460	0.1265	1.199
14	-0.1238	0.805	-0.2008	0.694	0.1181	1.186
15	-0.1155	0.818	-0.0703	0.889	0.1232	1.194
16	-0.0884	0.861	-0.1615	0.746	0.1031	1.162
17	-0.0758	0.881	-0.1803	0.716	0.0911	1.143
18	-0.0660	0.896	-0.1005	0.842	0.1318	1.208
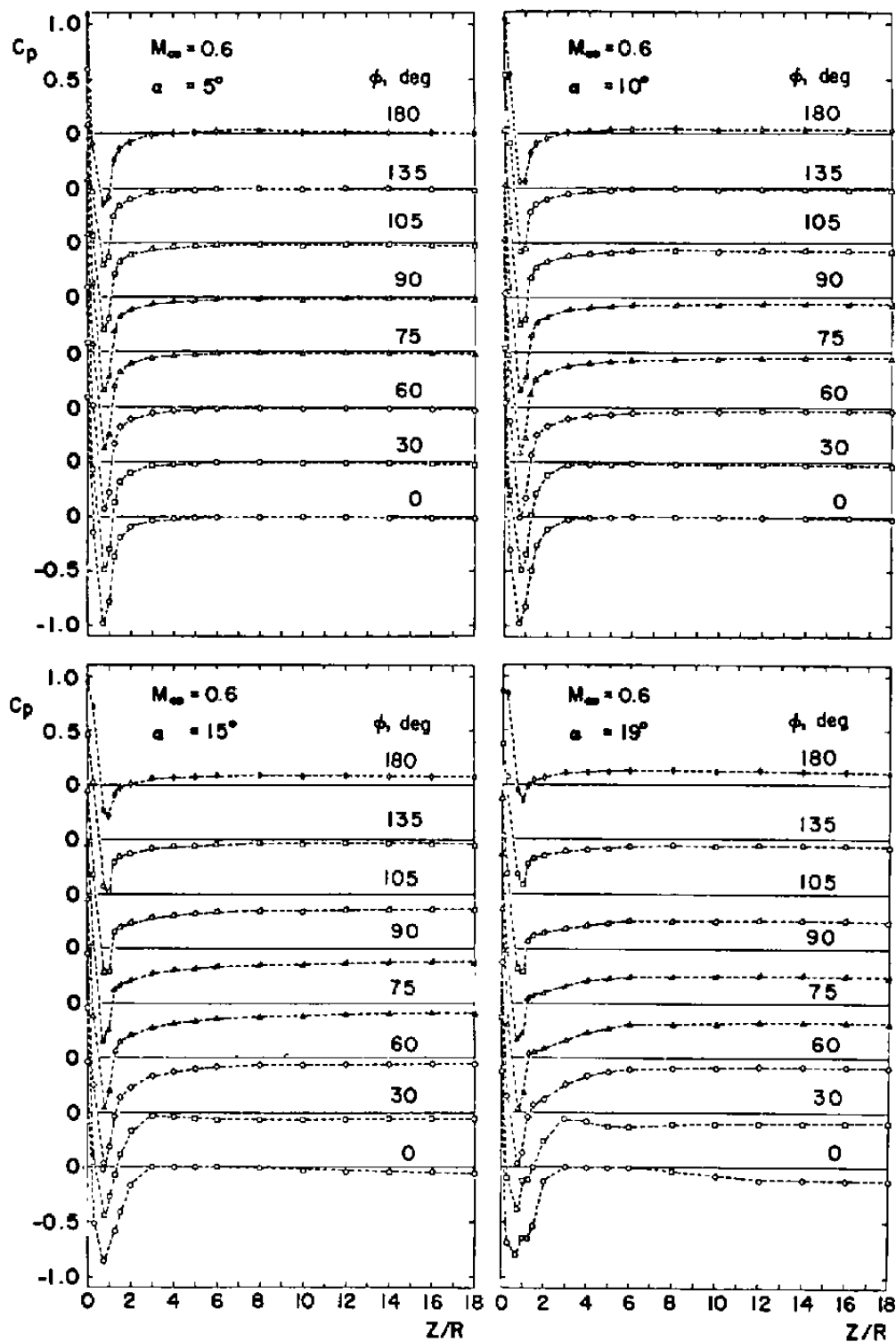
Figure A-1. Measured surface pressure distribution for hemisphere-cylinder at incidences.
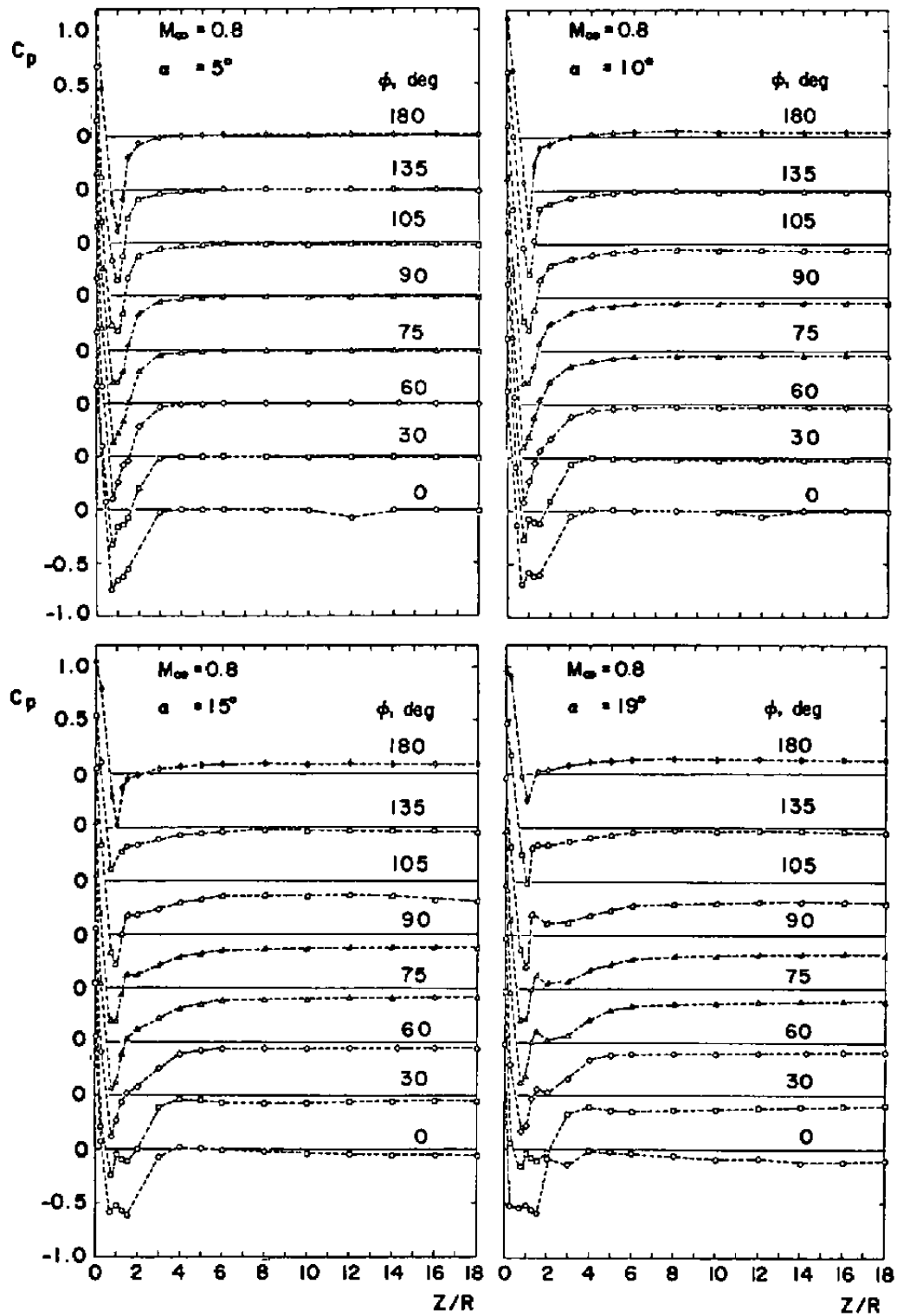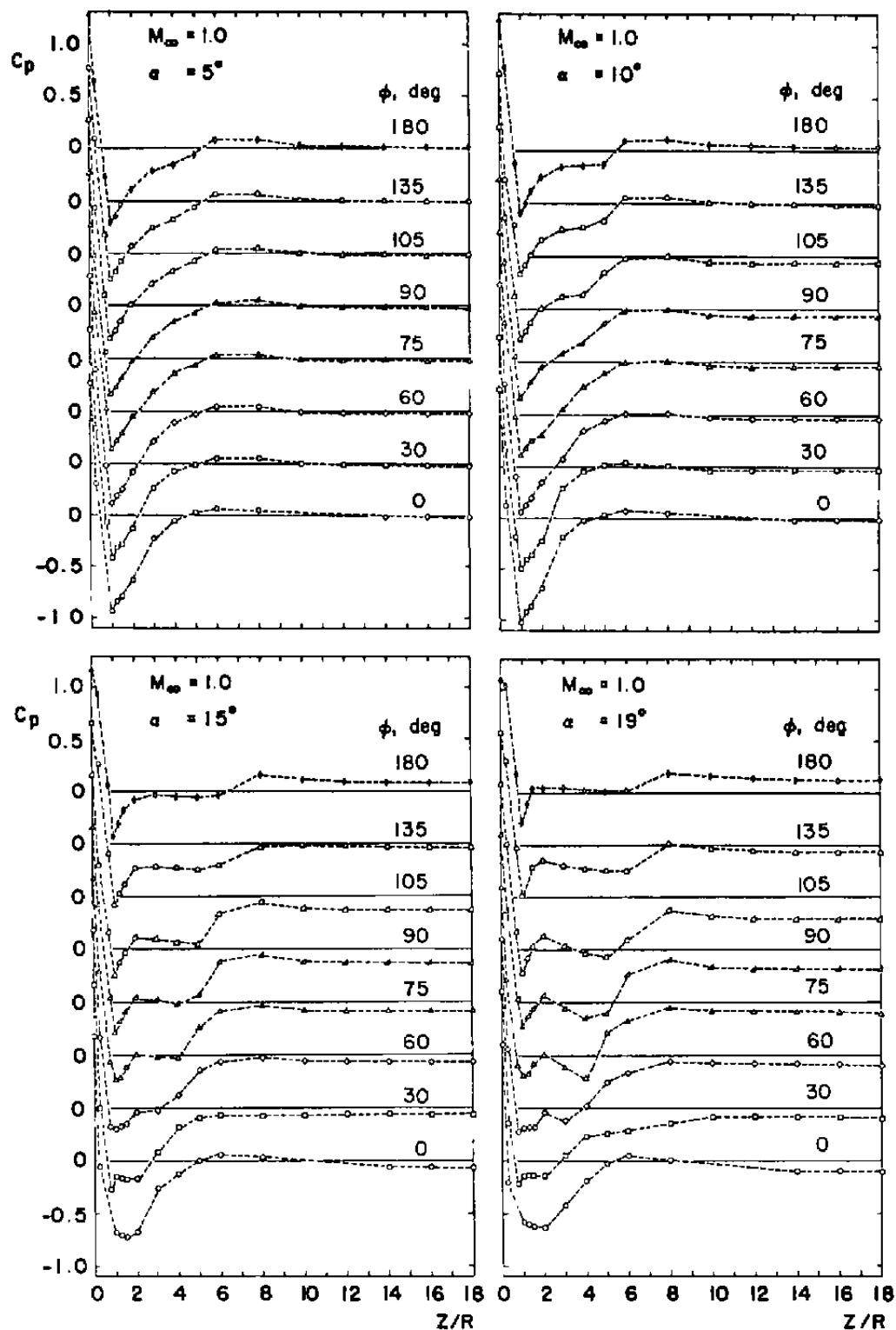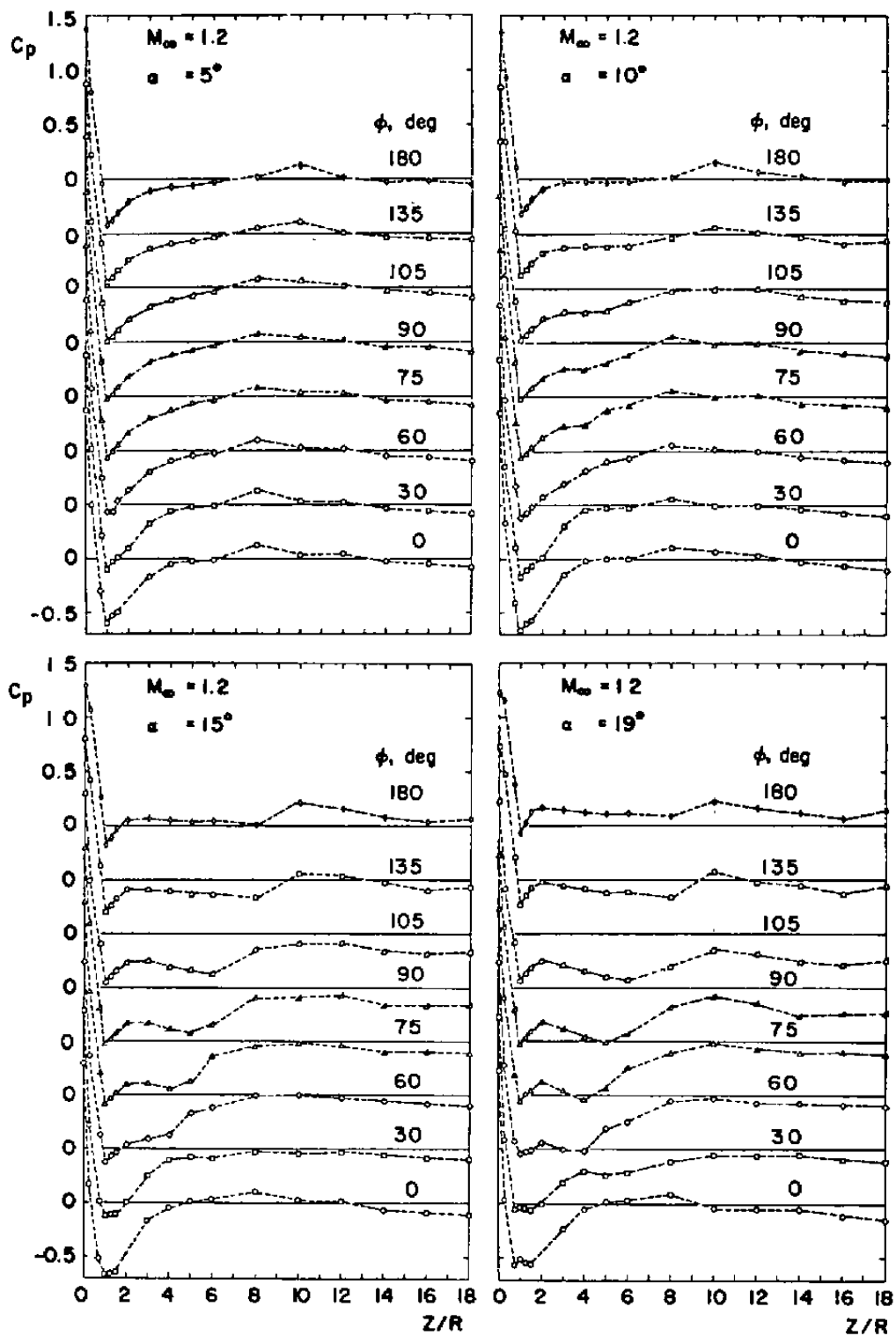
Figure A-1. Continued.

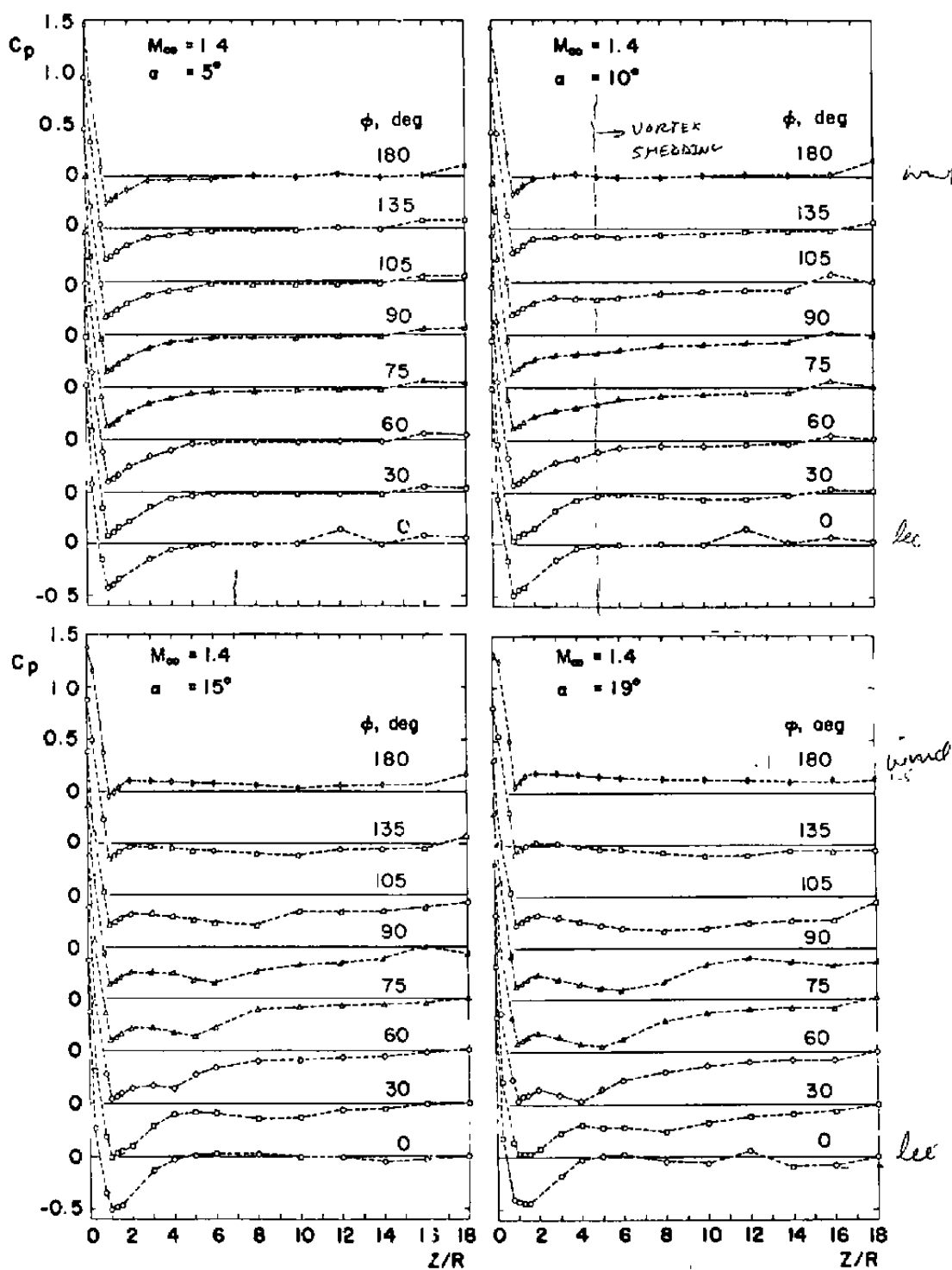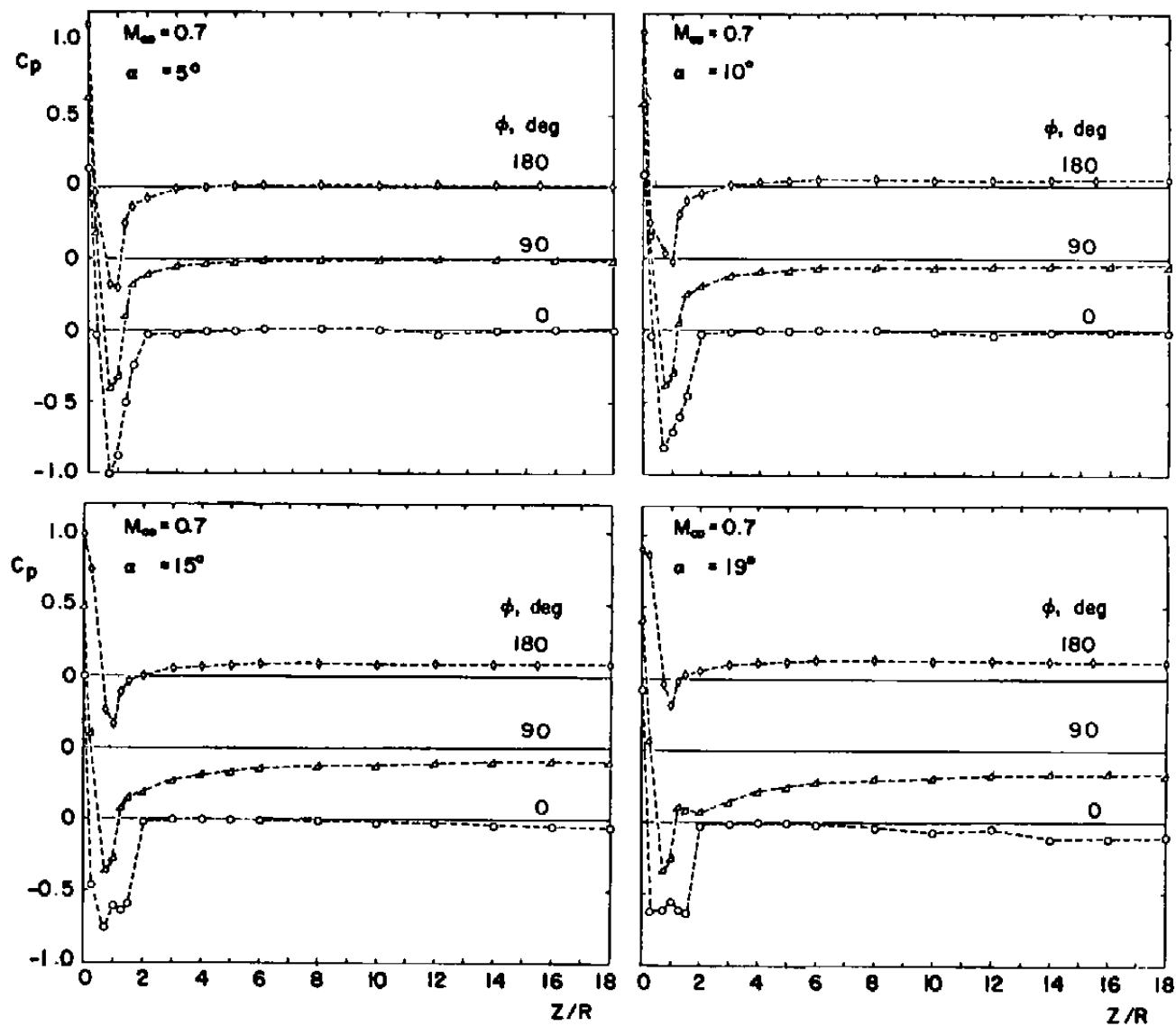Figure A-1. Continued.

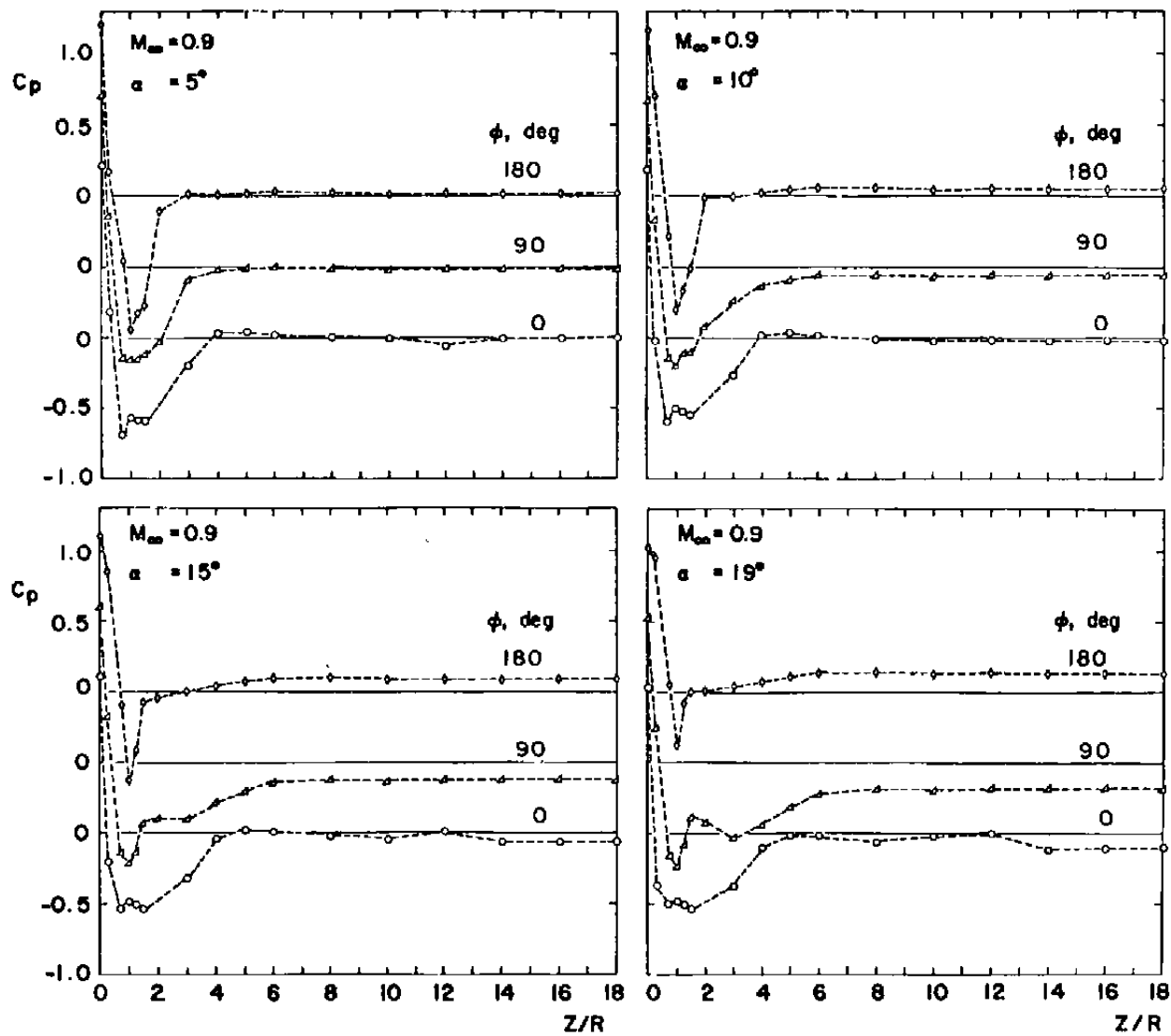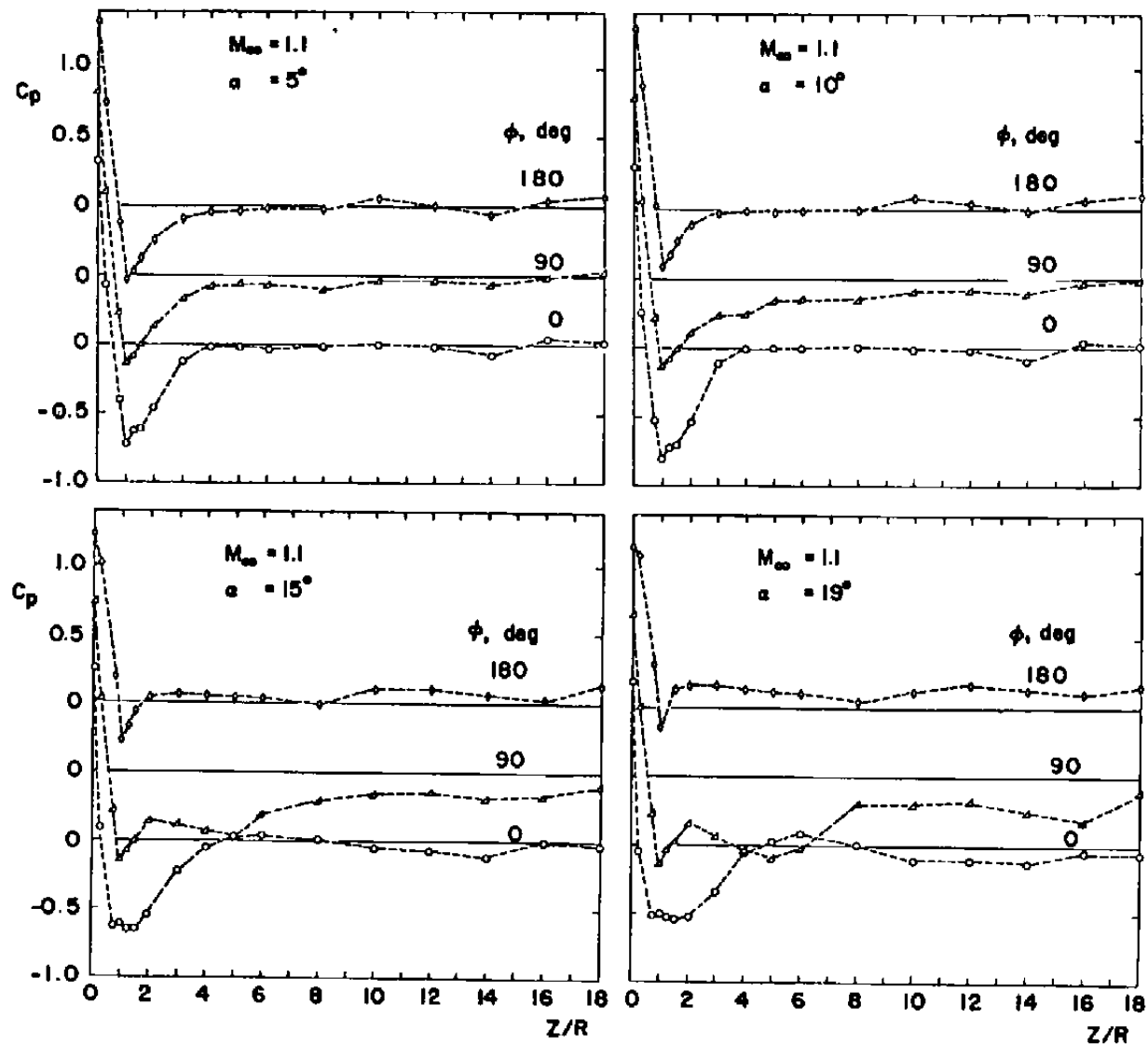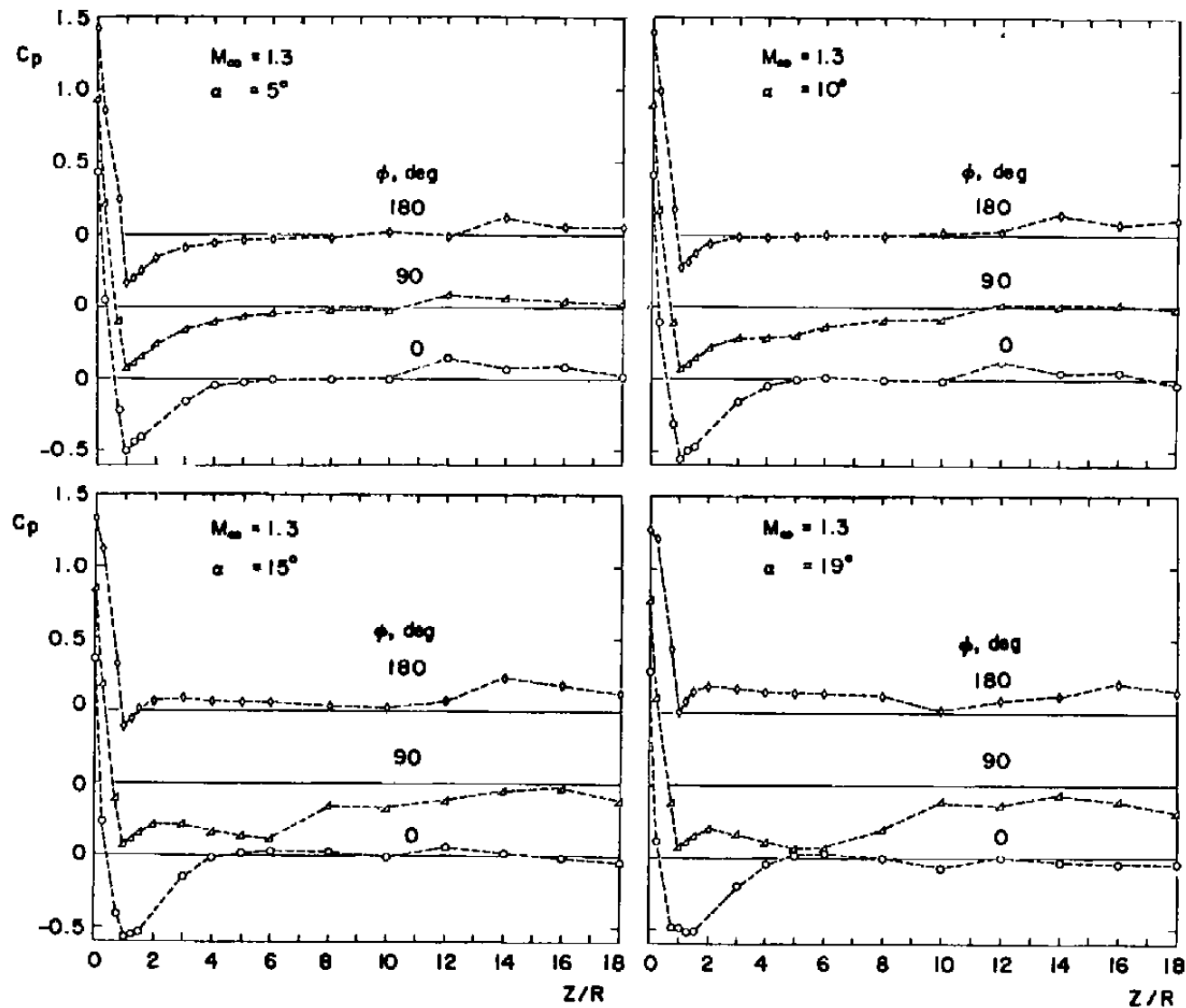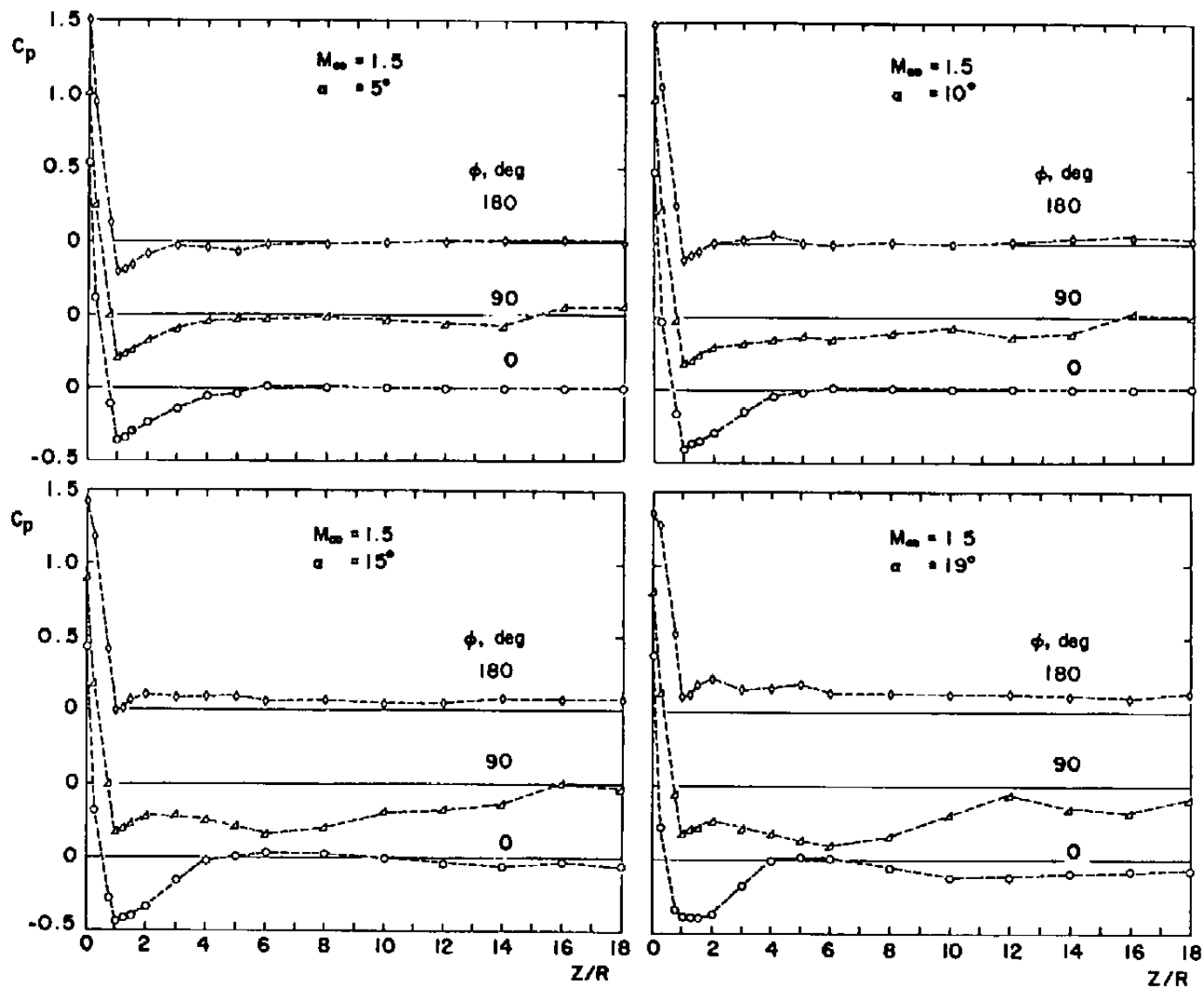Figure A-1. Continued.

98

Figure A-1. Continued.

99

Figure A-1. Continued.

Figure A-1. Continued.

$M_\infty = 1.1$

$a = 5°$

C_p

ϕ, deg

180

90

0

$M_\infty = 1.1$

$a = 10°$

ϕ, deg

180

90

0

$M_\infty = 1.1$

$a = 15°$

C_p

ϕ, deg

180

90

0

$M_\infty = 1.1$

$a = 19°$

ϕ, deg

180

90

0

Z/R

Z/R

Figure A-1. Continued.

Figure A-1. Continued.

Figure A-1. Concluded.

APPENDIX B
INTEGRATION OF SURFACE PRESSURE FOR
AERODYNAMIC COEFFICIENTS

The aerodynamic coefficients may be obtained from pressure data. In order to improve the accuracy, curve fitting, using least square fit, was first carried out and then integration was performed using the fitted curves instead of the data, which are not uniformly spaced. A brief description of the curve fitting and the integration is given in the following:

1. Curve fitting. In the nose portion, least square curve fitting was carried out with respect to θ first using C_P values at orifice No. 2 ($\theta = 0$), 3 ($\theta = 43$ deg), 4 ($\theta = 73$ deg), and 5 ($\theta = 90$ deg). In addition, a stagnation pressure C_{P_s} is located at θ_s with

$$\theta_s = -\beta \text{ for } \theta < \frac{\pi}{2}$$

$$= \beta \text{ for } \phi > \frac{\pi}{2}$$

(B1)

where

$$\beta = \tan^{-1} \left(\frac{\sin \alpha}{\sqrt{\cos^2 \alpha + \tan^2 \phi}} \right)$$

(B2)

and also $\left. \dfrac{\partial C_p}{\partial \theta} \right|_{\theta=\beta} = 0$ is imposed.

Next, curve fitting with respect to ϕ was carried out with $\phi = 0$, 30, 60, 75, 90, 105, 135, and 180 deg for a constant θ. In addition, the symmetry condition is imposed

$$\frac{\partial C_p}{\partial \phi} = 0 \quad \text{at } \phi = 0 \text{ and } \pi$$

(B3)

The above scheme of curve fitting in ϕ was also used for the cylinder portion.

2. Integration for aerodynamic coefficients. With all the fitted C_p curves, the integration for the drag coefficient can be obtained by

$$C_d = \frac{2}{\pi} \int_0^{\pi/2} \int_0^\pi C_p (\theta,\phi) \sin\theta \cos\theta \, d\phi \, d\theta \qquad (B4)$$

and sectional normal-force coefficient is given by

$$C_n = \frac{2}{\pi} \int_0^{\pi/2} \int_0^\pi C_p (\theta,\phi) \sin^2\theta \cos\phi \, d\phi \, d\theta \qquad (B5)$$

for the nose portion and

$$C_n = \frac{2}{\pi} \int_0^\pi C_p (\phi) \cos\phi \, d\phi \qquad (B6)$$

for the cylinder portion.

The above integration for sectional normal-force coefficient was carried out at $\Delta\theta = 5$ deg for the nose portion and at each (Z/R) station where data were taken. The integration for total normal-force coefficient and center of pressure are given as follows:

$$C_N = \int_0^{L/R} C_n \, d\left(\frac{\ell}{R}\right) \qquad (B7)$$

and

$$C_M = \int_0^{L/R} C_n \left(\frac{\ell}{R}\right) d\left(\frac{\ell}{R}\right) \qquad (B8)$$

$$(Z/R)_{c.p.} = \frac{C_M}{C_N} \qquad (B9)$$

where L is the total length of the body and ℓ is the distance from the nose at each station. A computer program was written to perform the above integration.

APPENDIX C
A BRIEF REVIEW OF PREDICTION METHODS FOR
AERODYNAMIC COEFFICIENTS FOR BODY OF REVOLUTION
AT LARGE INCIDENCE

C.1 THEORETICAL MODELS

Because of the complexity of the flow field involved, the
theoretical prediction method for the aerodynamic coefficients for a
missile-type body of revolution at large incidence is far from satis-
factory. A brief review of current available prediction methods is
presented in this section.

Among the published theoretical prediction methods, the fundamental
models used can be classified into three categories, namely: (I) cross-
flow drag model, (II) vortex model, and (III) numerical solution to the
approximate Navier-Stokes equation. Current development of each cate-
gory is discussed as follows:

(I) Crossflow drag model - The development of this model can be
found in Ref. 1. The idea is that a crossflow lift attributed to flow
separation is directly added to the lift predicted by slender body
potential theory. The crossflow lift in turn may be expressed by a drag
coefficient. The crossflow drag coefficient has since been studied in
detail to cover a large range of Reynolds number, Mach number, and body
geometry, etc. (Ref. C-1). Impulsive flow analogy for unsteady drag
has also been applied with limited success (Ref. C-2).

This model, because of its empirical nature, is very easy to use
and has been applied to predict aerodynamic coefficients for a missile-
type body from 0- to 180-deg incidence and has been shown to be in good
agreement with experimental data (note: not so satisfactory for the
axial force, see Ref. 1). The defects of this model are (1) it depends
heavily on experimental information, therefore, for a body geometry or

flow condition which has not been tested, the prediction can fail. As an example, the predicted aerodynamic coefficients for the hemisphere-cylinder discussed in the main text are not satisfactory, and (2) this model does not provide any information about the flow field around the body, hence, the effects of wings or other appendages added to the body for design purpose are not known.

(II) Vortex model – The development of a vortex model is a result of experimental observation. For a slender body of revolution (or the nose not too blunt), the changes in the leeside flow patterns may be described in the following sequences as shown in Fig. C-1. At low incidence, $\alpha \lesssim 20$ deg, a pair of steady symmetric vortices prevails, (see Fig. C-1a). At moderate incidence, 20 deg $\lesssim \alpha \lesssim 50$ deg, vortex shedding becomes asymmetric with two or more vortex cores as shown in Fig. C-1b. At still higher incidences, 50 deg $\lesssim \alpha \lesssim 70$ deg, the asymmetrical vortex sheddings become unsteady with the location of vortex cores randomly changing with time, (see Fig. C-1c). Finally, for 70 deg $\lesssim \alpha \to 90$ deg, the leeside flow field may be described by a turbulent wake as shown in Fig. C-1d. The vortex model is an attempt to simulate the leeside flow field by incompressible vortices in the crossflow plane and compute the force introduced by the vortices on the body.

There are two types of vortex models that can be distinguished as follows:

(a) Vortex model for replacing the crossflow drag – This model replaces the empirical crossflow drag of model (I) by a pair of concentrated vortices as was done in Refs. C-3, C-4, and Ref. 19, or pairs of vortices (multivortex) as was done in Ref. C-5. The lift as predicted by the slender potential theory is still maintained. The strength of the vortex or vortices is determined by satisfying the Kutta condition and the point of separation is considered to be given by experi-

ment or other theoretical means. By using the impulsive flow analogy, the position and strength of the vortices can be computed for each axial station along the body. Both the concentrated and the multivortex model have been modified to account for asymmetrical vortex shedding at high incidences (up to 50 deg) in Refs. C-6 and C-7. In Ref. C-7, the compressibility effect is accounted for through Gothert's rule. The improvement of this vortex model over the crossflow model is that it gives some feeling about the flow field around the body. The disadvantage is that to establish the flow separation location can be as difficult as obtaining the aerodynamic forces experimentally or theoretically.

(b) Diffusive vortex model - This model is developed in Ref. C-8. The assumptions are (i) the three-dimensional, incompressible steady flow is equivalent to the two-dimensional, incompressible unsteady flow (like impulsive flow), and (ii) in the two-dimensional crossflow plane the leeside flow field may be represented by a distribution of inviscid point vortices superimposed on the unseparated potential flow solution. The strength and separation location for the pointed vortices are provided by unsteady two-dimensional, laminar boundary-layer calculation and a diffusion model is added to the point vortices. In addition, a rear shear layer at the rear of the cylinder in the absence of the boundary layer is introduced to satisfy the nonslip condition there. Hence, the nonslip condition is satisfied on the body surface in the crossflow plane (but not in the axial direction). Forces acting on the body are obtained by the integrating of pressure distribution over the body. Despite the complexities involved in the computation of this method, a final empirical adjustment of the wake vortex strength may be required to provide good comparison with

experimental data. This method is valid for incompressible or low subsonic flow only and restricted to symmetric vortex shedding.

(III) Numerical solution to the approximate Navier-Stokes equation – Two approaches along the line of solving approximate Navier-Stokes equations are described as follows:

(a) Application of equivalence principle. The equivalence principle in Ref. C-9 is similar to the assumption (i) of the diffusive vortex model (IIb), or the steady motion of a viscous, compressible fluid in three dimensions is equivalent to time-dependent viscous, compressible flow in two dimensions (Ref. C-9). The time-dependent, two-dimensional, compressible Navier-Stokes equations are then solved numerically in the crossflow plane (instead of using the diffusive vortex model as in Ref. C-8) for a circular section varying with time. Good comparison for surface pressure between theory and experiments has been reported in Ref. C-9 for an ogive-cylinder at α = 10 deg and M_∞ = 1.98. How well this prediction method might be for higher incidence or arbitrary Mach number has not been investigated. The weak point of this method is that the theoretical grounds for the equivalence principle are not sound.

(b) A solution to the compressible, three-dimensional Navier-Stokes equations by neglecting the viscous, streamwise terms has been reported for pointed and blunt nose cone in Refs. C-10 and C-11. Good agreement of surface pressure between theory and experiment is obtained for incidence up to 15 deg, at a Mach number greater than 6 and a Reynolds number in the order of 10^6/ft. This method, however, is restricted to cone shape bodies only and for M_∞ > 3. It has not been tested for incidence higher than 15 deg. The approximation of neglecting

the viscous, streamwise terms can be a serious restriction to
the range of applicability in the aspect of incidence, Mach
number, and nose geometry.

C.2 COMMENTS

From the brief description of the available theoretical models in
Section C.1, some comments about these theories as applied to the
hemisphere-cylinder case, or more generally a blunt nose body of revolu-
tion, may be made. The comparison of the crossflow drag model (I) has
been described in the main text and is found to be unsatisfactory in the
transonic flow regime for $\alpha > 10$ deg. The reasons may be twofold, (1)
the insufficient data base for determination of crossflow drag coeffi-
cient at the transonic regime and (2) the inaccuracy of the lift pre-
dicted by slender body potential theory in the transonic regime and for
blunt nose bodies.

The vortex model of IIa has been applied to a hemisphere-cylinder
and other blunt nose bodies in incompressible flow as given in Ref. 19.
Generally, the results are only good qualitatively. Since this model
requires information of separation angle in the crossflow plane, as
shown in Fig. 17, the influence of Mach number and incidence is signi-
ficant for a blunt body in the transonic flow regime and such information
is just as difficult to obtain as the direct measurement or calculation
of the force and moment, hence, it is not so convenient to apply.
However, the method of Ref. C-7 may be promising. In Ref. C-7, a set
of empirical constants was used in the computation, and the author found
that the results were not too sensitive to the input of separation
angle. Therefore, if sets of empirical constants can be determined for
certain categories of body geometries, flow conditions, and incidence
ranges, this method may serve a good purpose for engineering application.

The assumption that three-dimensional steady flow is equivalent to time-dependent, two-dimensional flow is without theoretical basis and can only be considered as semi-empirical. For blunt nose bodies in the Mach number range studied in this report, two separation regions can exist simultaneously in the three-dimensional steady flow; it is impossible for a two-dimensional unsteady flow as such to depict correctly the physical situation. Therefore, such assumption must be made with great caution.

The appearance of bubble-type separation at the nose and the concentrated vortices on the leeside forebody also rule out the assumption of neglecting the viscous, streamwise terms in an attempt of solving Navier-Stokes equations for the flow field of blunt nose bodies of revolution at incidences.

From the above discussion, a satisfactory prediction method is still not available at this time, particularly for blunt nose bodies of revolution at large incidence. The flow field for the hemisphere-cylinder investigated in this report will serve as a guide for future development of the prediction method.

REFERENCES

C-1. Thomson, K. D. "The Estimation of Viscous Normal Force, Pitching Moment, Side Force and Yawing Moment on Bodies of Revolution at Incidences Up to 90°." WRE-Report-782, October 1972.

C-2. Kelly, H. R. "The Estimation of Normal Force, Drag, and Pitching-Moment Coefficients for Blunt-Based Bodies of Revolution at Large Angles of Attack." Journal of the Aeronautical Sciences, Vol. 21, No. 8, August 1954.

C-3. Mello, J. F. "Investigation of Normal Force Distributions and Wake Vortex Characteristics of Bodies of Revolution at Supersonic Speeds." Journal of the Aero/Space Sciences, March, 1959, pp. 155-168.

C-4. Bryson, A. E. "Symmetric Vortex Separation on Circular Cylinders and Cones." Journal of Applied Mechanics, Vol. 26, December 1959, pp. 643-648.

C-5. Angelucci, S. B. "A Multivortex Method for Axisymmetric Bodies at Angle of Attack." Journal of Aircraft, Vol. 8, No. 12, 1971, pp. 959-966.

C-6. Wardlaw, A. B., Jr. "Prediction of Normal Force, Pitching Moment, and Yawing Force on Bodies of Revolution at Angles of Attack up to 50 Degrees Using a Concentrated Vortex Flow-Field Model." NOLTR 73-209, October 1973.

C-7. Wardlaw, A. B., Jr. "Multivortex Model of Asymmetric Shedding on Slender Bodies at High Angle of Attack." AIAA Paper 75-123, 13th Aerospace Science Meeting, January 1975.

C-8. Marshall, F. J. and Deffenbaugh, F. D. "Separated Flow Over a Body of Revolution." Journal of Aircraft, Vol. 12, No. 2, 1975, pp. 78-85.

C-9. Walitt, L. and Trulio, J. G. "A Numerical Method for Computing Three-Dimensional Viscous Supersonic Flow Field about Slender Bodies." NASA-CR 1963, November 1971.

C-10. Lubard, S. C. and Helliwell, W. S. "Calculation of the Flow on a Cone at High Angle of Attack." AIAA Paper 73-636, 6th Fluid and Plasma Dynamic Conference, July 1973.

C-11.   Lubard, S. C. and Rakich, J. V.   "Calculation of the Flow on a
          Blunted Cone at High Angle of Attack."   AIAA Paper 75-149,
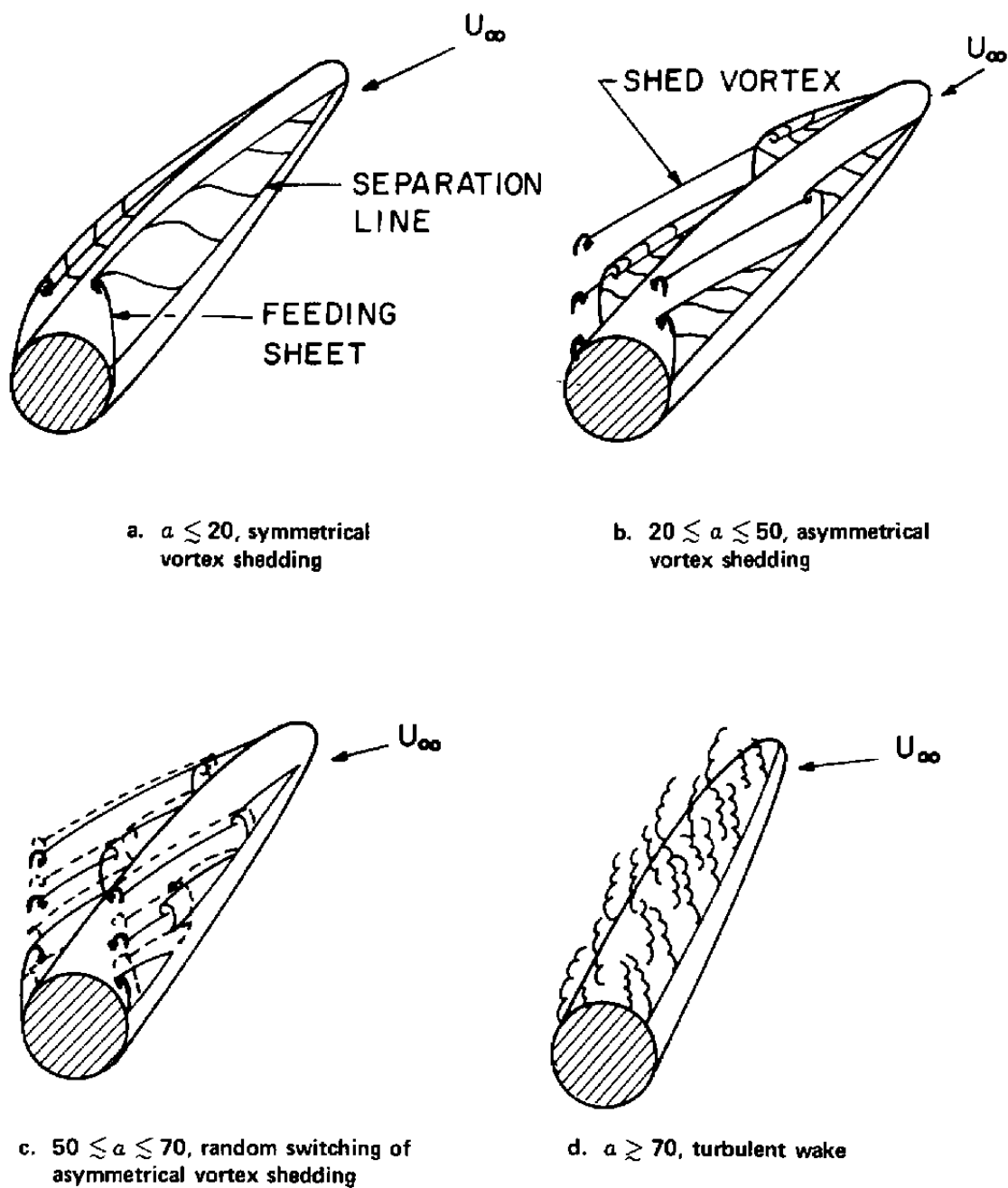   13th Aerospace Sciences Meeting, January 1975.

a. $a \lesssim 20$, symmetrical vortex shedding

b. $20 \lesssim a \lesssim 50$, asymmetrical vortex shedding

c. $50 \lesssim a \lesssim 70$, random switching of asymmetrical vortex shedding

d. $a \gtrsim 70$, turbulent wake

Figure C-1.

NOMENCLATURE

C_A — Axial-force (forebody only) coefficient, $F_a / \frac{1}{2} \rho_\infty U_\infty^2 (\pi R^2)$

C_n' — Local normal force per unit length

C_N — Total normal-force coefficient, $F_N / \frac{1}{2} \rho_\infty U_\infty^2 (\pi R^2)$

C_P — Pressure coefficient, $(p - p_\infty) / \frac{1}{2} \rho_\infty U_\infty^2$

F_a, F_N — Axial and normal force, respectively

M_∞ — Mach number

R — Radius of cylinder

Re — Reynolds number

S_1, S_2 — Primary and secondary separation points, respectively

U, V — Axial and radial (vertical) velocity components

V_1, V_2, V_3 — Possible appearance of vortices

Y, Z — Radial (or vertical) and axial distance

$(Z/R)_{c.p.}$ — Location of center of pressure from nosetip

α — Angle of attack, deg

ϕ — Circumferential angle starting from leeside plane of symmetry

ψ_s — Angle of separation in the crossflow plane

Δ — Shock standoff distance

SUBSCRIPT

∞ Condition at free stream

p   For small entrained particles in the fluid medium